AFCRL-70-0111

TRAVEL TIMES AND BODY WAVE MAGNITUDE

Seweryn J. Duda
School of Engineering and Earth Science
SAINT LOUIS UNIVERSITY
St. Louis, Missouri 63156

Contract No. AF 19(628)-5100
Project No. 8652
Task No. 865200
Work Unit No. 86520001

SCIENTIFIC REPORT No. 8

February 1970

Contract Monitor: Henry A. Ossing
Terrestrial Sciences Laboratory

Prepared for

Air Force Cambridge Research Laboratories
Office of Aerospace Research
United States Air Force
Bedford, Massachusetts 01730

This research was supported by
ADVANCED RESEARCH PROJECTS AGENCY
ARPA Order No. 292, Amendment 45
Project Code No. 5810

87

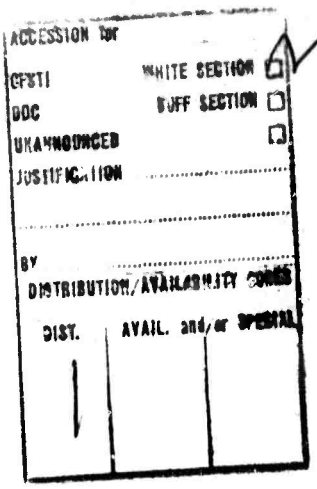

Qualified requestors may obtain additional copies from the Defense Documentation Center. All others should apply to the Clearinghouse for Federal Scientific and Technical Information.

AFCRL-70-0111

TRAVEL TIMES AND BODY WAVE MAGNITUDE

Seweryn J. Duda
School of Engineering and Earth Science
Saint Louis University
St. Louis, Missouri 63156

Contract No. AF 19(628)-5100
Project No. 8652
Task No. 865200
Work Unit No. 86520001

SCIENTIFIC REPORT No. 8

February 1970

Contract Monitor: Henry A. Ossing
Terrestrial Sciences Laboratory

Prepared for

AIR FORCE CAMBRIDGE RESEARCH LABORATORIES
OFFICE OF AEROSPACE RESEARCH
UNITED STATES AIR FORCE
BEDFORD, MASSACHUSETTS 01730

This research was supported by

ADVANCED RESEARCH PROJECTS AGENCY
ARPA Order No. 292, Amendment 45
Project Code No 5810

TRAVEL TIMES AND BODY WAVE MAGNITUDE

ABSTRACT

The $\overline{Q}$-charts used presently for magnitude determinations were obtained mainly from direct observations of ground motion amplitudes of several components of seismic waves (e.g. PZ, PH, SH) as functions of epicentral distance.

After the compensation of the amplitudes of body waves for the radiation pattern at the focus, the amplitude variation is caused mainly by geometrical spreading. No lateral velocity heterogeneities are permitted. Indications are given that the effect of anelasticity upon the amplitudes is secondary for magnitude scales.

Amplitude observations alone can serve for the definition of a magnitude scale applicable to events at only one particular focal depth. In order to assign the same magnitude to two earthquakes of identical "size" regardless of the focal depth, the velocity-depth and eventually anelasticity-depth profile of the Earth must be known.

A set of new $\overline{Q}$-charts, obtained independently or direct amplitude observations, for PZ-, PH-, and SH-waves is presented. A refinement in the magnitude definition warrants the magnitude figures obtained with the new $\overline{Q}$-charts to be uniform with regard to focal depth. Examples show the new $\overline{Q}$-charts to decrease the scatter of magnitude determinations between stations.

Since the efficiency in generating longitudinal and transverse waves is most probably not the same for all events, separate P-wave and S-wave magnitudes are advocated.

BLANK PAGE

TRAVEL TIMES AND BODY WAVE MAGNITUDE

by Seweryn J. Duda

1. Introduction

The classification of seismic events according to their relative and absolute size is an obvious need. The magnitude scale, originally proposed by Richter (1935), is the most widely accepted means serving the purpose. Though it would be theoretically more satisfactory to express the size of seismic events in terms of the kinetic energy radiated across the focal surface (sphere) during the event, practical difficulties forbid at present the attempt to determine energy for a large number of events, or on a routine base. The practical difficulty in determining the kinetic energy of an event contributes to the continuing success of the magnitude scale. The disturbing question, whether a unique relation exists between the magnitude and the kinetic energy corresponding to an event, is thereby left open, and will be answered most probably in the negative with the increase of observational accuracy.

The magnitudes published presently by various stations scatter, and differences of one magnitude unit between two stations are not rare. The scatter of magnitude determinations can be caused by numerous factors. Gutenberg (1945) realized the severity of the problem, and proposed corrections to be applied to the individual magnitude determinations. Station corrections compensating for the local structure beneath the observatory, and regional corrections compensating for the prevailing mechanism and anomalies along the ray paths between a given region and an observatory have been worked out (see, e.g., Båth, 1956). The procedure of obtaining and applying them is tedious, and it is not surprising that rather few observers know the corrections applicable to their station for earthquakes in a particular region. Since horizontal heterogeneities exist in the real Earth, regional and station corrections will remain necessary for the decrease of scatter of individual magnitude determinations. In addition, however, it seems worthwhile to check the consistency of the presently used magnitude scale against evidence offered by new observations.

The magnitude problem involves several aspects of seismic wave generation and propagation. The most important ones are the radiation pattern of the focus, the geometric spreading and the absorption of seismic waves along the ray path. Recent work by Jarosch (1969) and Chandra (1969) has shown that if a source model is postulated and a fault plane

solution obtained, the variation of amplitudes due to the resulting radiation pattern can be accounted for, and the scatter of magnitude figures obtained at different stations is decreased. This aspect of the magnitude problem shall be omitted here. Consequently, we assume throughout the present paper that the amplitudes of longitudinal and transverse waves leaving the focus are already compensated for the radiation pattern, and are virtually the same in all directions.

The elastic waves generated at the focus may be supposed to cover a wide frequency spectrum. The lowest and highest frequencies are the subject of only occasional recording: low frequency waves have small amplitudes which usually escape detection and high frequency waves are attenuated through scattering already at short distances from the focus. Only waves in an intermediate frequency range are eventually recorded at all possible epicentral distances, and thus are of interest e.g. for magnitude studies. Without specifying it exactly we will limit ourselves in the following to the latter frequency range of seismic waves.

During the passage from the focus to the observatory the amplitudes of seismic waves are subject to change due to two principal factors:

1) the velocity heterogeneity, and

2) the anelasticity of the Earth.

Amplitudes as a function of epicentral distance, when obtained from direct observations, are then the result of both geometrical spreading (frequency independent), and absorption (in general frequency dependent). It is known that geometrical spreading has a substantially bigger effect upon the amplitudes of seismic waves than absorption. We will show that the effect of the absorption is below the accuracy of present amplitude measurements. The observed amplitudes of seismic waves can be, therefore, compared with those computed under the assumption of a certain velocity model for the Earth.

$\overline{Q}$-charts for magnitude determination from P- and S-waves are obtained, absolutely independently of direct amplitude observations.

II. P-waves

1. Amplitude variation along the Earth's surface.

We consider the earthquake focus as a point source of longitudinal and transverse waves. A point source, as used

also in other seismological problems, leads unfortunately to some theoretical difficulties by producing a singularity at the source itself.

The earthquake focus is assumed to be situated inside the Earth or at its surface, the focal depth under consideration ranging from 0 km to 800 km. The (spherical) Earth is assumed to have a radial velocity heterogeneity. No horizontal velocity gradients are permitted. The velocity distribution of P-waves as published by Herrin et al. (1968) is here accepted (Fig. 1). The feature of the distribution most important for the present study is the monotonic increase of velocity with depth. Thus, the travel time curve is continuous for all focal depths, and no extensive shadow zones are possible.

The amplitudes, A, of seismic waves along the surface of the Earth are proportional to:

$$(1) \qquad A \sim \sqrt{\frac{\sin i_h}{R_o^2 \cdot \sin \Delta \cdot \cos i_o} \cdot \left| \frac{d\, i_h}{d\, \Delta} \right|}$$

with

i_h - angle of incidence at the focus

i_o - angle of incidence at the Earth's surface

Δ - epicentral distance

R_o - radius of the Earth

(see e.g. Bullen, 1953).

Applying formula (1), the variation of the total P-wave amplitude along the Earth's surface was computed for epicentral distances ranging from 0° to 100°, and for foci at 21 depths (0, 15, 40, 50, 75, 100, 125, 150, 200, 250, etc., through 800 km). Fig. 2-22 show the amplitudes as a function of epicentral distance relative to that at 80° epicentral distance.

The choice of the amplitude at 80° as norm is due to the comparative "quiescence" of all amplitude variation curves in the range from about 40° to 80°. It would have been improper for the normalizing amplitude to be chosen from among distances shorter than 40° or larger than 80°. As seen from the figures, the amplitudes become at those distances occasionally very small, or even vanish. The shadow zones occur whenever the slope of the travel time curve remains unchanged for two adjacent epicentral distances. However, the extent of the

shadow zones does not exceed about 0.5°.

A slight instability is visible on the amplitude variation curves (Fig. 2-22). We interpret this as due to the required twofold numerical differentiation of travel times given at 0.5 degree distance intervals with an accuracy of 0.01 sec. A higher accuracy in the travel times would presumably result in a more stable amplitude variation curve. On the other hand, it is conceivable, though outside the scope of the present paper, that if the amplitude variation curve would be stabilized by some criterion, the travel times could be obtained by inversion with a higher accuracy. For our present purpose the instability is of only slight practical importance.

In the Fig. 2-22 we see a bulge in the amplitude variation curves - especially for shallow focal depths. The peak lies at about 18°, and the preceding trough at about 12° epicentral distance. As can be readily seen, e.g. from Fig. 3, the amplitudes increase by a factor of about 3 over a distance of 6°.

It is worthwhile to compare the amplitude variation in this distance range with that reported by Gutenberg (1959) on the base of direct amplitude observations. According to Gutenberg's measurements, "the amplitudes of longitudinal waves decrease about exponentially with increasing distance and reach a minimum at $\Theta = 15^{\circ}$. At this distance they increase suddenly by a factor of more than ten." The graph published by Gutenberg is seen on Fig. 23, and was used originally by him as one of the evidences for the existence of the low velocity layer in the upper mantle.

Comparing the observations with our calculations (e.g. Fig. 3), we see that the amplitude behavior reported by Gutenberg may also be in agreement with a velocity model not containing a low velocity layer. Regardless of the interpretation, it is reassuring that a characteristic feature of the amplitude variation has been recognized earlier by direct amplitude observation. This indicates that body wave amplitudes are essentially capable of yielding information on certain details of the velocity-depth structure of the Earth.

For the surface focus, the amplitude at zero epicentral distance tends to infinity. For foci at greater depths, the amplitude at zero epicentral distance is finite and decreases with the increase of focal depth.

Table 1 g the amplitudes at zero epicentral distance for foci at de between 0 km and 800 km, relative to the amplitude at 80°. The amplitudes decrease with increasing focal depth and are affected basically by the velocity distribution down to the greatest focal depth.

As mentioned earlier the P-wave amplitudes at the surface of the Earth remain fairly unchanged in the range from about 40° to 80° epicentral distance, independent of focal depth. Over most of the distance range, the amplitudes remain usually within 3 orders of magnitude for shallow foci, and within 2 orders of magnitude for deep foci. For a focal depth of 800 km, the ratio of the largest to the smallest amplitude in the entire observable range is even less than 100.

The knowledge of the variation of seismic wave amplitudes along the surface of the Earth is fundamental for any magnitude scale.

As defined, the body wave magnitude, m, is computed from the formula:

$$m = \log \frac{A_c}{T} + \overline{Q} \qquad (2)$$

where

A_c - ground amplitude at station for a particular component in microns

T - corresponding period, in seconds,

c - PZ, PH, PPZ, PPH, SH

$\overline{Q}$ - tabulated quantity depending on wave type, seismograph component, and epicentral distance.

The log is to the base 10; for simplicity the regional and station corrections are assumed to cancel each other. The quantity $\overline{Q}$ (denoted by various authors as Q, q, A, σ, or β) compensates the observed ratio of amplitude and period for the general decrease with epicentral distance. Thus, $\overline{Q}$ increases usually with epicentral distance.

For m = 0, $\overline{Q}$ represents the negative logarithm of the amplitude/period ratio of any given epicentral distance:

$$\overline{Q} = - \log \frac{A_c}{T} \qquad (3)$$

and the amplitude/period ratio is:

$$\frac{A_c}{T} = 10^{-\overline{Q}} \quad . \qquad (4)$$

For an arbitrary magnitude the amplitude/period ratio is:

$$(5) \qquad \frac{A_c}{T} = 10^m * 10^{-\bar{Q}}$$

If $\bar{Q}$ is known, the amplitude/period ratio as function of epicentral distance can be readily computed from (4). Up to a constant factor, the curve is representative for any magnitude. The curve is numerically equal to the amplitude variation of a 1 second wave, and is proportional to the amplitude variation of a wave with an arbitrary period. Consequently, $10^{-\bar{Q}}$ is proportional to the variation with epicentral distance of any Fourier component of the ground motion.

Numerous investigators have published or modified $\bar{Q}$ charts, especially for shallow foci. For deep foci, the only $\bar{Q}$-values available seem to be those published by Gutenberg and Richter (1956).

Using (4) we compute A_{PZ}/T and A_{PH}/T as functions of epicentral distance. Dividing by the cosine and sine of the angle of incidence correspondingly, we obtain the variation of the total amplitude along the surface of the Earth (divided by T). The total amplitudes so obtained should be equal.

The computations were carried out for the $\bar{Q}$-values corresponding to PZ and PH for a shallow focus as published by Gutenberg and Richter (1956), Vaněk and Stelzner (1960), and Vaněk, et al. (1962). From Fig. 24 it is seen that the total amplitudes obtained from $\bar{Q}$ (PZ) and $\bar{Q}$ (PH) respectively, diverge somewhat, indicating that the sets of $\bar{Q}$-values are not consistent.

Each of the curves represents an amplitude variation of the P-wave along the Earth's surface, as resulting from direct observations and averaging processes.

Obviously, the observed amplitude variation results not only from geometrical spreading but also from absorption and from possible lateral heterogeneities.

Comparing Fig. 24 with the Fig. 3, the latter representing the computed amplitude variation due to geometrical spreading alone for a shallow focus, we see a general agreement. The difference between any of the curves in Fig. 24 and the curve in Fig. 3 is not greater than the differences between the curves in Fig. 24 themselves. The agreement becomes poor if details are concerned, apparently due to the scatter of the observational amplitude data and possibly to regional differences in the velocity structure, i.e. to lateral velocity heterogeneities.

From the above we conclude that the P-wave amplitude variation along the surface of the Earth is principally due to the vertical velocity heterogeneity in the Earth. The share of anelasticity in causing the amplitude variation seems to be below the present observational accuracy.

The conclusion permits one to use the amplitude variation curves based on the newest travel time tables (and the underlying velocity model), as given in Fig. 2-22, for the computation of a set of $\bar{Q}$ values, independent of direct amplitude observations.

2. Amplitude variation along interface inside the Earth.

A source of seismic waves situated at a particular focal depth produces amplitudes at the Earth's surface, which vary with epicentral distance. If the amplitudes are observed and measured, they can be readily used as a base for a magnitude scale for all seismic events at this particular focal depth. The local magnitude scale for California earthquakes may serve as an example. The amplitudes so observed will be inapplicable to a different focal depth.

However, a workable magnitude scale must be uniform with respect to focal depth, and, obviously, assign the same magnitude to two events of identical "size," which occurred at different depths. This is theoretically only possible if a velocity-depth and an anelasticity profile of the Earth is assumed.

This difficulty was realized already by Gutenberg (1945) who reported the computation of the amplitude variation at the Earth's surface for sources at a few focal depths. The computations served as a frame into which the amplitude variation curves obtained from direct observations were fitted.

Anelasticity inside the Earth is of secondary importance for a magnitude scale even at the present level of routine amplitude observations, and is neglected in the present paper.

But even with this simplification a certain ambiguity remains in the definition of the magnitude scale, which can be expressed through the question: When should two events at different focal depths be assigned the same magnitude?

While Gutenberg's answer is not apparent from his paper, we propose the following approach.

A point source of elastic waves inside the Earth is assumed to produce equal amplitudes in all directions. Due to the velocity heterogeneity, the amplitudes around the focus vary in general in a different way than they would

while spreading in a homogeneous medium. Only in the horizontal direction, where the velocity gradient vanishes, do amplitudes change as if propagation would occur in a homogeneous medium (Duda, 1970). Consequently, we assign the same magnitude to two events at different focal depths, if the amplitudes produced at the levels of the foci at a constant distance, d, are identical (see Fig. 25). A distance of 111 km is assumed for the reason that the region within which imperfect elastic processes occur during an earthquake has linear dimensions smaller than this distance for most earthquakes, even with biggest magnitudes. The distance obviously coincides with the length of an arc of 1^{o} at the surface of the Earth.

A different distance would yield slightly different numerical values for the $\overline{Q}$-charts presented below. We do not see any way to avoid this arbitrariness in the definition of the magnitude. We believe, however, that with our assumption a possibly consistent and uniform set of $\overline{Q}$-charts for all focal depths is obtained.

Thus, the amplitudes at a horizontal distance of 111 km at the level of the focus must be known.

Our procedure is to reduce the travel times along the Earth's surface for the focal depths, h, as function of epicentral distance Δ, so as to obtain the travel times along the interface at depth h as function of the distance Δ_B (Fig. 25). The travel time τ needed for the portion BA of the ray path is given by:

$$\tau = \int_{R_o - h}^{R_o} \frac{r * dr}{\sqrt{r^2 - (p*v)^2}}$$

where v is the wave velocity at distance r from the center of the Earth, and p is the path parameter of the ray emerging at distance Δ. This travel time is subtracted from the observed travel time, the difference being t_B. The angular distance between B and A is given by:

$$\delta = p \int_{R_o - h}^{R_o} \frac{dr}{r \sqrt{\left(\frac{r}{v}\right)^2 - p^2}}$$

Subtracting δ from the corresponding epicentral distance Δ, we obtain Δ_B. Knowing t_B as a function of Δ_B, the amplitude variation along the interface at the depth h is computed. At $\Delta_B = 0$ a singularity in the amplitude curve is observed for all focal depths.

The amplitudes along the interface are normalized with respect to the amplitude at the surface of the Earth and at the epicentral distance of 80°. The amplitude at the point A, A_A, with epicentral distance Δ, is related to the amplitude at point B, A_B, with distance Δ_B by:

$$A_B^2 = A_A^2 \cdot \left(\frac{R_o}{R_o - h} \right)^2 \cdot \frac{\cos i_o}{\cos i_h} \cdot \frac{\sin \Delta}{\sin(\Delta - \delta)} \cdot \frac{\left| \frac{d\, i_h}{d\, \Delta} \right|_B}{\left| \frac{d\, i_h}{d\, \Delta} \right|_A} ,$$

the symbols being defined in Fig. 25.

Evidently, the same amplitude was used for normalizing the amplitudes along the interface, as, previously, along the surface of the Earth.

The amplitudes along the interface decrease in general monotonically with distance, and the variation is fairly smooth, especially at greater focal depth. Fig. 26 shows the variation in the distance range $0\text{-}14^\circ$ for all 21 focal depths considered. Each figure shows how much larger is the amplitude at the level of the focus, at distances up to 14°, as opposed to the amplitude observed at the surface of the Earth at 80° epicentral distance.

The limit of 14° was assumed due to the fact that at about this distance the amplitudes become larger by one order of magnitude over those at the surface of the Earth at 80° epicentral distance. It was unexpected to find that the amplitudes at distances from 0° to 14° along the interface fall into four groups, depending on the focal depth. The least square approximation by a formula

$$(6) \qquad \begin{aligned} A &= C \cdot \mathrm{EXP}\,(-D \cdot \ln \Delta) = \\ &= C \cdot 10^{-D} \cdot \log \Delta \end{aligned}$$

with Δ in degrees is indicated on Fig. 26 by circles, and the numerical values of the constants C and D are given for the appropriate depth ranges. (Log denotes the logarithm to the base 10, and ln - to the base e.) In the depth ranges 0 - 40 km, and 50 - 125 km, the approximation was possible only for the distance range 0° - 10°, without producing an excessive standard deviation; in the depth ranges 150 - 450 km, and 500 - 800 km the approximation covers the distance range

0° - 14° . From Fig. 26 it is seen that, e.g., at 1° distance from the focus the amplitudes are about 1.5 times larger for a focus in the depth range 150 - 450 km, over a focus in the depth range 0 = 14 km, if the amplitude at the Earth's surface at 80° epicentral distance is equal to one in both cases.

The knowledge of the amplitudes close to the focus at any focal depth renders possible a magnitude definition uniform for all focal depths.

3. $\overline{Q}$-charts for P-waves.

According to Gutenberg and Richter (1956) "... a formal definition for m may be phrased as follows,

(7) $$m - 7.0 = q$$

at a distance of 90° for normal shallow focal depths, where $q = \log \frac{W}{T}$ refers to PZ and the station constant is taken as zero ..." This means that for a zero magnitude and a shallow focus $\frac{A_{PZ}}{T}$ at 90° epicentral distance amounts to 10^{-7} μ/sec, and $\overline{Q}(PZ)$ at 90° is 7.0.

Knowing that for a shallow focus the angle of incidence at 90° is $i_o = 14.7^{\circ}$, and with $\tan i_o = \frac{A_{PH}}{A_{PZ}}$, at 90° $\overline{Q}(PH) = 7.58$.

Accepting the formulation of Gutenberg and Richter, the total amplitude (for a 1 sec wave) at a distance of 111 km from the focus for zero focal depth and zero magnitude was computed.

This amplitude was assumed to exist at a horizontal distance of 111 km from foci at any focal depth. For a magnitude different from zero, the corresponding amplitudes are 10^{m} times larger.

Before the $\overline{Q}$-values can be computed, a refinement is necessary. We require in our magnitude definition that the amplitudes at the point C, at a distance, d, from the focus be equal for all focal depths (see Fig. 25). The amplitudes at a point D, after the wave has traveled (along the ray path) the distance d in a direction other than horizontal, generally will be different for the given focal depths, due to the vertical velocity heterogeneity in the neighborhood of the focus. We have computed the amplitudes at the points D for angles of incidence $0^{\circ} \leq i_h \leq 90^{\circ}$. Whereas for foci in the

Earth's mantle the amplitude diverges only up to 7% from the amplitude in the direction perpendicular to the velocity gradient, for foci in the crust a variation of up to 20% is found. For details see Duda, 1970.

Consequently, for a given magnitude the amplitudes along the ray path at a distance of 111 km from the focus were taken such as to produce equal amplitudes in the direction perpendicular to the velocity gradient at all focal depths.

With the amplitude variation curves discussed earlier (Fig. 2-22), knowing the angles of incidence at the surface for all epicentral distances, and taking into account the free surface effect at the station, it is possible to obtain the sets of $\overline{Q}(PZ)$ and $\overline{Q}(PH)$. Fig. 27a, b, c, and 28a, b, c, show the corresponding $\overline{Q}$-values for 21 focal depths as functions of epicentral distance.

The vertical arrows in the figures indicate a local shadow zone: at the corresponding epicentral distances $\overline{Q}$ is theorteically equal to infinity. We do not attribute to the local shadow zones any practical significance; we interpret them rather as the result of the finite accuracy of the travel time tables, as noted earlier. We interpret similarly the slight instability in the $\overline{Q}$-values, apparent usually at the second place to the right of the decimal point.

Fig. 29 and 30 present the $\overline{Q}$-values of Figures 27 and 28 in the form of isometric maps, with the epicentral distance and focal depth as isometric parameters.

III. S-waves.

1. Amplitude variation along the Earth's surface.

For magnitude determinations, various authors have preferred the horizontal component of the shear wave over the vertical (Gutenberg, Richter, 1956; Vaněk, Stelzner, 1960, Vaněk et al., 1962). The preference is based on the fact that in the prevailing number of cases the horizontal component of the S-waves is larger than the vertical.

Referred to as SH in magnitude studies, the horizontal component of the S-wave is not identical with the horizontally polarized component of the S-wave and referred to also as SH, especially in focal mechanism studies.

If the focus would produce only horizontally polarized S-waves, both SH would be identical; if the focus would produce only vertically polarized S-waves, the second SH would vanish, whereas, in general, the first would not. The bias

in the nomenclature is perhaps symptomatic for the practical difficulty in using S-waves for magnitude determinations.

The S-wave travel-time curve enables one to find the amplitude variation along the Earth's surface, using formula (1). The variation will apply to both the vertically and horizontally polarized component of the S-wave, at least as long as no velocity anisotropy is permitted.

The computation was performed for the S-wave travel times by Jeffreys and Bullen, 1967. The underlying velocity model is shown in Fig. 1, according to Jeffreys, 1952. The corresponding focal depths are 0, 33, 96, 160, 223, 287, 350, 413, 477, 540, 603, 667, 731, 794 km.

The amplitude variation curves show an instability. This arises from the fact that over most of the epicentral distance range the S-wave travel times are given with an accuracy of only 0.1 sec at distance intervals of 1.0 degree, compared to 0.01 sec at 0.5 degree for P-waves. Consequently the round-off error causes the slope of the S-wave travel time curve to remain constant over certain distance ranges, resulting in an apparent local shadow zone, if the necessary numerical differentiation is performed between two adjacent slopes, corresponding to epicentral distances 1° apart. In order to achieve a higher degree of stability, the distance interval was increased. Fig. 31-44, corresponding to a distance interval of 4°, show the amplitude of S-waves along the surface of the Earth as functions of epicentral distance, if referred to the amplitude at 80° epicentral distance. It is clear that differentiation over a greater distance interval results in the possible loss of some details. For the calculation of $\bar{Q}$-charts, the smallest possible epicentral distance interval was chosen, producing, however, a number of local shadow zones. (See below.)

Again, the amplitude curves of S-waves show a bulge between 15° and 20° epicentral distance, followed by a rapid decrease of the amplitude. Between 40° and 80° the amplitudes change only slowly, as previously seen for the P-waves.

In Table 2 the S-wave amplitudes at zero epicentral distance for foci at all given focal depths are given, relative to the amplitude at 80°. A comparison with Table 1 reveals that the corresponding P-wave amplitudes are generally larger, indicating that the variation range of P-wave amplitudes is greater than that for S-waves.

The amplitude variation corresponding to the $\bar{Q}$-values for SH published by various authors is shown in Fig. 45 (Gutenberg, Richter, 1956; Vaněk, Stelzner, 1960; Vaněk et al., 1962). The underlying $\bar{Q}$-values for shallow foci

were obtained from direct observations and averaging. A comparison of the amplitude variation with that based on geometrical spreading alone (e.g. Fig. 32) yields a general agreement, indicating that factors other than geometrical spreading influence the amplitudes of S-waves to a lesser degree than is observable with the present accuracy of amplitude measurements.

2. Amplitude variation along interface inside the Earth.

In order to arrive at a set of $\overline{Q}$-values for S-waves, defining a magnitude uniform for all focal depths, again the amplitudes must be known at short distances from the focus.

Fig. 46 displays the S-wave amplitudes at the level of the focus as a function of epicentral distance in the range from 0° to 14°, keeping the amplitude at the Earth's surface at 80° equal to one. Similarly as for P-waves, the amplitudes fall into several groups. The amplitudes for foci between 413 and 794 km are smaller than for foci above, and the amplitudes for foci in the crust are smallest. The least square approximation by the formula (6) is shown in Fig. 45 by circles, together with the numerical values of the constants C and D. Unfortunately, the approximation for a surface focus is crude, which makes the extrapolation to epicentral distances smaller than 1° problematic. It is, however, fairly certain that the amplitudes for a surface focus are distinctly smaller than the amplitudes in the next focal depth range. From the least square approximation it can be seen that, e.g., at a distance of 1°, the amplitude for foci in the depth range 33-350 km is almost seven times larger than for a surface focus.

Some complications are introduced by this result into the $\overline{Q}$-charts for S-waves. Namely, making the amplitudes of S-waves equal at 111 km from the focus at all depths yields an amplitude, e.g., at 80° seven times larger for a surface focus than for a focus at 33 km depth. Consequently the $\overline{Q}$(SH)-value for a surface focus will be smaller by log 7(=0.8) than that for a focus at 33 km depth. A corresponding complexity in the isometric form of the $\overline{Q}$(SH)-chart, though perfectly consistent and in agreement with the magnitude definition, is seen for zero focal depth in Fig. 49.

3. $\overline{Q}$-charts for S-waves.

When the body wave magnitude was originally defined, it was supposed that identical magnitude figures can be obtained from both P-waves and S-waves, for all earthquakes. This can be so only if the relative efficiency of P-wave and S-wave generation remains unchanged for all earthquakes. Neglecting

the fact that such a magnitude scale would be inapplicable to events other than earthquakes, the assumption seems strong, even in the light of the present accuracy in individual amplitude determinations.

Assuming a certain ratio of the efficiency in P-wave and S-wave generation, one assumes simultaneously a certain - not necessarily known - earthquake mechanism. Attempting to define a magnitude scale which does not discriminate between a P-wave magnitude and an S-wave magnitude, one presupposes a certain earthquake mechanism common to all earthquakes.

We have tried to settle the problem as follows. The magnitude charts, as published by Gutenberg and Richter (1956) for PZ and SH are considered (see Fig.47). The difference between the $\overline{Q}$-values is computed at 10° distance intervals and a number of focal depths, as seen in Table 3. Averaging in lines and columns, and converting, the ratio of amplitude/period for P-waves and S-waves, respectively, is obtained. It is seen that in average the ratio is slightly below one, and

$$\frac{A_P}{T_P} = 0.837 \cdot \frac{A_S}{T_S} \tag{8}$$

Here, T_P and T_S are the prevailing periods of P- and S-waves recorded at teleseismic distances with the amplitudes A_P and A_S, correspondingly. Putting

$$T_S = 4 \cdot T_P , \tag{9}$$

in accordance with observations, i.e., assuming the period of S-waves to be four times longer than that of P-waves, we have:

$$A_S \cong 5 \cdot A_P , \tag{10}$$

i.e., the S-wave ground amplitudes are about five times larger than the P-wave ground amplitudes, recorded at teleseismic distances.

There is a substantial scatter in the ratio for individual epicentral distances and focal depth as seen in Table 3. No systematic trend can be ascertained. It is clear that (8) is a consequence of the focal mechanism, as well as of differential absorption and scattering of P- and S-waves along the ray path.

A fairly widely accepted focal model of earthquakes is a double couple point source (type II source). According to theory the ratio of the maximum S-wave amplitude to the maximum P-wave amplitude on the focal sphere is proportional to the cube of the ratio of the corresponding wave velocities numerically equal to 5-6 (see Stauder, 1962, for the formulae).

Consequently, at the focal sphere the S-waves should have amplitudes 5-6 times larger than the P-waves, regardless of the wave period. As seen from formula (10), this is also the amplitude ratio observed on the average at teleseismic distances, which indicates, if the differential absorption is excluded, that the double couple point source mechanism is representative, on the average, of most earthquakes.

It seems, however, unwarranted to expect the ratio of the maximum S-wave and P-wave amplitudes to be the same for all seismic events. Yet the magnitude scale should be applicable to seismic events with all possible focal mechanisms. Thus, S-waves and P-waves may not be able in all individual cases to yield the same magni ude, and it seems more appropriate to refer to the correspondingly determined S-wave magnitude and P-wave magnitude, than to one and only body wave magnitude, especially if the magnitudes determined from P-waves and from S-waves show a systematic difference. This problem was discussed already by Vaněk et al (1962). Because of the general independence of S-wave and P-wave amplitudes at the focal sphere, we are left with a certain liberty in defining the S-wave magnitude.

In analogy with Gutenberg and Richter's formal definition for m in (7), we put

$$m - 6.95 = q \tag{11}$$

at a distance of 90° for a normal shallow focus, with $q = \log \frac{A}{T}$ referring to SH. The numerical value in (11) becomes obvious by inspecting Fig. 47b. In (11) m refers to the magnitude determined from S-waves.

Using the amplitude variation curves for S-waves (Fig. 31-44), taking the free surface effect into account and keeping the S-wave amplitudes at a horizontal distance of 111 km to be the same for foci at all possible depths, a set of $\overline{Q}$-values was computed and is presented in Fig. 48a, b. Fig. 49 shows the $\overline{Q}$-values on an isometric map.

IV. Examples.

Five earthquakes were used to compare the magnitude figures obtained by using Gutenberg, Richter's (1956) $\overline{Q}$-charts, and our new $\overline{Q}$-charts. Each of the earthquakes was recorded at 21-49 stations. The focal depths varied between 181 and 639 km. Seismograms from WWSS stations were used exclusively. The calculations were performed and made available to the author by Dr. Umesh Chandra.

Table 4 identifies the earthquakes, and shows the P-wave magnitude obtained with both $\overline{Q}$(PZ)-charts, together with the resulting standard deviation (SD). An inspection of the first two lines shows a decrease of the standard deviation in 4 out of 5 cases, a deterioration corresponding to the earthquake in Fiji Island.

The second two lines in Table 4 show the two sets of magnitudes and standard deviations, obtained from amplitudes, compensated for the radiation pattern at the focus. Also here the same 4 out of 5 earthquakes show a decrease of the standard deviation, after the new $\overline{Q}$(PZ)-charts were applied.

In all cases the application of the new $\overline{Q}$-charts results in magnitude figures larger than those obtained from the Gutenberg-Richter (1956) $\overline{Q}$-charts.

V. Discussion and Conclusions.

The original magnitude definition for local shocks in California was based on the amplitude variation with epicentral distance of a particular phase recorded on one kind of instrument (Richter, 1935). When the body wave magnitude for teleseisms was defined, the amplitude of P- and S-phases was found to vary erratically, whereas the amplitude/period ratio on which the definition was finally based, proved to be a more stable quantity. From the point of view of the wave propagation theory, the stability of the amplitude/period ratio is not easily understandable (since the period remains unchanged and the amplitude varies along the ray path).

We have found previously that the observed amplitude/period ratio (Fig. 24) and the calculated amplitude (e.g. Fig. 3) vary with epicentral distance in parallel. In addition, the periods of the phases used for the magnitude calculations presented in Table 4 were found not to differ from each other by more than 20%. Here the recordings were obtained on one kind of instrument (WWSS, long-period). Thus, it seems feasible that amplitudes of body phases alone can serve as base of the magnitude scale, if only recordings of one kind of instrument are used.

A systematic difference exists in the magnitude figures arrived at, using Gutenberg-Richter 1956 $\overline{Q}$-charts, and the new $\overline{Q}$-charts, although the new $\overline{Q}$-charts reduce the scatter of magnitudes determined at individual stations, as compared with those from the Gutenberg-Richter 1956 $\overline{Q}$-charts. We consider it satisfying that the new $\overline{Q}$-charts offer the possibility to arrive at magnitude figures uniform for all focal depths in accordance with the magnitude definition used here. We have calculated the expected magnitude differences for a number of epicentral distances and focal depths, by subtracting the Gutenberg-Richter 1956 $\overline{Q}$-charts from the new $\overline{Q}$-chart for PZ (Table 5) and SH (Table 6). Since we have accepted the Gutenberg-Richter formal definition of the magnitude (7), the difference is zero for an epicentral distance of 90° and a shallow focus.

A negative difference in the Tables indicates that Gutenberg-Richter $\overline{Q}$-charts will yield a larger magnitude, and a positive difference - that the use of the new $\overline{Q}$-charts will result in a larger magnitude. For PZ waves and a shallow focus, the difference is seen not to exceed 0.20 units. With the increase of focal depth the difference increases, reaching at its maximum 0.77 units for 700 km focal depth. The differences are mostly positive, suggesting that the Gutenberg-Richter chart assigns P-wave magnitudes too small to earthquakes especially at larger focal depths.

For SH-waves and a shallow focus the difference does not exceed 0.27 units. However, for a surface focus negative differences appear, due to the small amplitude at a distance of 111 km from the focus, seen in Fig. 46. For increasing focal depth, the difference becomes positive. Again, we conclude that generally the Gutenberg-Richter chart assigns S-wave magnitudes too small to earthquakes with larger focal depth.

As already mentioned, the Gutenberg-Richter charts are based mainly on direct amplitude observations, which should include virtually the effects of both velocity heterogeneity and anelasticity upon the amplitudes, whereas the new $\overline{Q}$-charts are obtained assuming that velocity heterogeneity is the principal factor affecting the amplitudes. If the systematic difference in the magnitude figures were due to the anelasticity effect, the Gutenberg-Richter $\overline{Q}$-charts should over-compensate the observed amplitudes, and result in magnitude figures generally <u>larger</u> than those based on the new $\overline{Q}$-charts. Since the <u>opposite</u> is true, the anelasticity effect cannot account for the observed difference. We interpret the difference between the magnitudes obtained by using the Gutenberg-Richter (1956) $\overline{Q}$-charts and the new $\overline{Q}$-charts seen in Tables 5 and 6 as due to the different velocity-depth profiles used in the construction of

the $\bar{Q}$-charts. Tables 5 and 6 indicate that earthquake catalogues assign magnitudes which are consequently too small to earthquakes at greater depths.

The result of Tables 5 and 6 is of tectonophysical significance, if related to the strain energy release as a function of focal depth. It has been found (Båth, Duda, 1963) that the maximum possible magnitude decreases with focal depth. However, in view of Tables 5 and 6 deep focus earthquakes may reach magnitudes at least equal to the magnitudes of shallow focus earthquakes. Though there are fewer deep than shallow focus earthquakes, the proportional energy release in deep focus earthquakes is thus apparently larger than hitherto believed.

Acknowledgments

My sincerest thanks are due to Fr. William Stauder, S.J., for discussions on the problem, and to Dr. Carl Kisslinger and Fr. William Stauder, S.J., for reading the manuscript.

Dr. Umesh Chandra kindly made available to me some of his results prior to publication.

This research was supported by the Advanced Research Projects Agency and was monitored by the Air Force Cambridge Research Laboratories under Contract AF 19(628)-5100, as part of the Project VELA UNIFORM.

References

Båt ., M., 1956, The problem of earthquake magnitude determination, Publ. bureau central seismologique international (A), vol. 19, pp. 5-93.

Båth, M., S. J. Duda, 1963, Strain release in relation to focal depth, Geofisica Pura e Applicata, vol. 56, pp. 93-100.

Bullen, K. E., 1953, An introduction to the theory of seismology, Cambridge at the University Press, 296 pp.

Chandra, U., 1969, Personal communication.

Duda, S. J., 1970, The amplitudes of elastic waves in heterogeneous media, in preparation.

Gutenberg, B., 1945, Magnitude determination for deep-focus earthquakes, Bull. Seism. Soc. Am., vol. 35, pp. 117-130.

Gutenberg, B., 1959, Physics of the Earth's interior, Academic Press, 240 pp.

Gutenberg, B., G. F. Richter, 1956, Magnitude and energy of earthquakes, Ann. geofisica, vol. 9, pp. 1-15.

Herrin, E., E. P. Arnold, B. A. Bolt, G. E. Clawson, E. R. Engdahl, H. W. Freedman, D. W. Gordon, A. L. Hales, J. L. Lobdell, O. Nuttli, G. Romney, J. Taggart, W. Tucker, 1968, 1968 Seismological tables for P-phases, Bull. Seism. Soc. Am., vol. 58, pp. 1196-1219.

Jarosch, H., 1969, Body wave magnitude and source mechanism, Trans. A.G.U., vol. 50, No. 4, p. 237 (abstract).

Jeffreys, H., 1952, The Earth, its origin, history and physical constitution, Cambridge at the University Press, 392 pp.

Jeffreys, H., K. E. Bullen, 1967, Seismological tables, London, Office of the British Association, pp. 16-21.

Richter, G. F., 1935, An instrumental earthquake scale, Bull. Seism. Soc. Am., vol. 25, pp. 1-32.

Stauder, W., S. J., 1962, The focal mechanism of earthquakes, in Advances in Geophysics, vol. 9, Academic Press, pp. 1-76.

Vaněk, J., J. Stelzner, 1960, The problem of magnitude calibrating functions for body waves, Ann. geofisica, vol. 13, pp. 393-407.

Vaněk, J., A. Zatopek, V. Karnik, N. V. Kondorskaya, Yu. V. Riznichenko, E. F. Savarensky, S. L. Solov'ev, N. V. Shebalin, 1962, Standardization of magnitude scales, Izv. Acad. Nauk SSSR, Geophys. Ser., English translation, pp. 108-111.

Table 1

1. Focal depth, km

2. Total amplitude of P-wave at the surface of the Earth for $\Delta = 0^{\circ}$, if the amplitude is 1.0 at $\Delta = 80^{\circ}$

1	2	1	2	1	2
0 km	∞	150 km	109	500 km	29
15	610	200	85	550	25
40	380	250	62	600	23
50	320	300	52	650	21
75	212	350	43	700	18
100	162	400	38	750	17
125	131	450	33	800	15

Table 2

1. Focal depth, km.

2. Amplitude of SH-wave at the surface of the Earth for $\Delta = 0^{\circ}$, if the amplitude is 1.0 at $\Delta = 80^{\circ}$.

1	2	1	2
0 km	∞	413 km	33
33	140	477	28
96	98	540	23
160	74	603	20
223	58	667	18
287	48	731	16
350	39	794	14

Table 3

Epicentral distance	10	20	30	40	50	60	70	80	90	100	
Focal depth											$\frac{A_P}{T_P} / \frac{A_S}{T_S}$
700 km	0.50	0.56	0.80	0.28	0.05	-0.20	0.00	0.06	-0.18	0.20	0.621
600	0.32	0.55	0.43	0.23	-0.11	-0.48	0.28	-0.30	-0.04	0.45	0.736
500	0.94	0.90	0.40	0.02	-0.39	-0.17	0.00	-0.23	-0.05	0.52	0.648
400	0.96	0.19	0.02	-0.12	-0.65	-0.02	0.13	0.22	0.11	0.42	0.748
300	0.47	0.34	0.16	-0.23	-0.56	0.00	-0.05	0.18	0.14	0.48	0.807
200	0.15	0.13	0.48	-0.09	-0.38	0.06	-0.04	-0.17	-0.20	0.23	0.961
100	-0.31?	-0.31	0.16	0.06	0.05	0.26	-0.05	-0.40	0.13	0.31	1.02
50	-0.10?	0.09	0.29	-0.04	0.10	0.29	-0.06	-0.15	0.10	-0.08	0.903
0	0.00	0.30	0.34	-0.20	0.07	0.29	-0.01	0.05	0.15	-0.10	0.814
$\frac{A_P}{T_P} / \frac{A_S}{T_S}$	0.472	0.472	0.455	1.02	1.59	0.993	0.951	1.23	0.961	0.537	0.837

Table 4

	October 25, 1965 22:34:24.4 Hokkaido, Japan 181 km 49 stations		November 3, 1965 01:39:03.1 Peru-Brazil 593 km 34 stations		March 17, 1966 15:50:33.1 Fiji Island 639 km 21 stations		February 15, 1967 16:11:11.8 Western Brazil 597 km 23 stations		March 24, 1967 09:00:19.5 Java Sea 600 km 21 stations	
	m	SD	m	SD	m	SD	m	SD	m	SD
with GR $\overline{Q}$(PZ):	6.35	0.27	6.16	0.22	6.25	0.29	6.32	0.27	6.17	0.26
with new $\overline{Q}$(PZ):	6.73	0.26	6.60	0.20	6.71	0.37	6.78	0.23	6.52	0.25
corrected for focal mechanism:										
	m	SD	m	SD	m	SD	m	SD	m	SD
with GR $\overline{Q}$(PZ):	6.29	0.16	6.24	0.27	6.23	0.27	6.31	0.19	6.22	0.30
with new $\overline{Q}$(PZ):	6.67	0.15	6.69	0.15	6.69	0.32	6.78	0.16	6.58	0.24

Table 5

Epicentral distance	20	30	40	50	60	70	80	90	100
Focal depth									
700 km	0.50	0.13	0.31	0.55	0.77	0.63	0.61	0.65	0.15 ?
600	0.05	0.13	0.28	0.42	0.73	0.52	0.69	0.44	0.06 ?
500	-0.10	0.29	0.32	0.53	0.59	0.48	0.69	0.48	0.06 ?
400	0.14	0.58	0.55	0.73	0.59	0.50	0.45	0.58	0.15 ?
300	0.15	0.52	0.70	0.69	0.69	0.45	0.46	0.57	0.20 ?
200	-0.09	0.33	0.47	0.59	0.36	0.40	0.47	0.52	0.15 ?
100	-0.01	0.29	0.14	0.05	-0.04	0.23	0.29	0.17	-0.10
50	-0.09	0.20	0.12	-0.06	-0.11	0.08	0.13	-0.02	-0.05
0	0.02	0.10	0.20	0.03	-0.12	-0.17	0.02	0.00	-0.10

Table 6

Epicentral distance	20	30	40	50	60	70	80	90	100
Focal depth									
700 km	0.71	0.94	0.62	0.62	0.59	0.64	0.68	0.29	0.33 ?
600	0.42	0.54	0.50	0.30	0.25	0.23	0.37	0.18	0.25
500	0.74	0.61	0.37	0.15	0.42	0.49	0.41	0.25	0.30
400	0.33	0.52	0.47	0.12	0.62	0.67	0.70	0.53	0.32
300	0.54	0.61	0.57	0.19	0.73	0.53	0.73	0.65	0.53
200	0.34	0.82	0.49	0.37	0.59	0.54	0.48	0.31	0.26
100	0.89	0.41	0.26	0.22	0.36	0.33	0.08	0.36	0.14
50	0.23	0.51	0.13	0.10	0.27	0.13	0.08	0.05	-0.18
0	-0.35	-0.44	-0.67	-0.53	-0.45	-0.79	-0.57	-0.58	-1.11

Figure Captions

Fig. 1	P-wave and S-wave velocities in the crust and upper mantle.
Fig. 2-22	Amplitudes of P-waves along the Earth's surface, relative to that at 80° epicentral distance.
Fig. 23	Amplitudes of P-waves at short epicentral distances, according to Gutenberg.
Fig. 24	Total P-wave amplitude variation (versus period), as computed from $\overline{Q}$-charts published by various authors for PZ and PH.
Fig. 25	Schematic representation of focus, ray path and station.
Fig. 26	Amplitudes of P-waves along interface at de. h of the focus.
Fig. 27a,b,c	$\overline{Q}$(PZ)-charts.
Fig. 28a,b,c	$\overline{Q}$(PH)-charts.
Fig. 29	Isometric $\overline{Q}$(PZ)-charts.
Fig. 30	Isometric $\overline{Q}$(PH)-charts.
Fig. 31-44	Amplitudes of S-waves along the Earth's surface relative to that at 80° epicentral distance.
Fig. 45	S-wave amplitude variation, as computed from $\overline{Q}$-charts published by various authors for SH.
Fig. 46	Amplitudes of S-waves along interface at depth of the focus.
Fig. 47	Q-charts for PZ, PH and SH from Gutenberg-Richter, 1956.
Fig. 48a,b	$\overline{Q}$(SH)-charts
Fig. 49	Isometric $\overline{Q}$(SH)-charts.

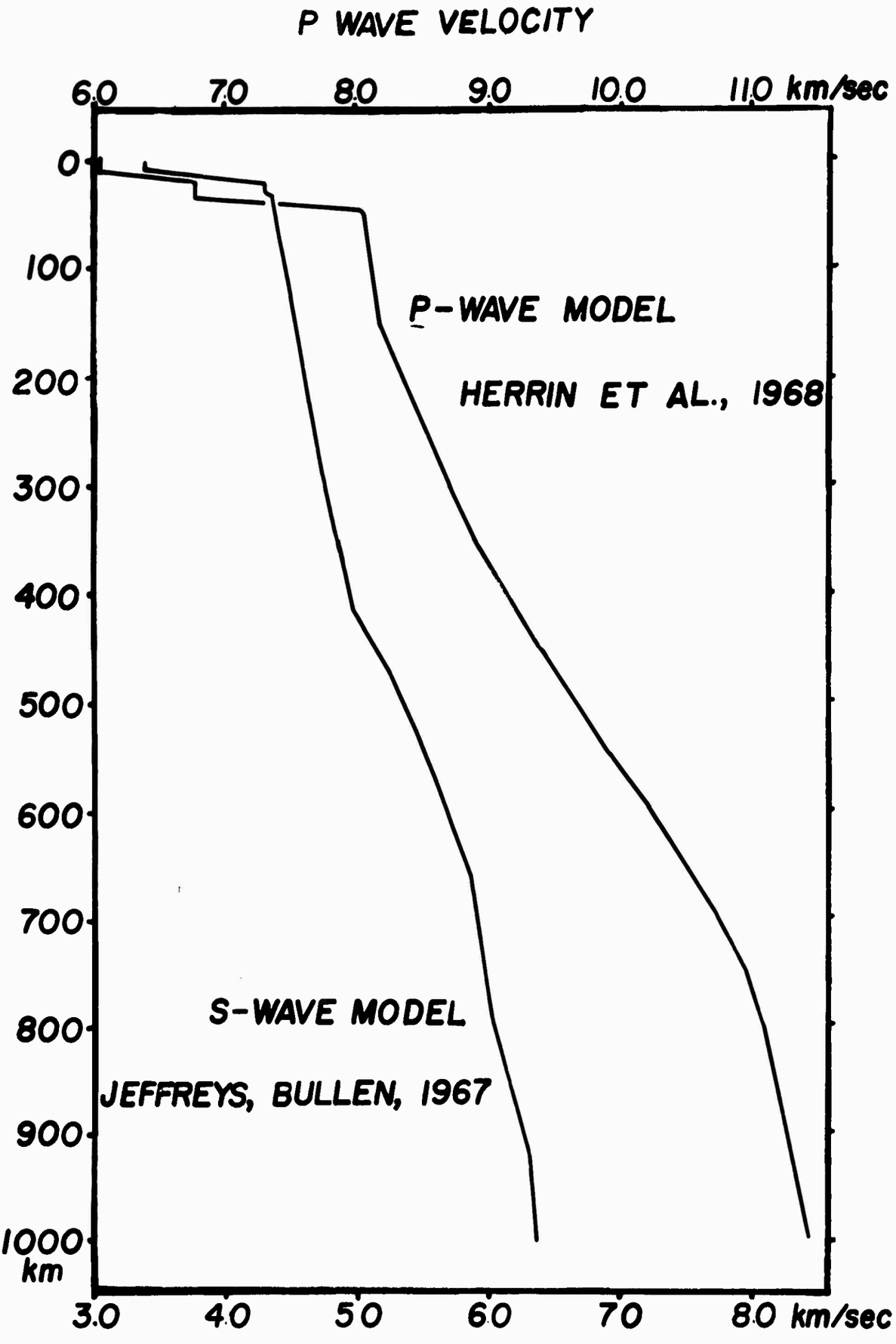
P WAVE VELOCITY
6.0
7.0
8.0
9.0
10.0
11.0 km/sec
0
100
200
300
400
500
600
700
800
900
1000
km
P-WAVE MODEL
HERRIN ET AL., 1968
S-WAVE MODEL
JEFFREYS, BULLEN, 1967
3.0
4.0
5.0
6.0
7.0
8.0 km/sec
S WAVE VELOCITY

FIG. 1

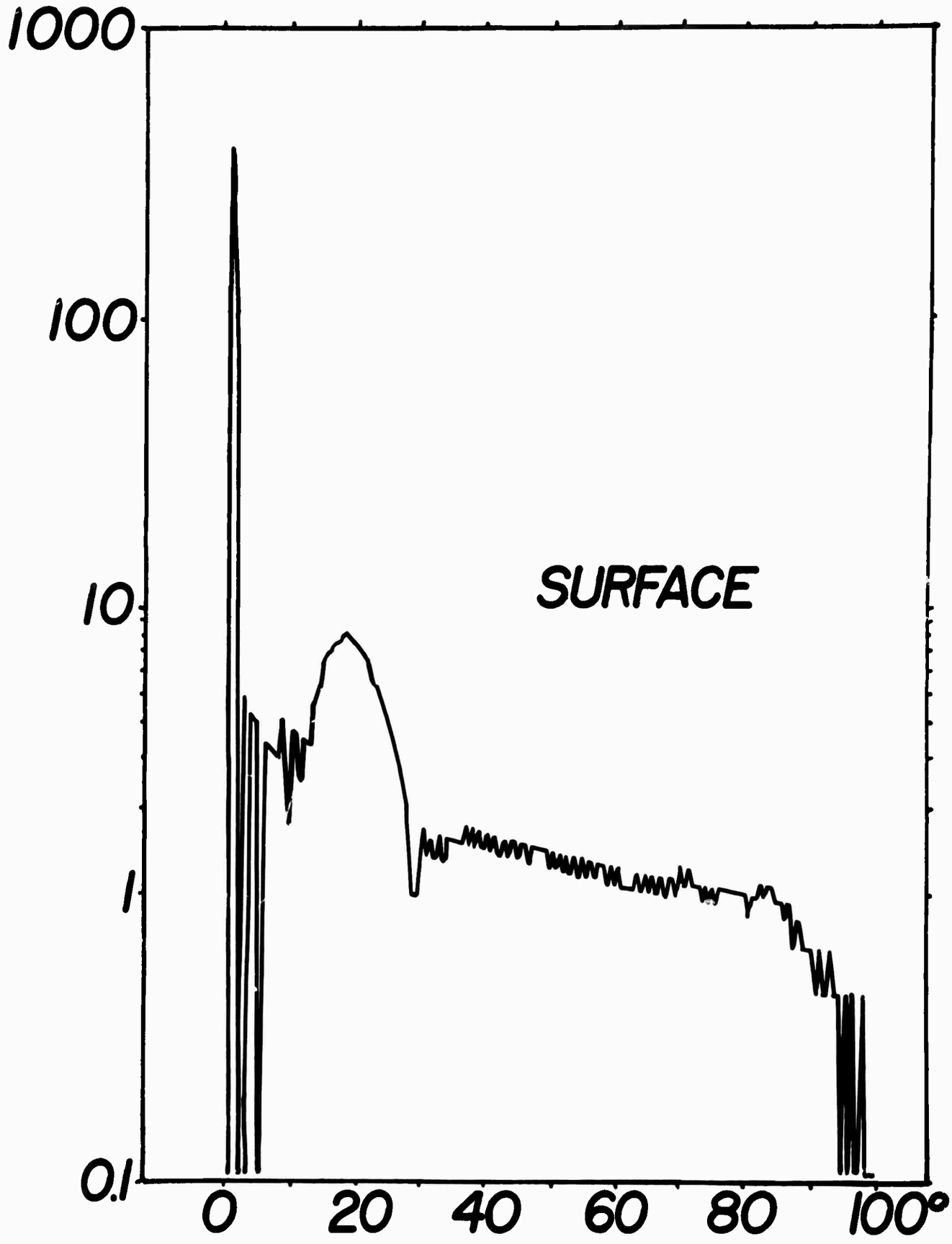

FIG. 2

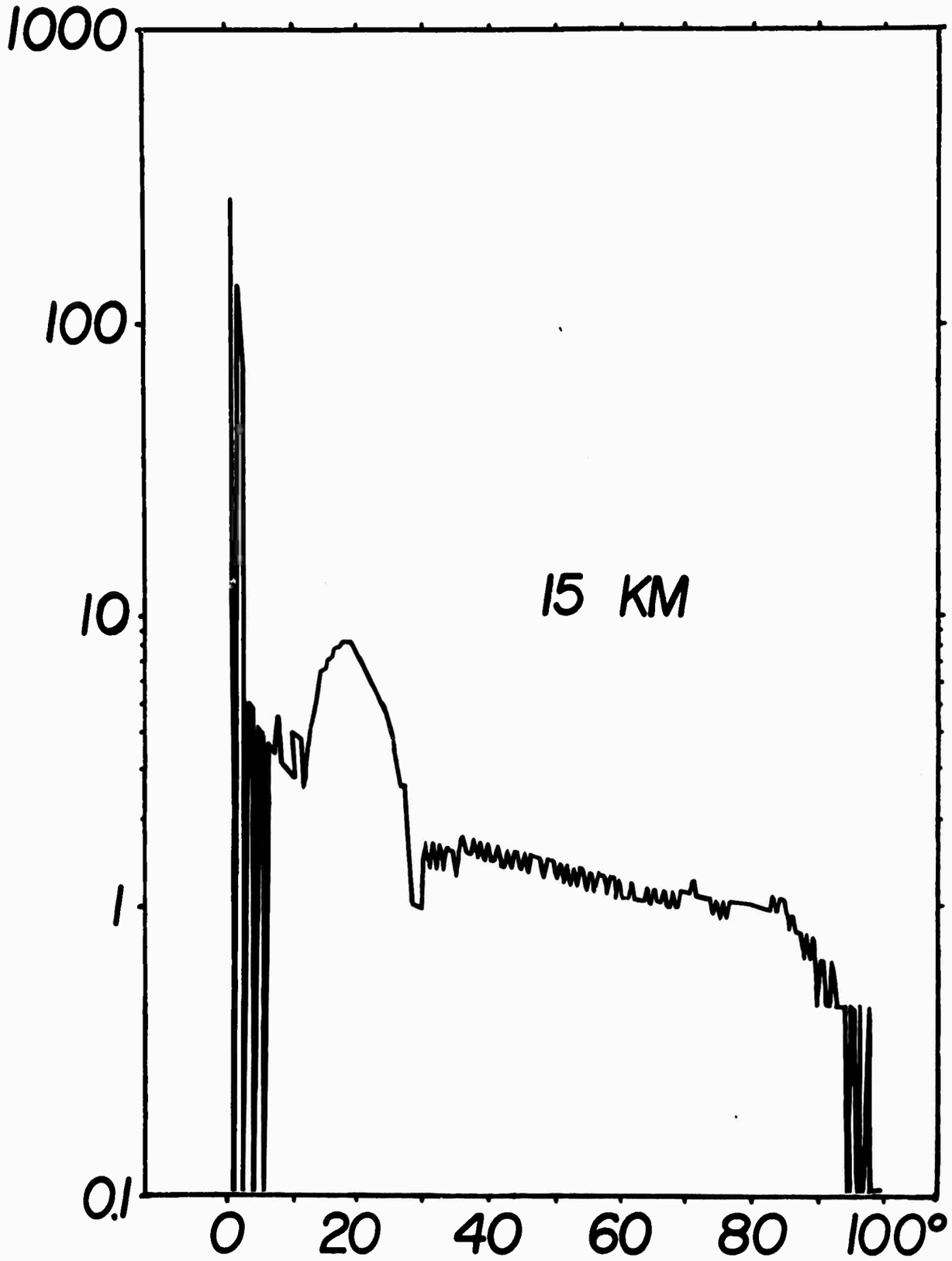

FIG. 3

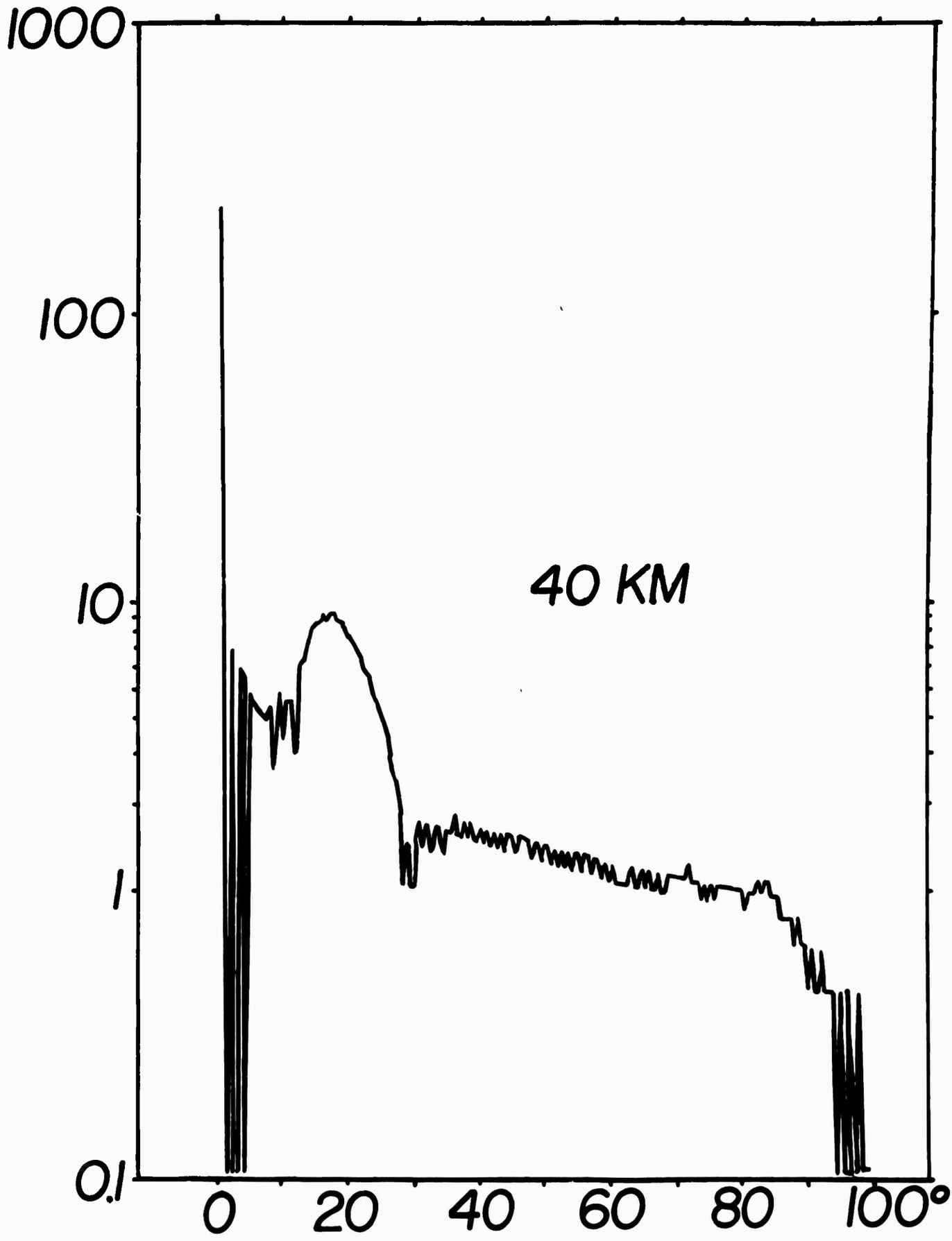

FIG. 4

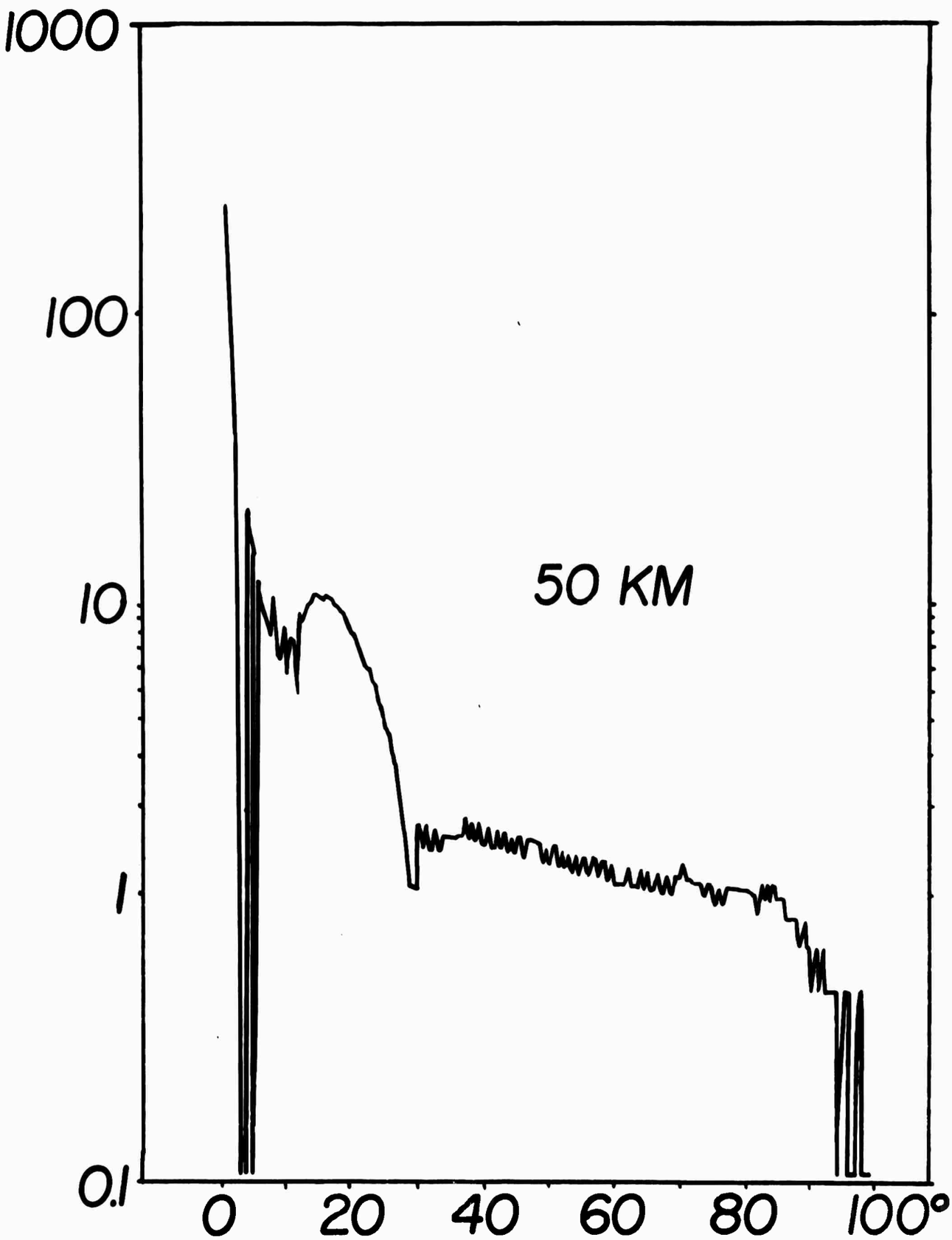

FIG. 5

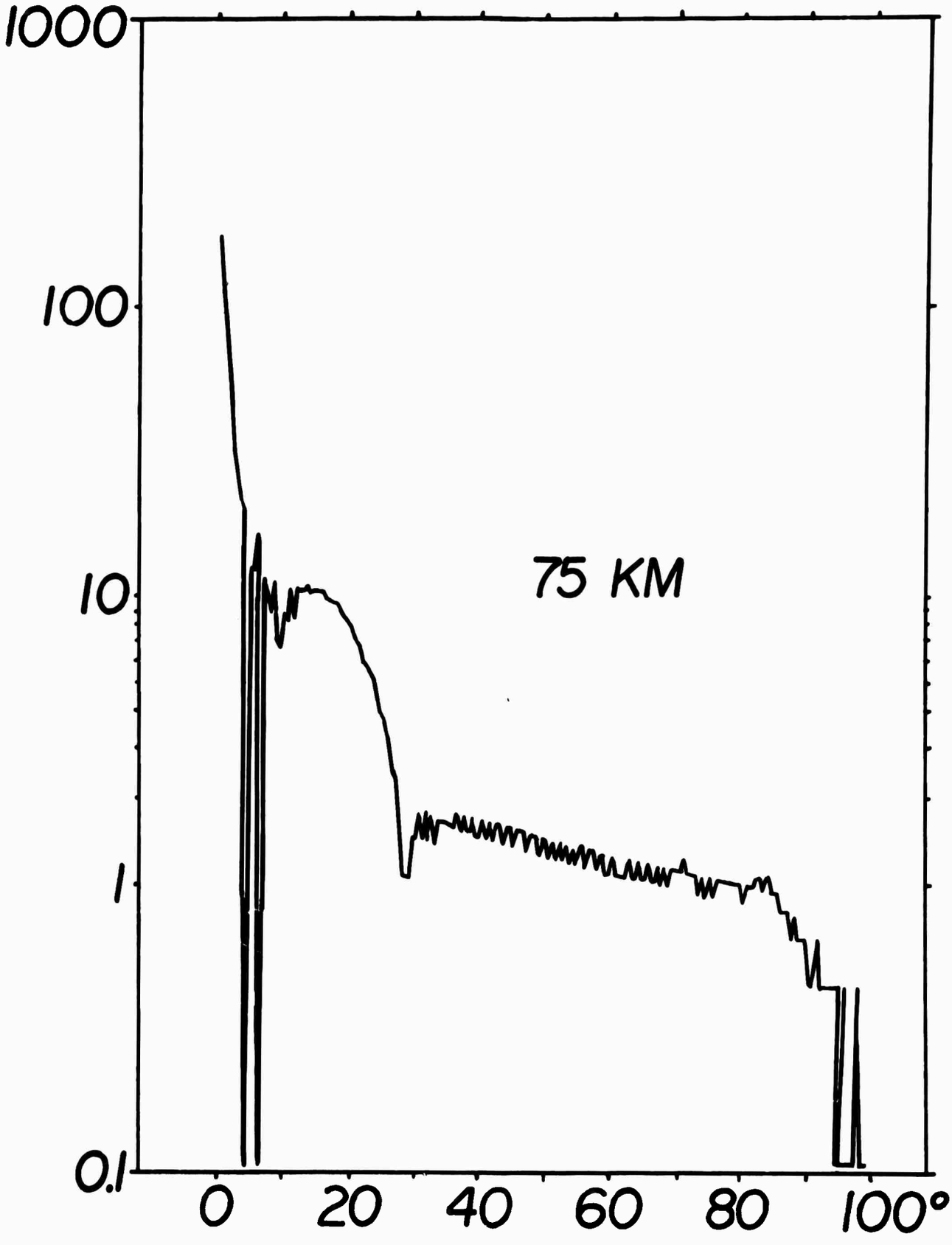

FIG. 6

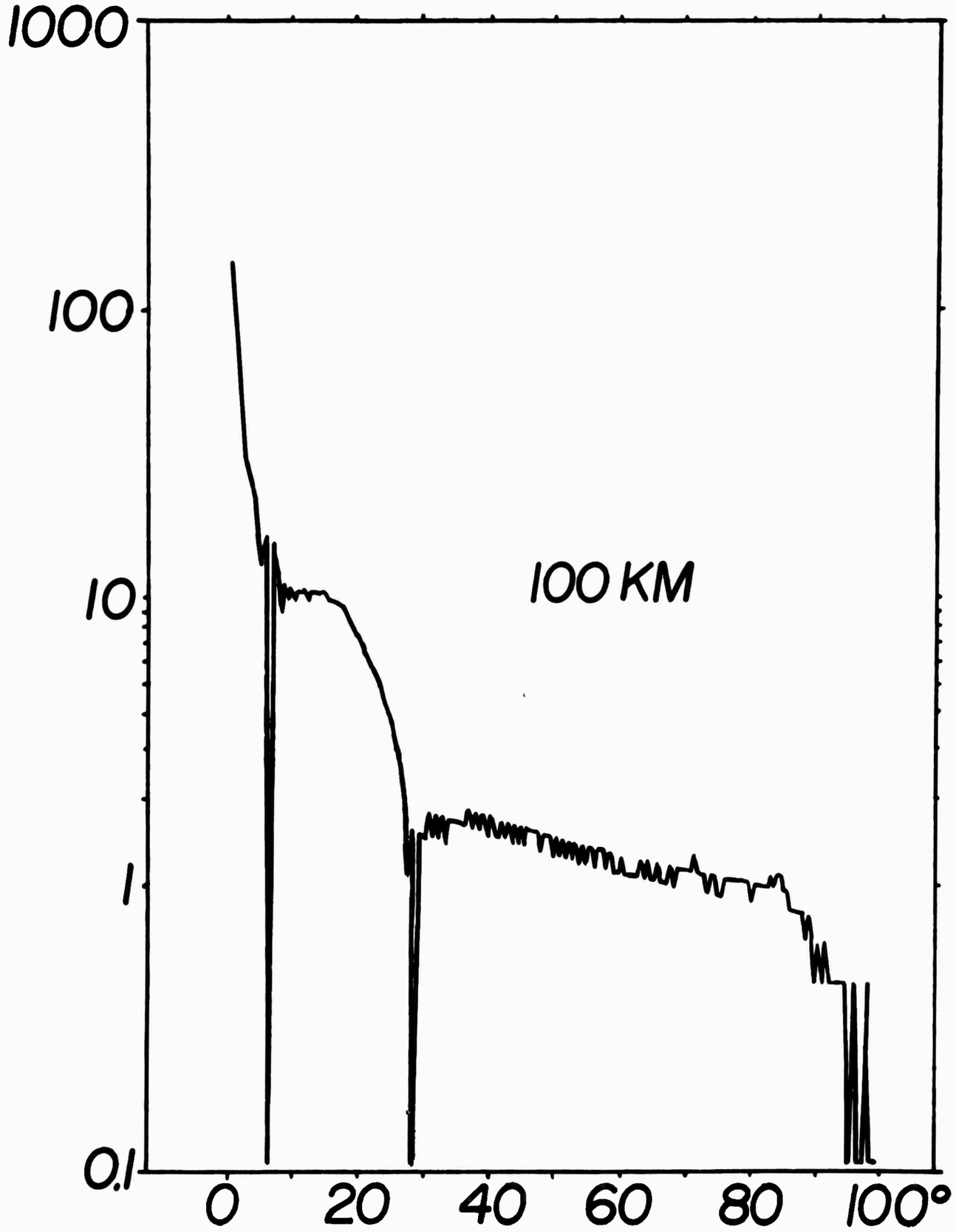

FIG. 7

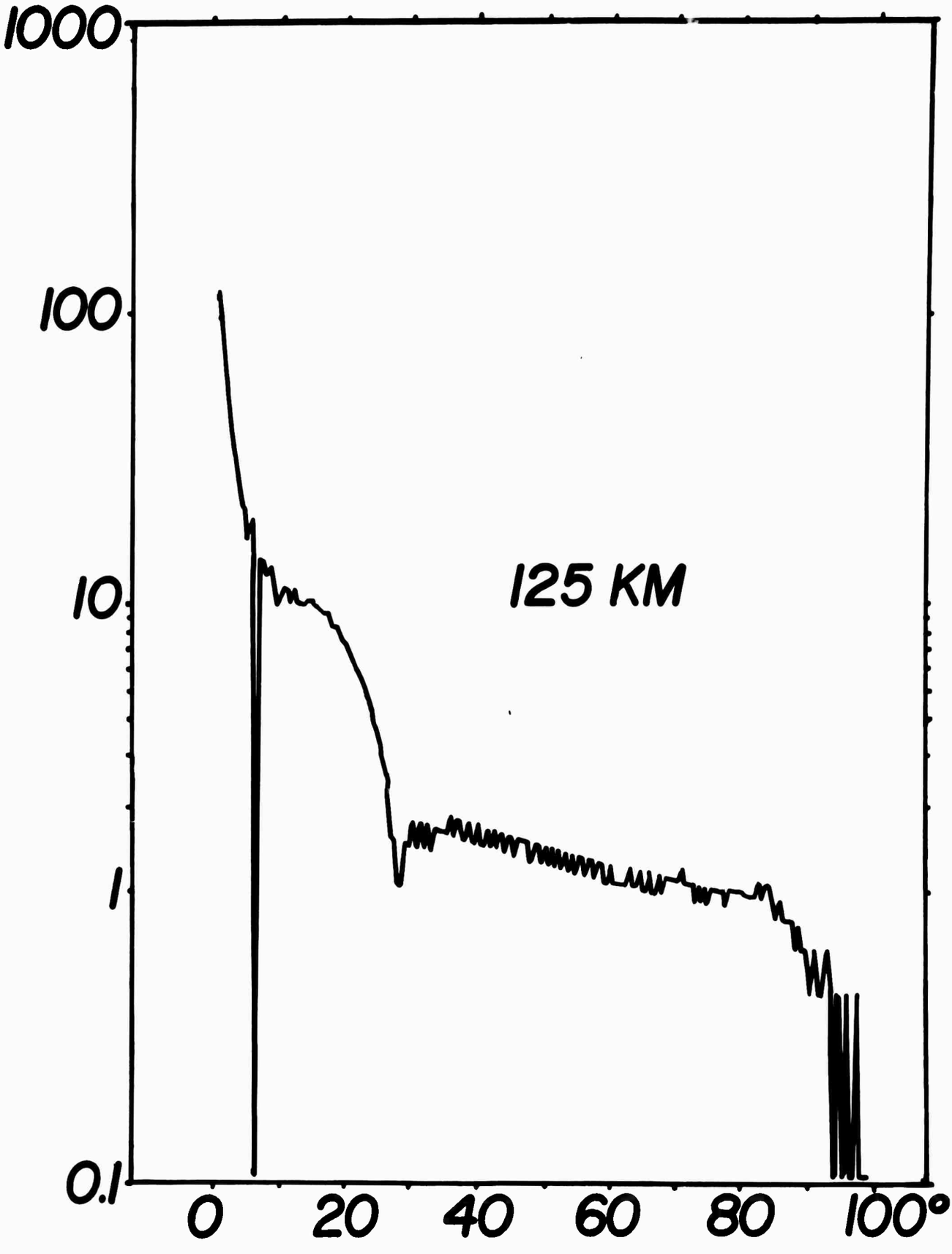

FIG. 8

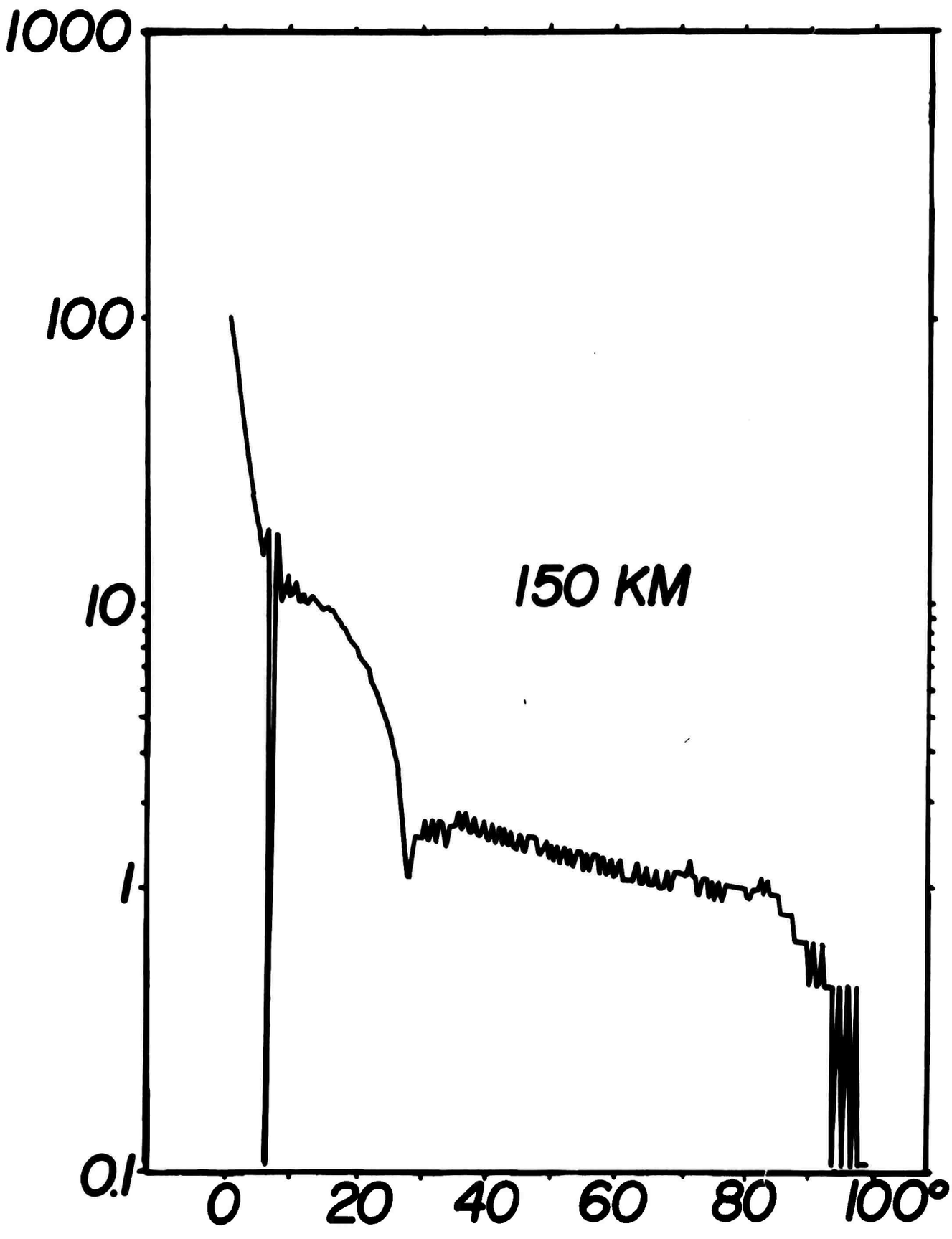

FIG. 9

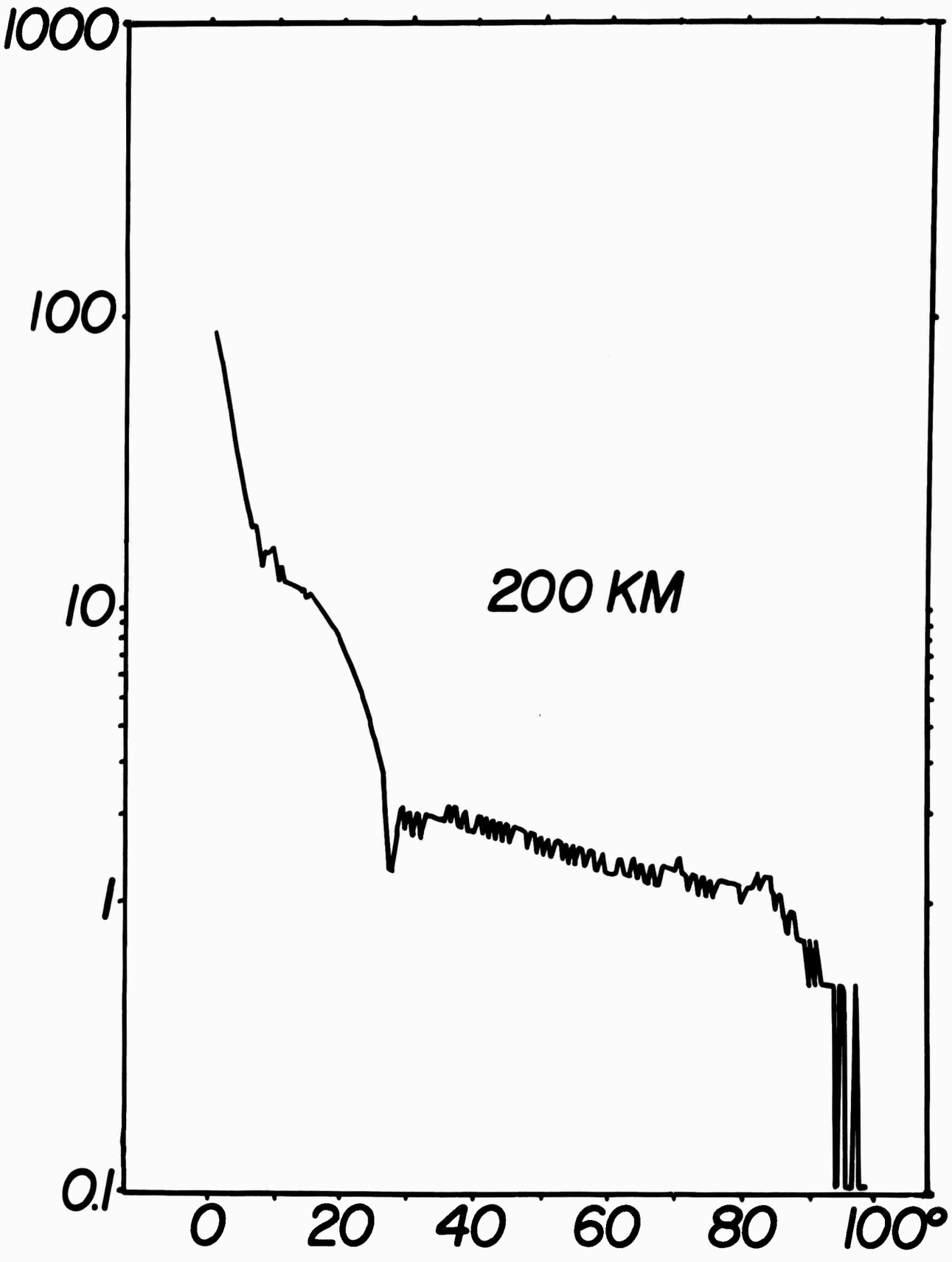

FIG. 10

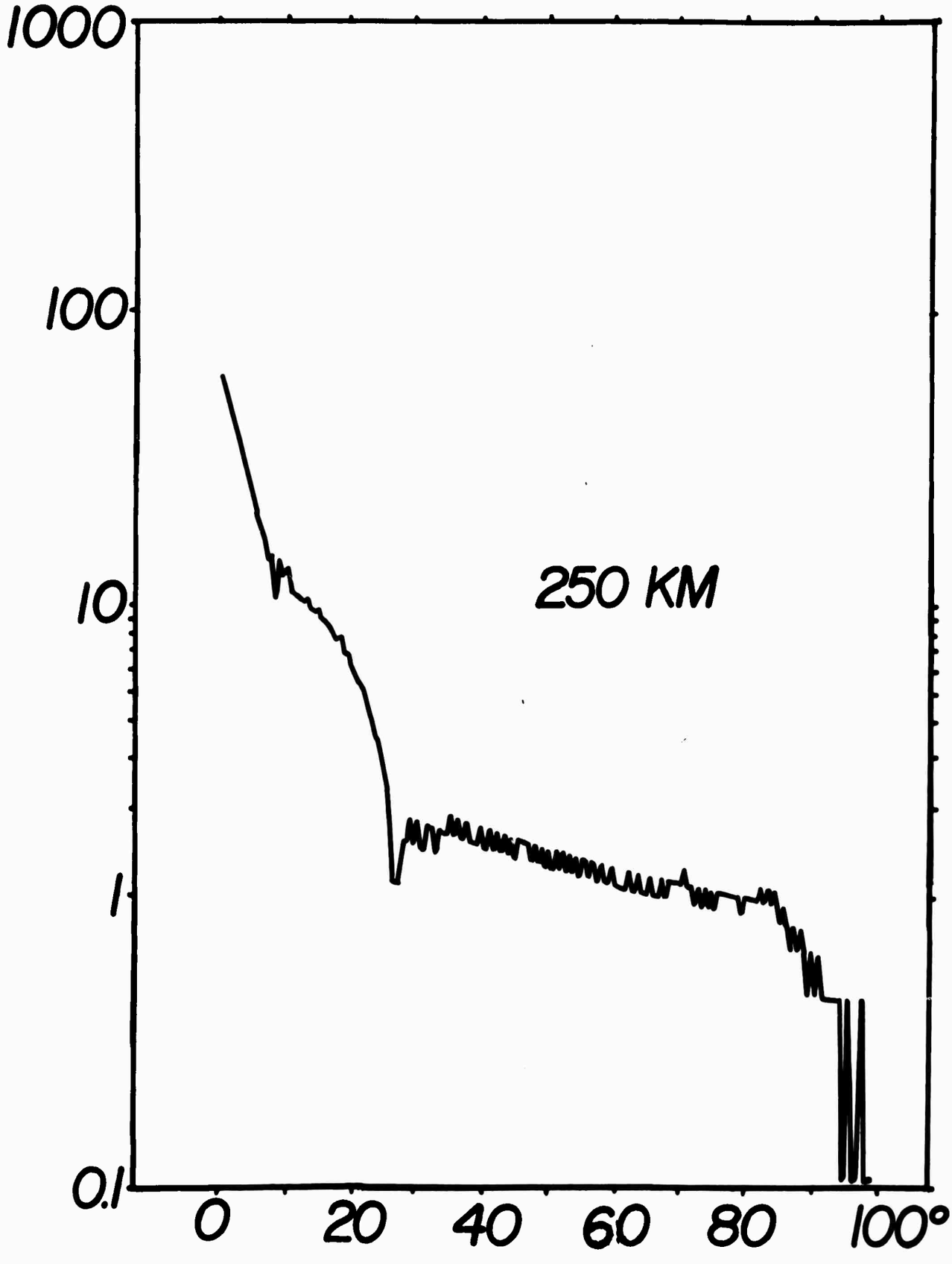

FIG. 11

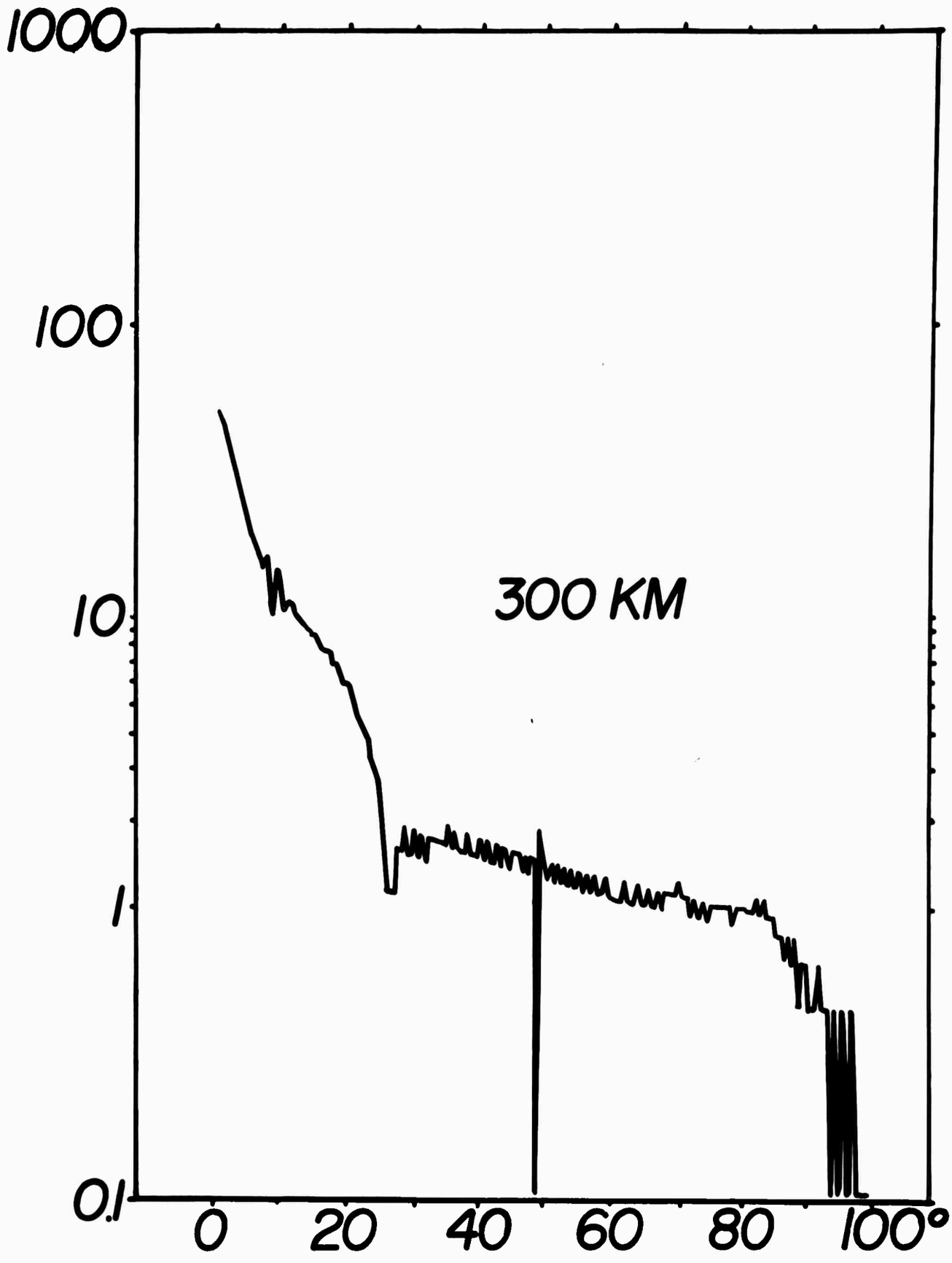

FIG. 12

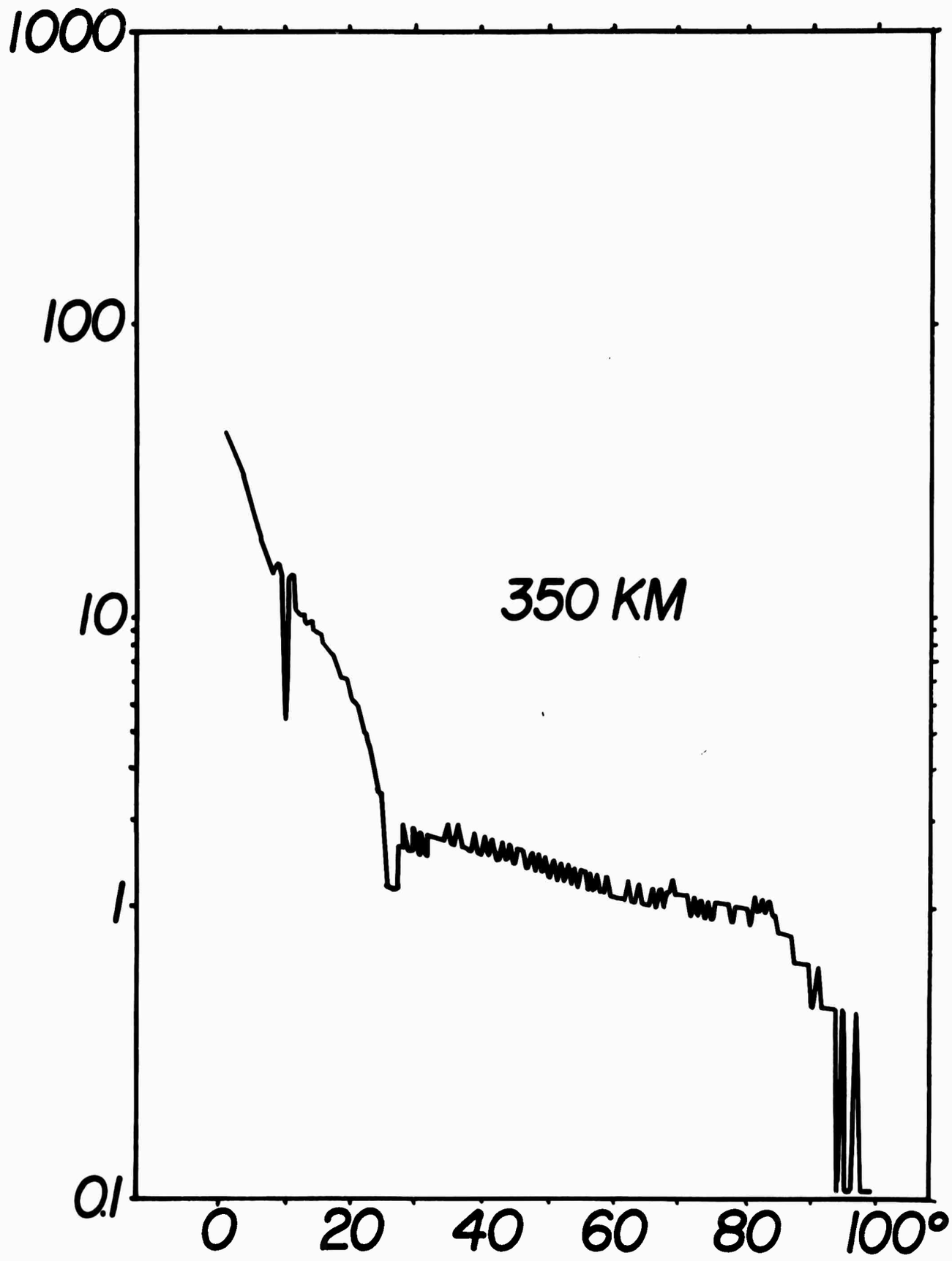

FIG. 13

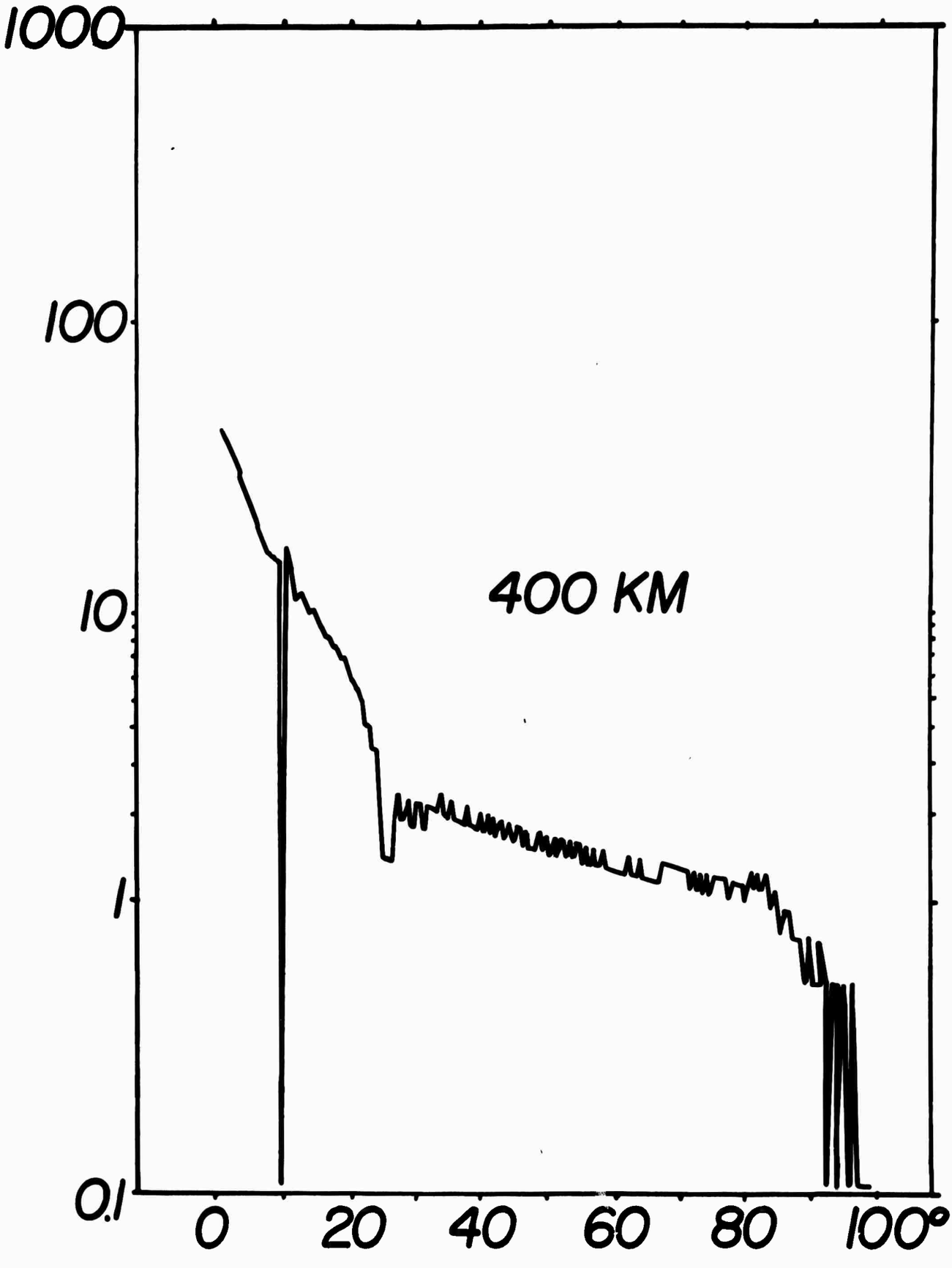

FIG. 14

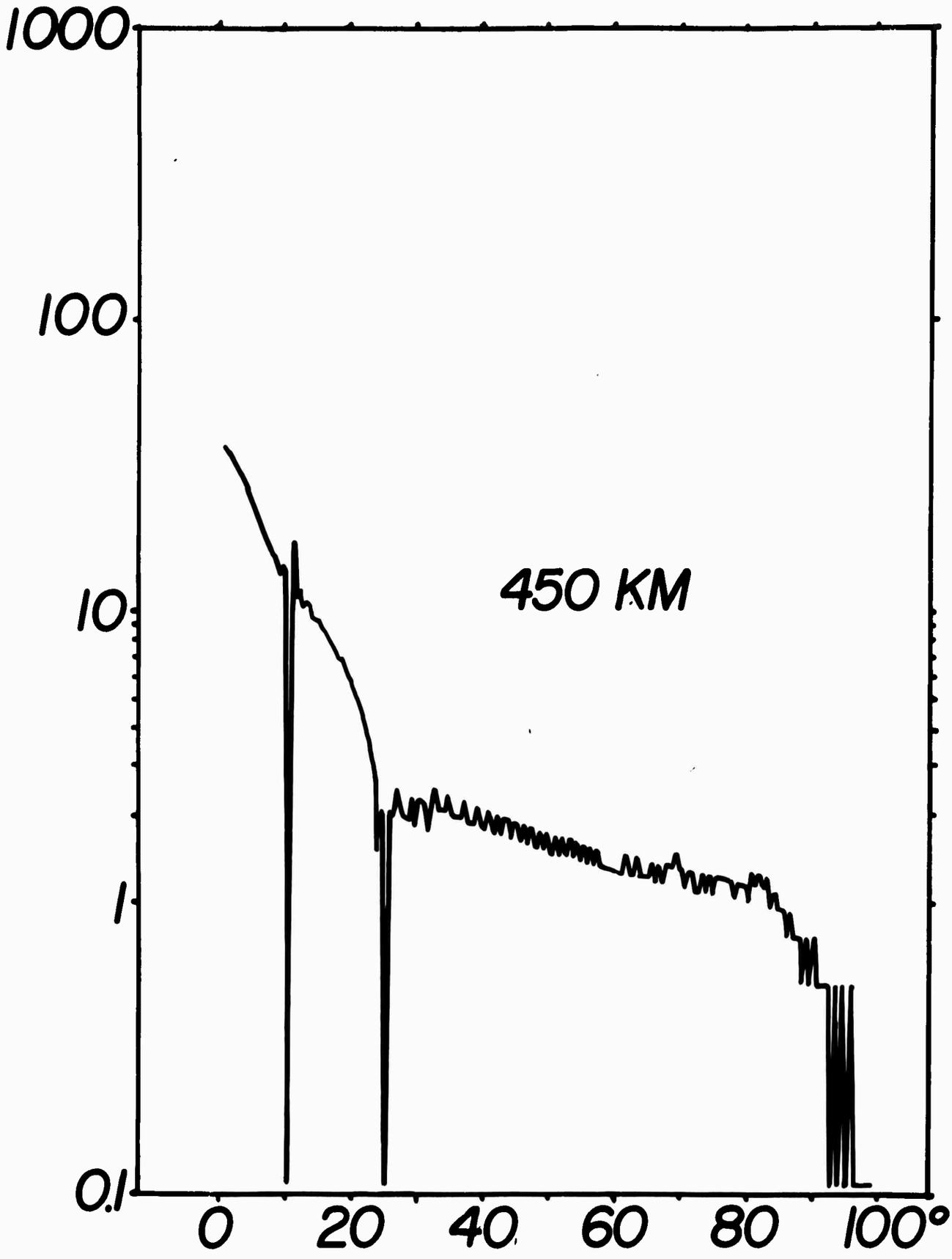

FIG. 15

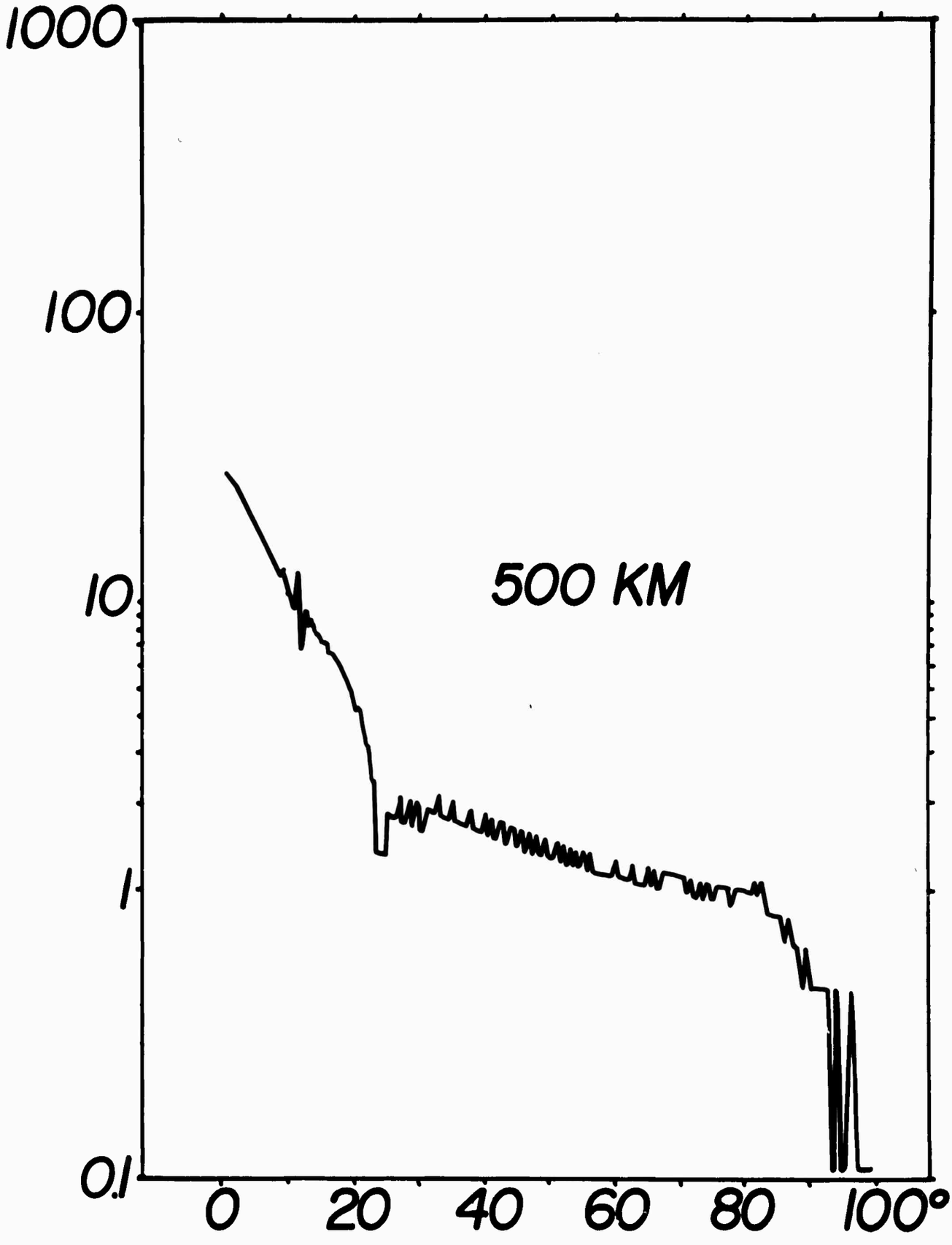

FIG. 16

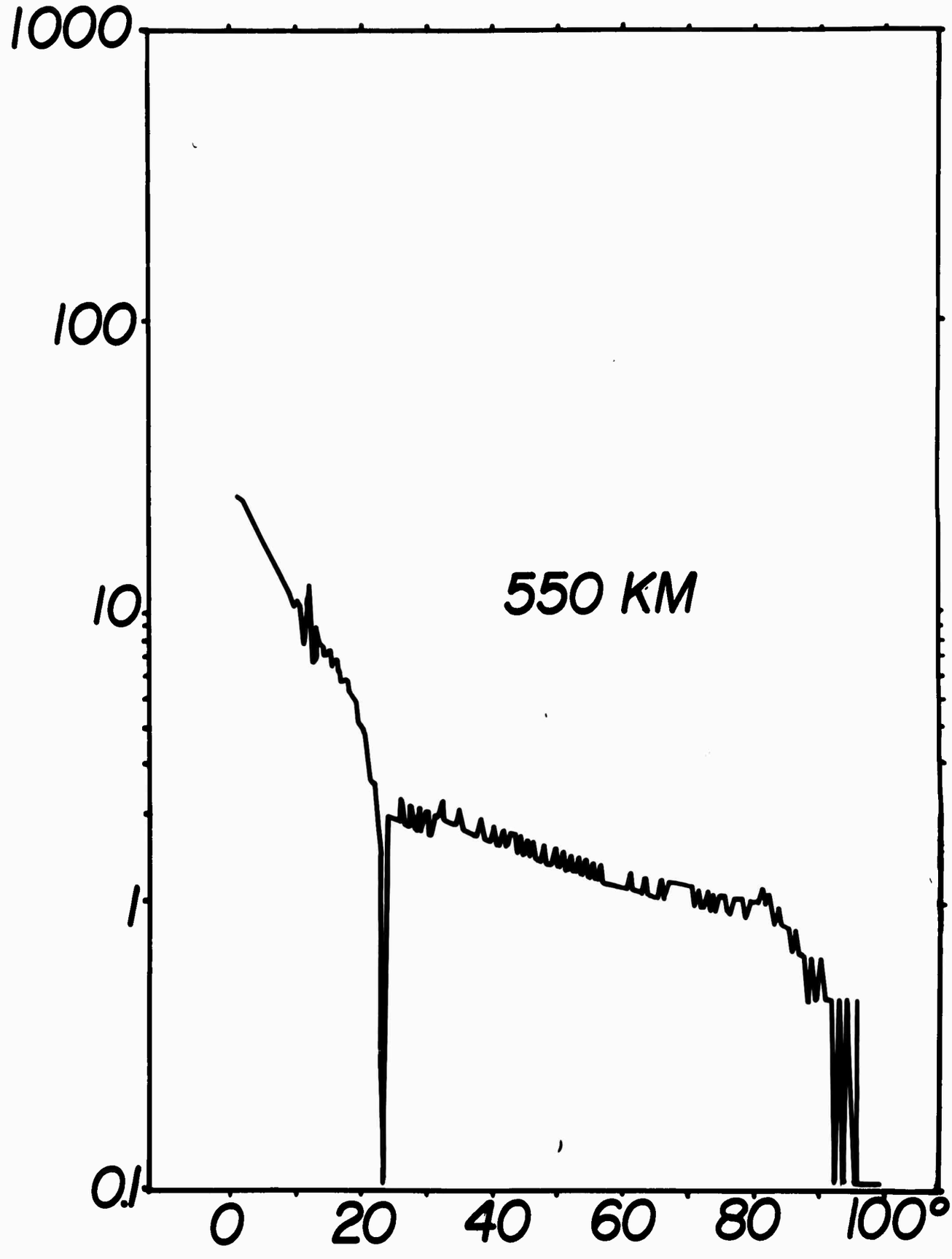

FIG. 17

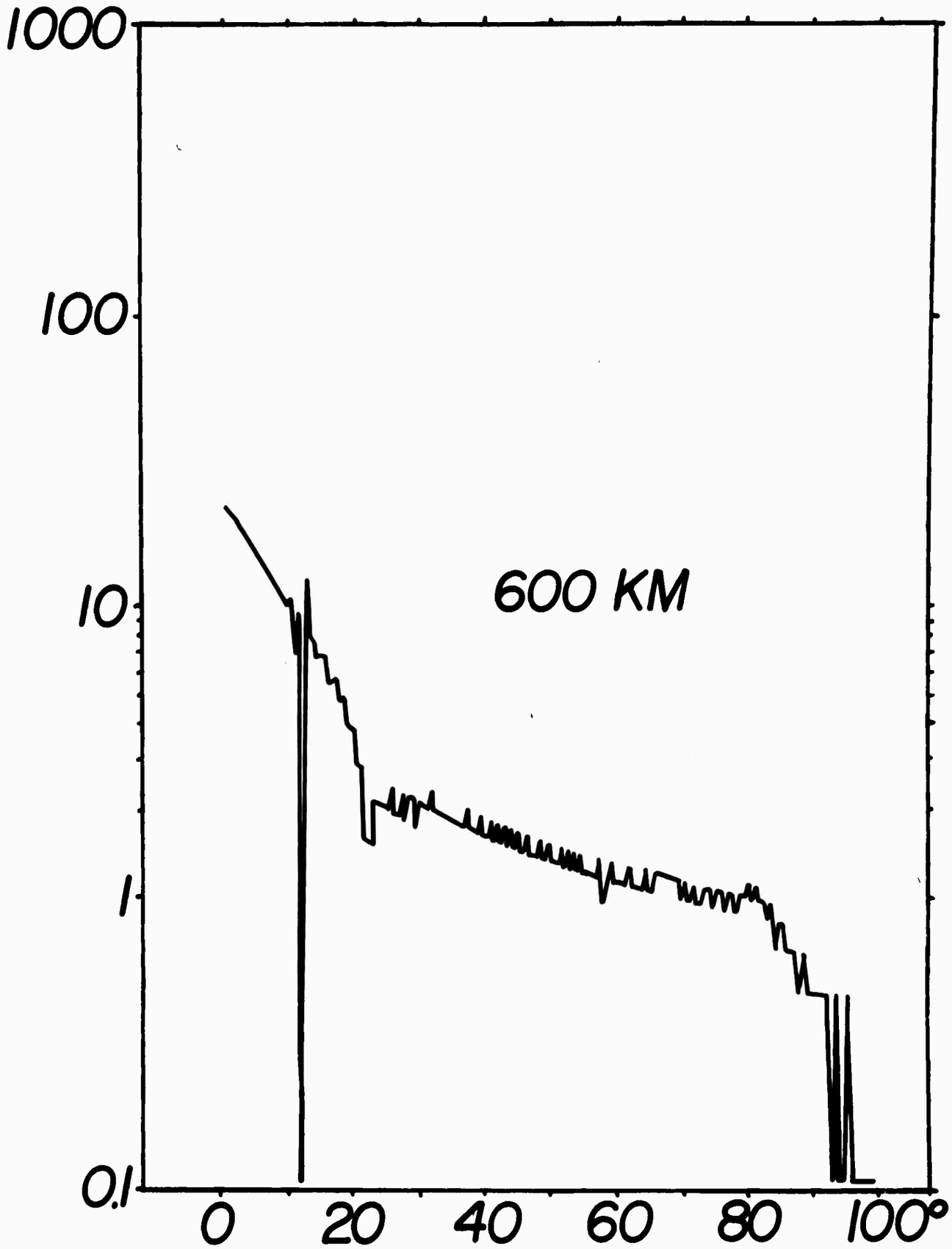

FIG. 18

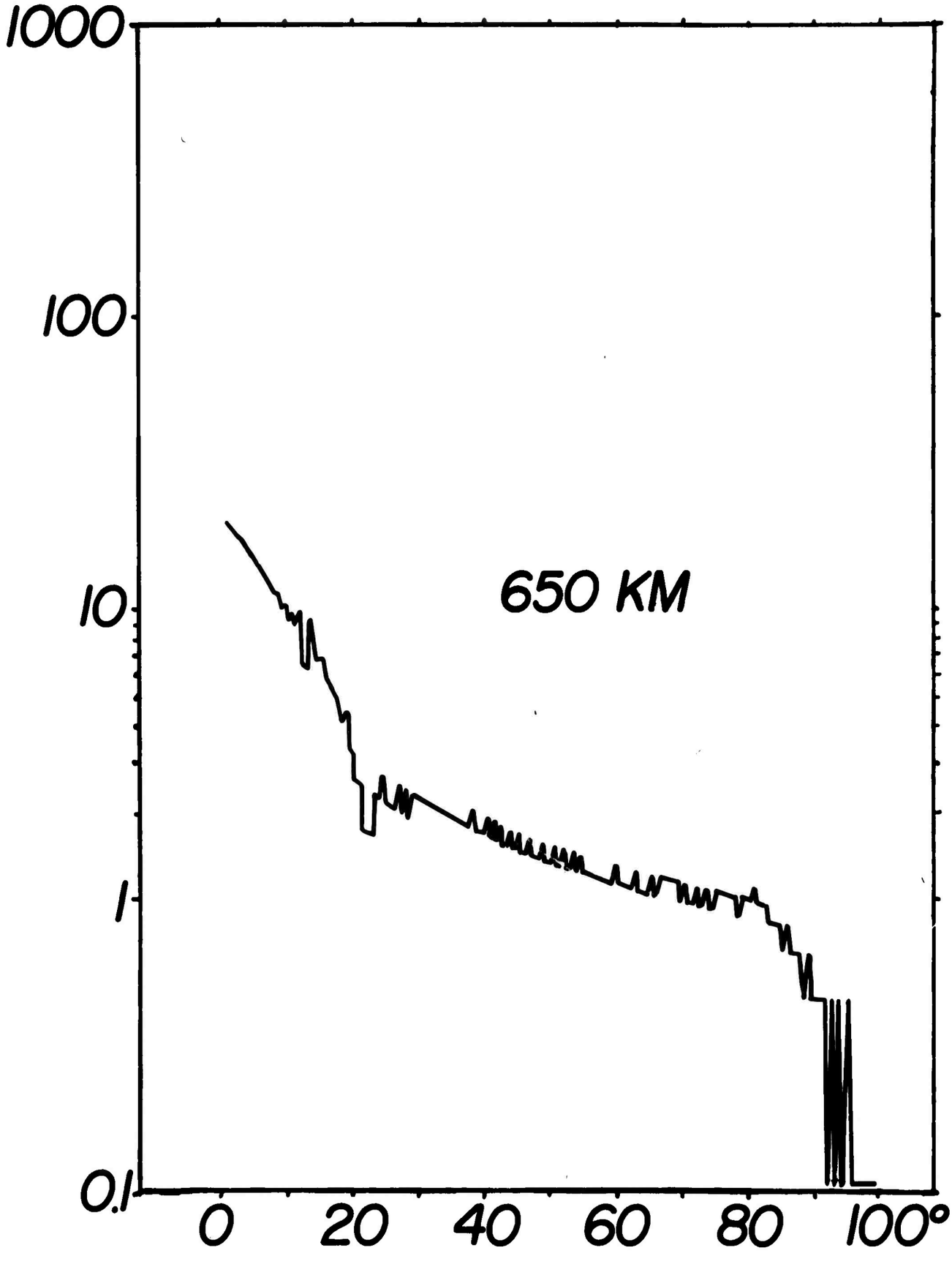

FIG. 19

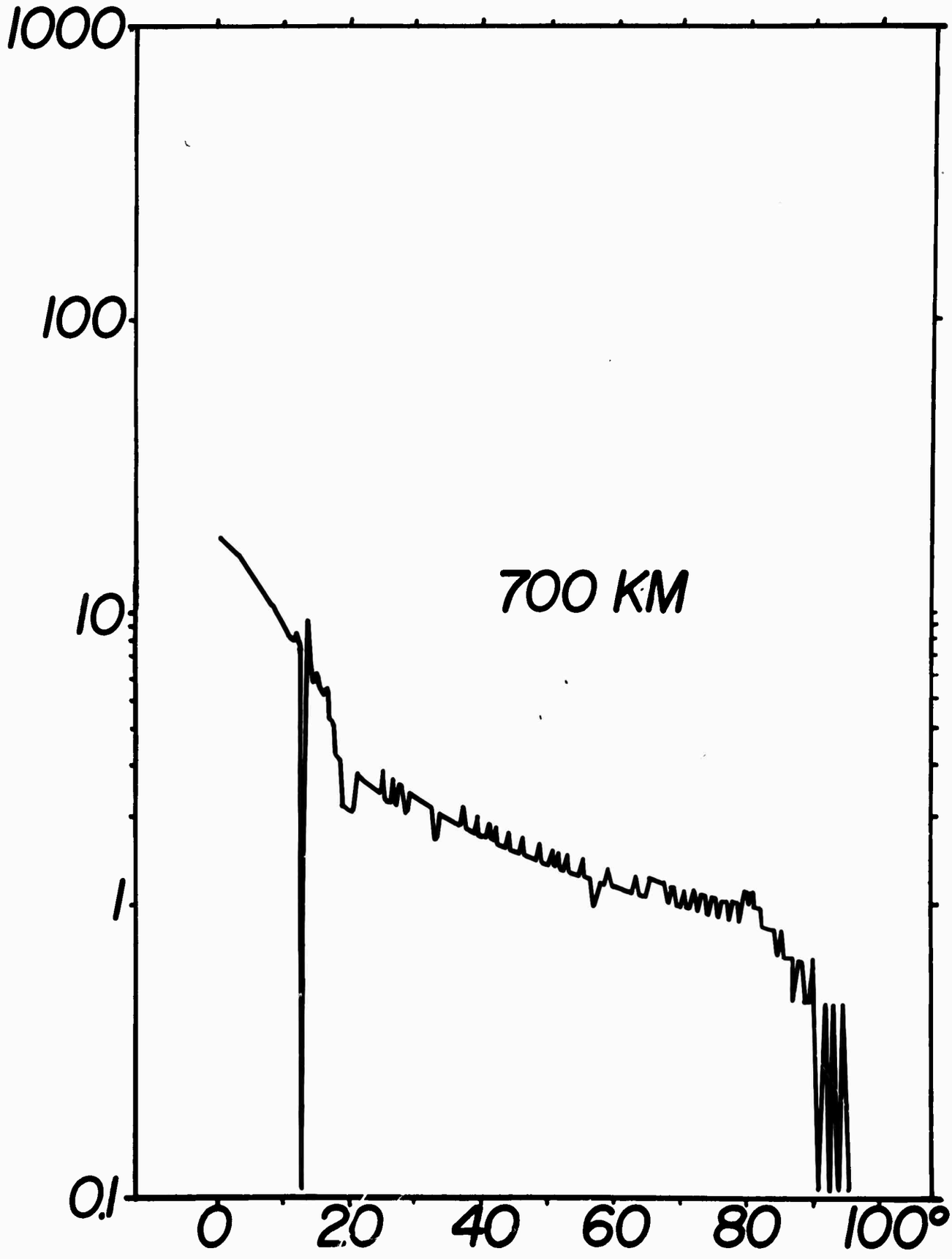

FIG. 20

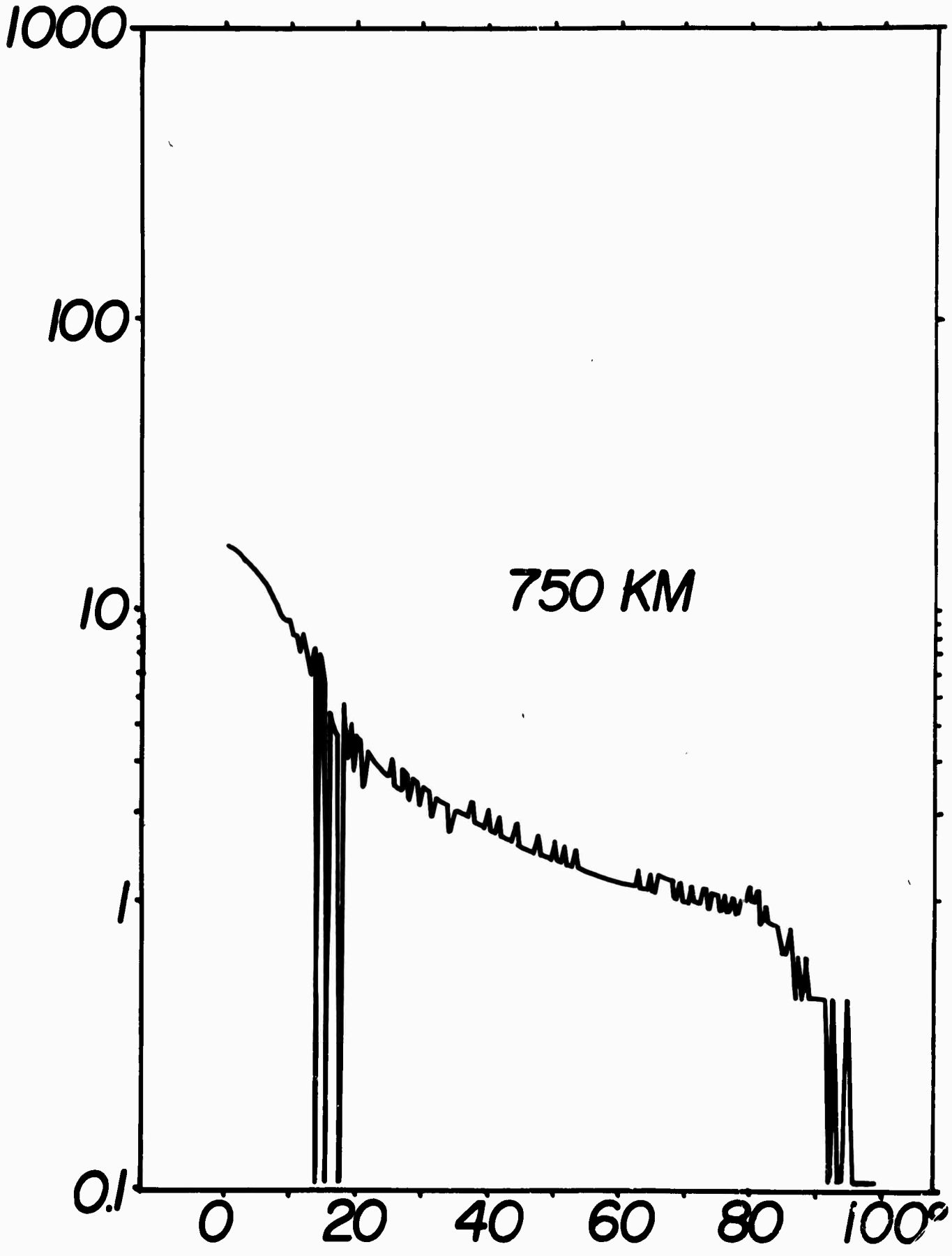
1000
100
10
1
0.1
750 KM
0
20
40
60
80
100°

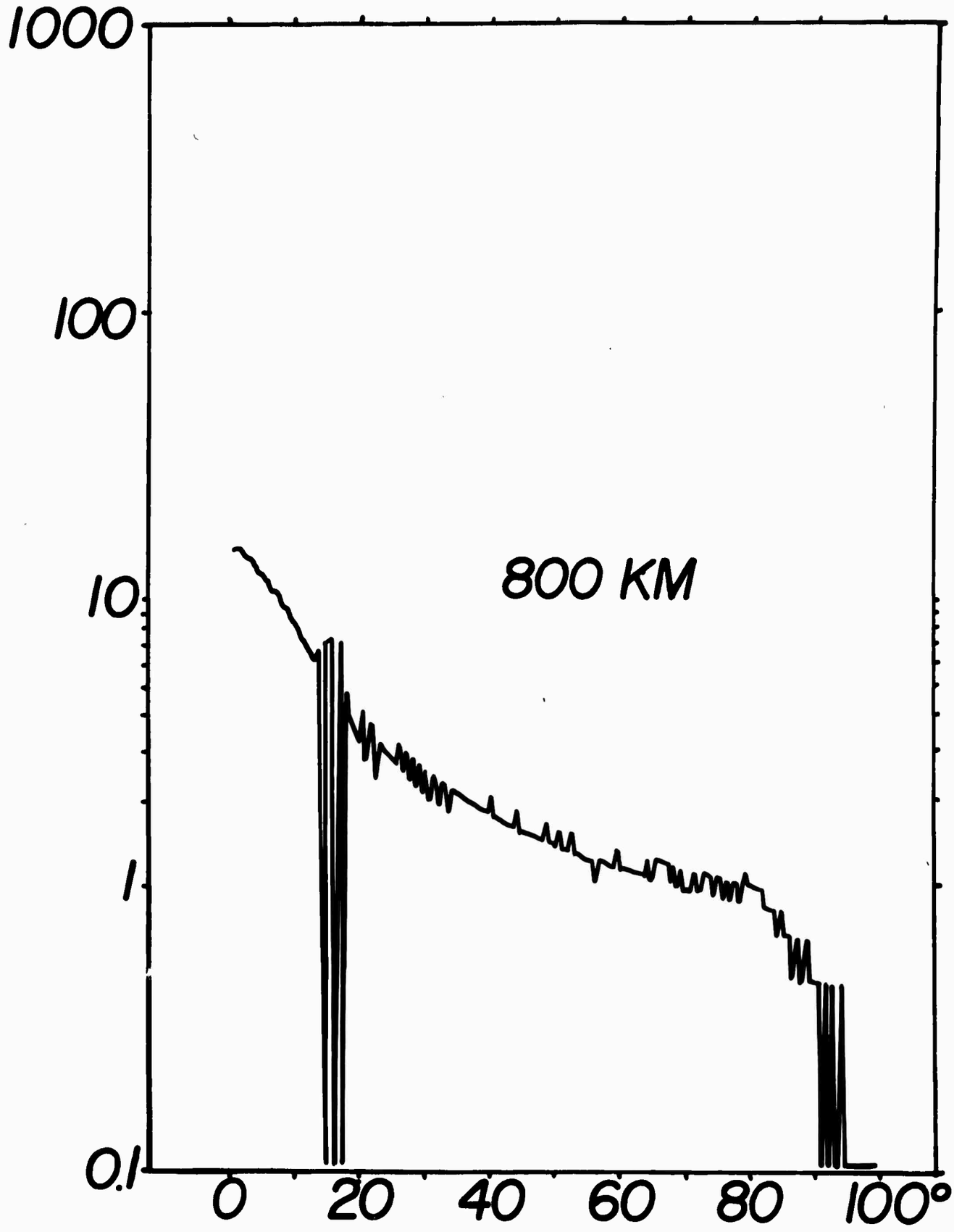

FIG. 22

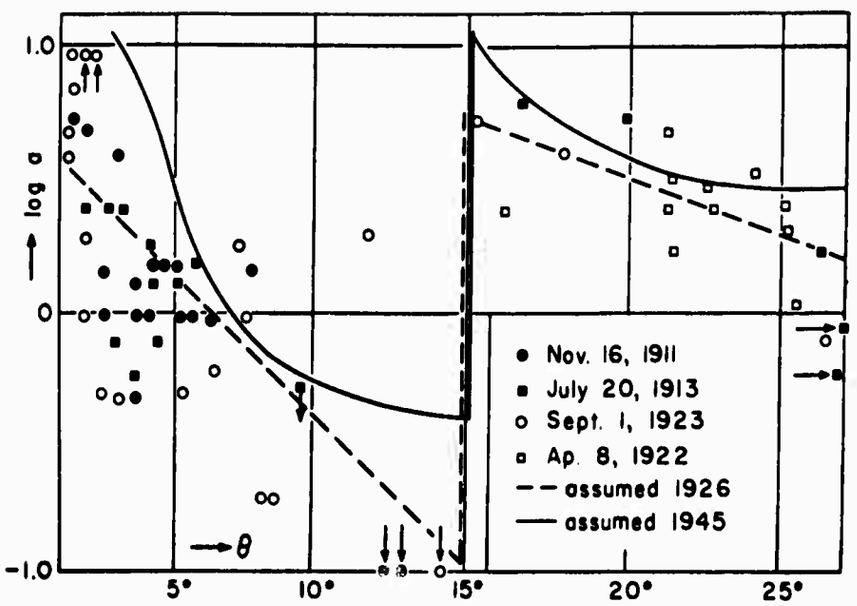

Logarithm of amplitudes a of longitudinal waves (P) as function of distance Θ, observed in earthquakes of 1911 and 1913 (epicenter in South Germany), 1922 (South of Spitsbergen), and 1923 (Japan), reduced to the same magnitude, and assumed curve in arbitrary units [Gutenberg, 1926]. The curve assumed by Gutenberg [1945] gives the average log a/T (T = period) for the vertical component of P in shallow shocks of magnitude 7 in various regions. Note that the units for the two curves are different, so that their vertical displacement is not significant.

FIG. 23

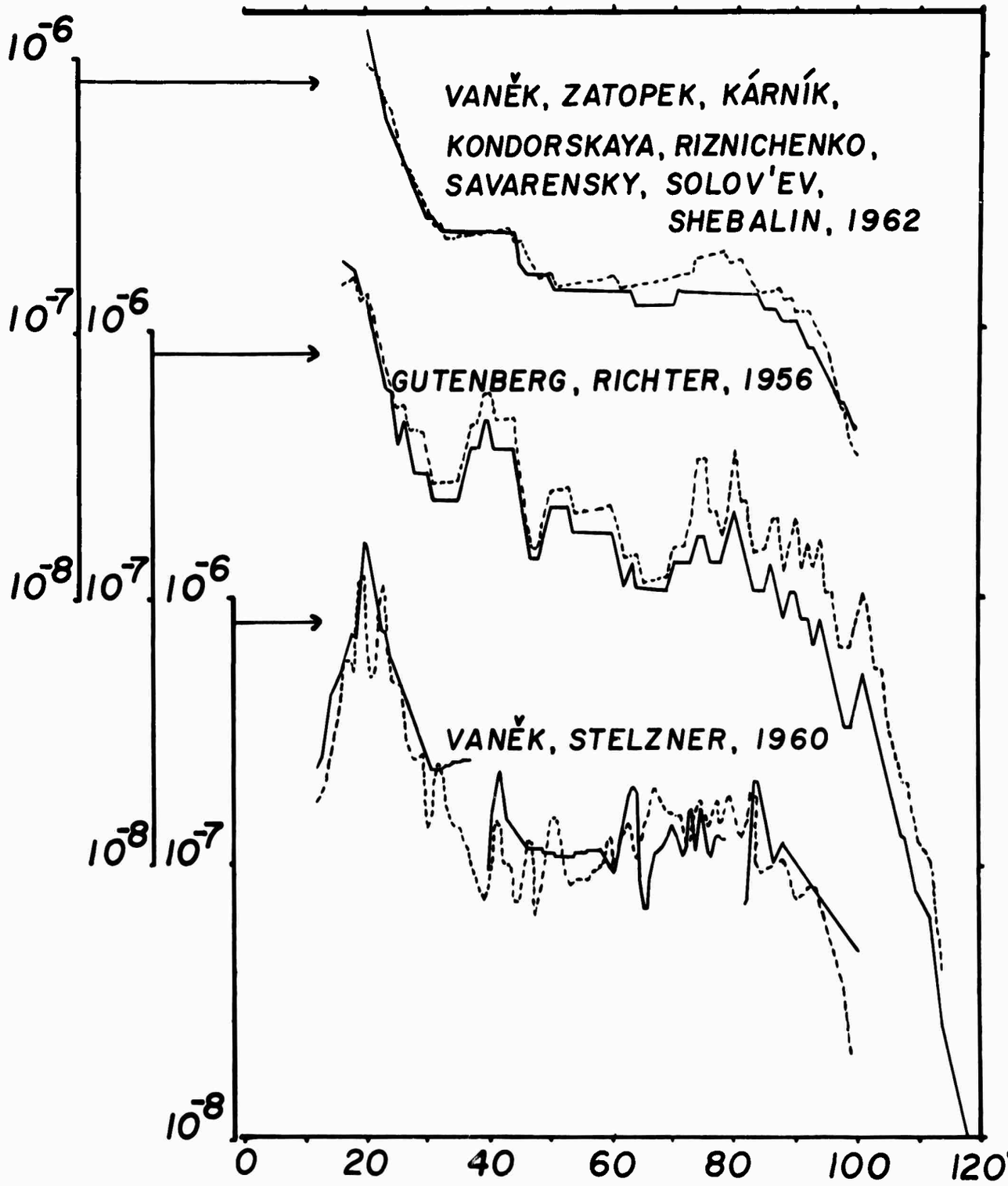
10^{-6}
VANĚK, ZATOPEK, KÁRNÍK,
KONDORSKAYA, RIZNICHENKO,
SAVARENSKY, SOLOV'EV,
SHEBALIN, 1962
10^{-7} 10^{-6}
GUTENBERG, RICHTER, 1956
10^{-8} 10^{-7} 10^{-6}
VANĚK, STELZNER, 1960
10^{-8} 10^{-7}
10^{-8}
0 20 40 60 80 100 120°

FIG. 24

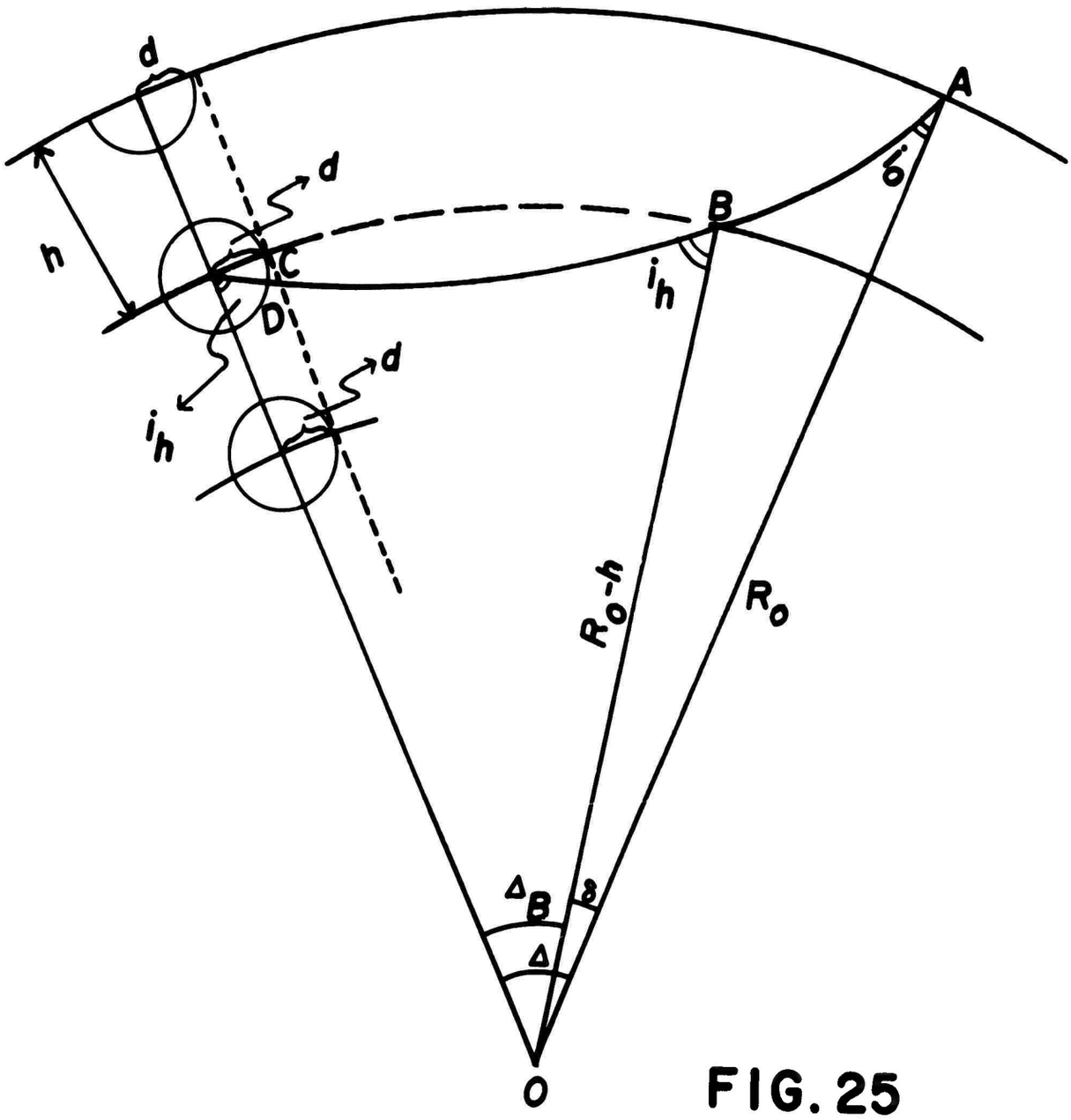

FIG. 25

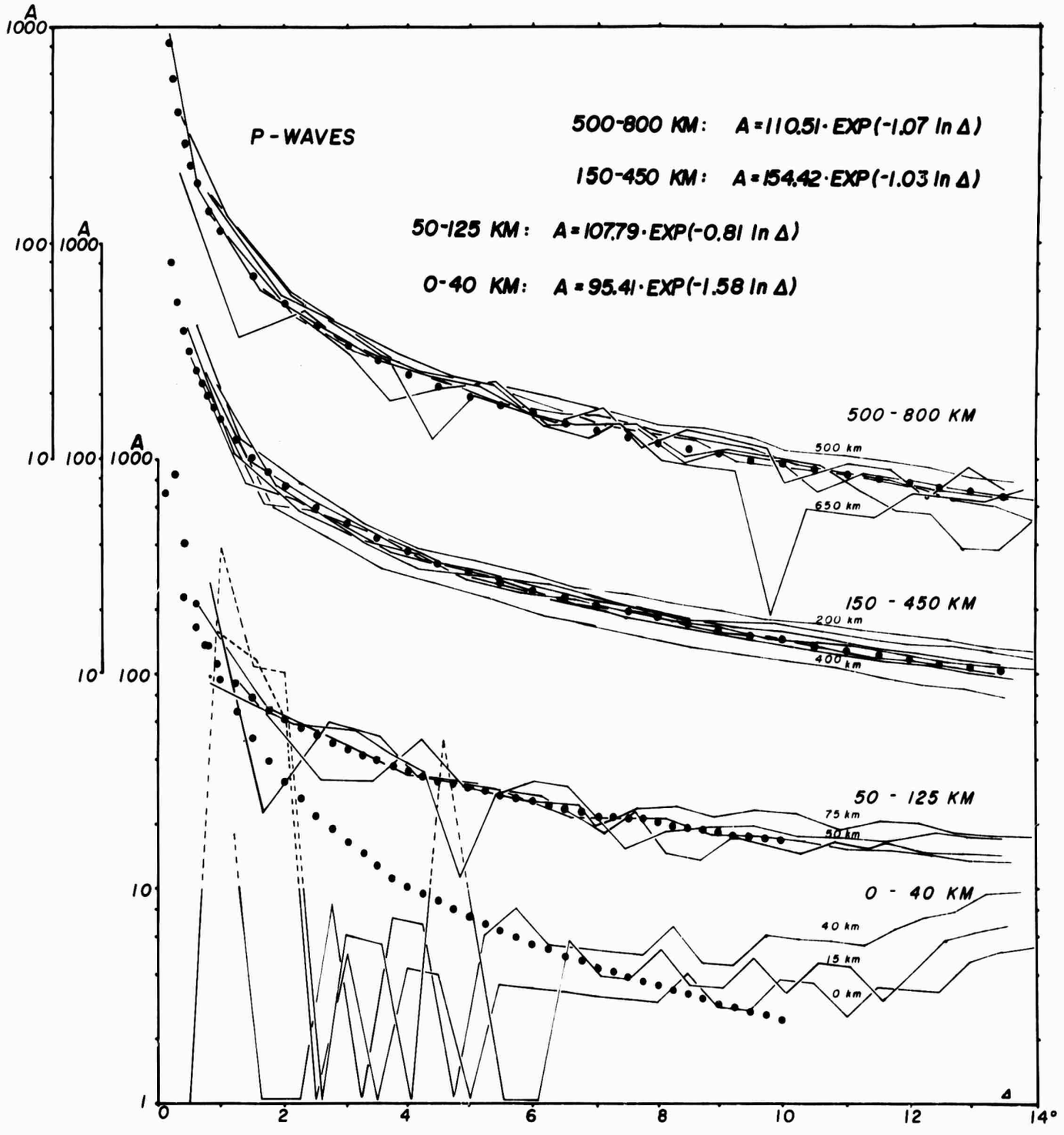
P - WAVES
500-800 KM: A = 110.51 · EXP(-1.07 ln Δ)
150-450 KM: A = 154.42 · EXP(-1.03 ln Δ)
50-125 KM: A = 107.79 · EXP(-0.81 ln Δ)
0-40 KM: A = 95.41 · EXP(-1.58 ln Δ)
500 - 800 KM
500 km
650 km
150 - 450 KM
200 km
400 km
50 - 125 KM
75 km
50 km
0 - 40 KM
40 km
15 km
0 km
A
Δ
1000
100
10
1
0
2
4
6
8
10
12
14°

FIG. 26

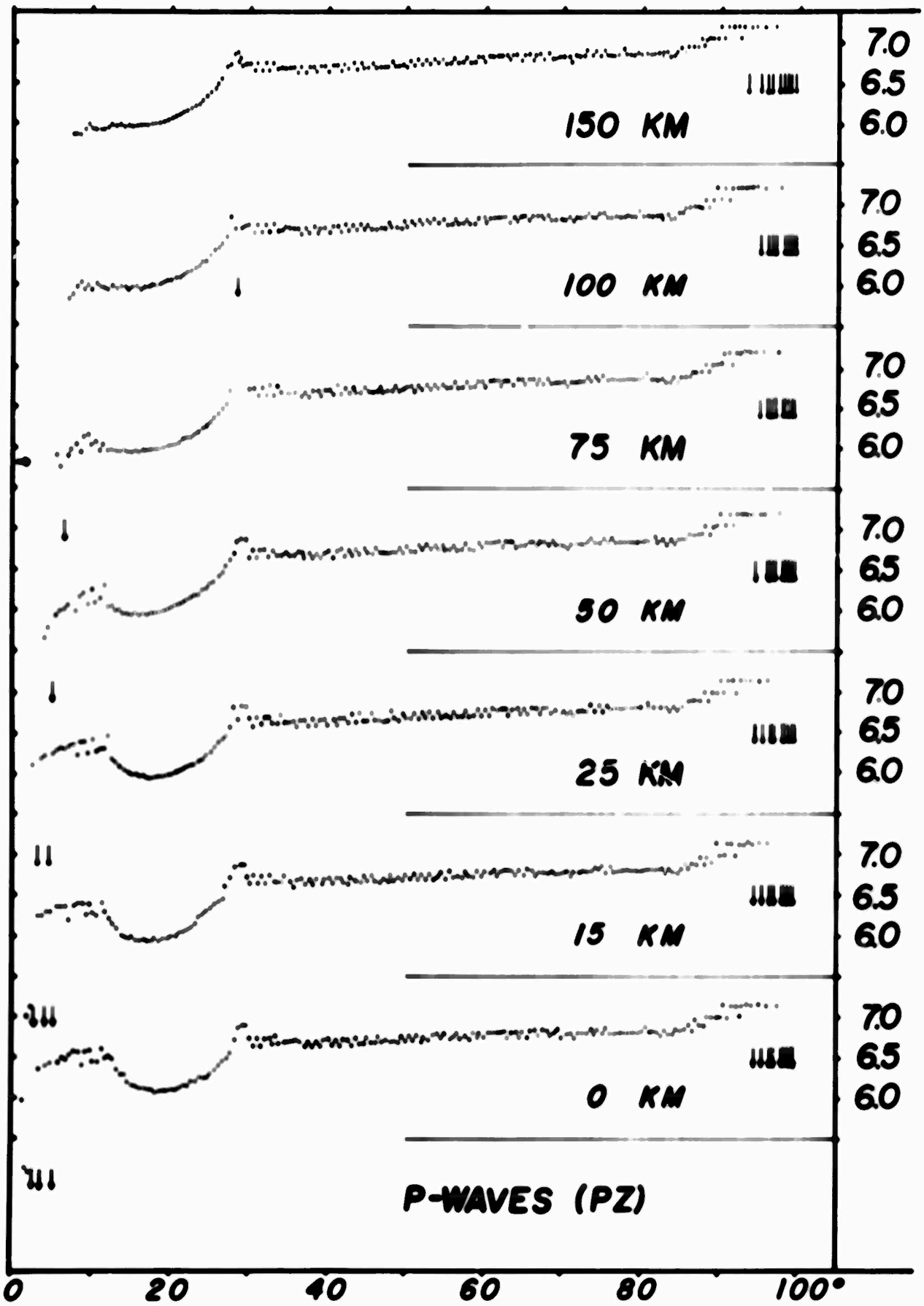
7.0
6.5
6.0
150 KM
100 KM
75 KM
50 KM
25 KM
15 KM
0 KM
P-WAVES (PZ)
0
20
40
60
80
100°

FIG. 27a

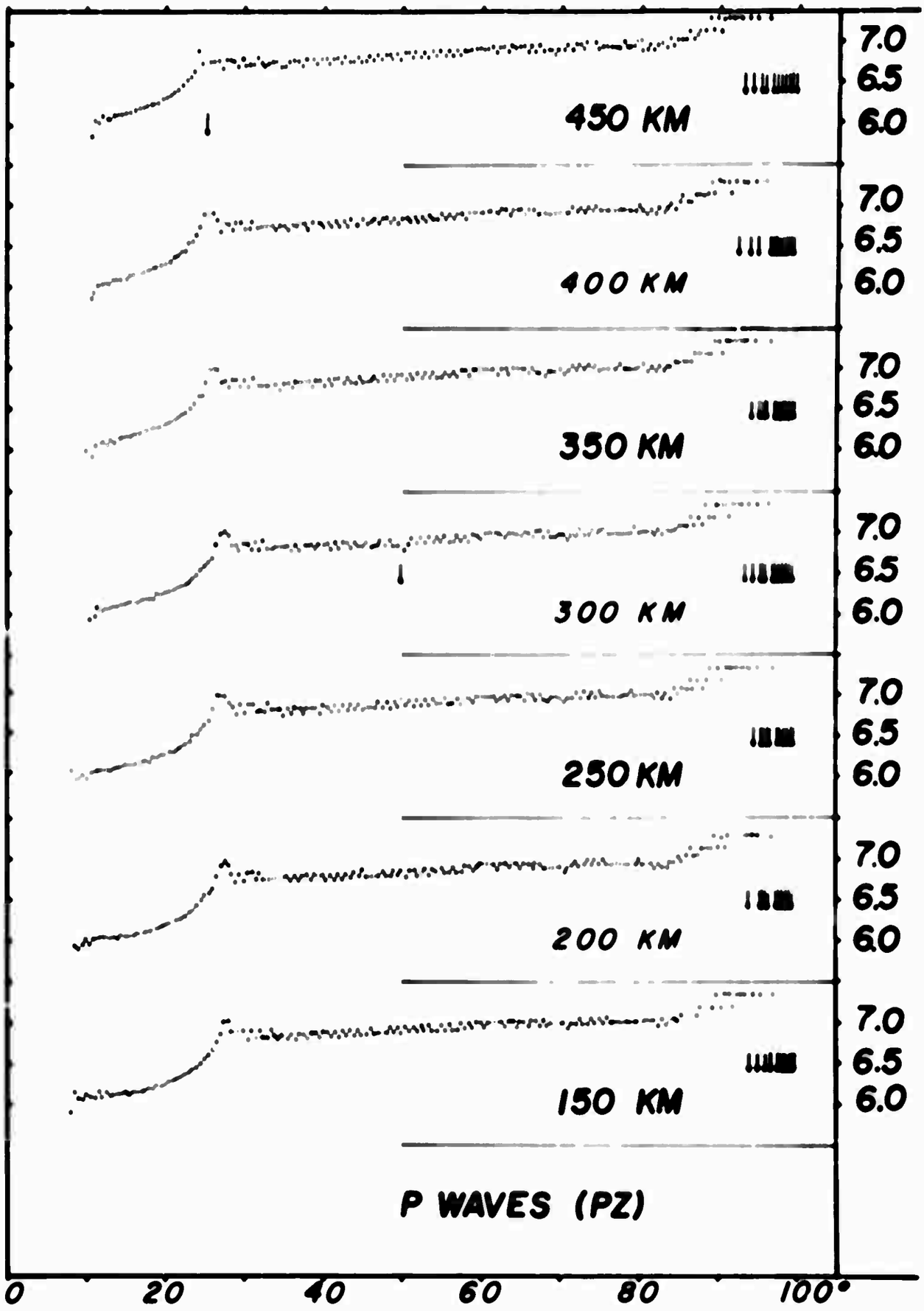
7.0
6.5
6.0
450 KM
400 KM
350 KM
300 KM
250 KM
200 KM
150 KM
P WAVES (PZ)
0
20
40
60
80
100°

FIG. 27b

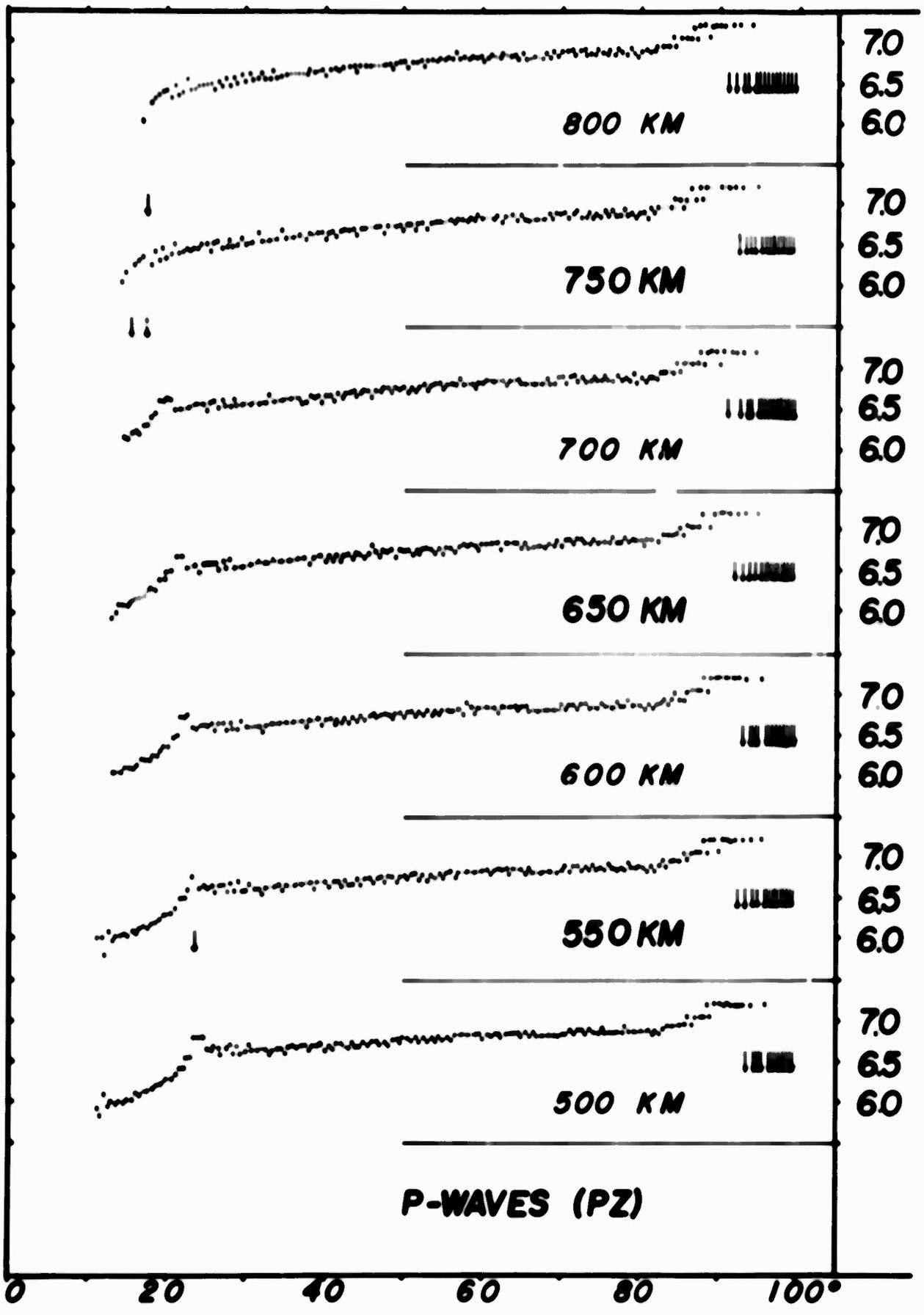
800 KM
750 KM
700 KM
650 KM
600 KM
550 KM
500 KM
7.0
6.5
6.0
P-WAVES (PZ)
0
20
40
60
80
100°

FIG. 27c

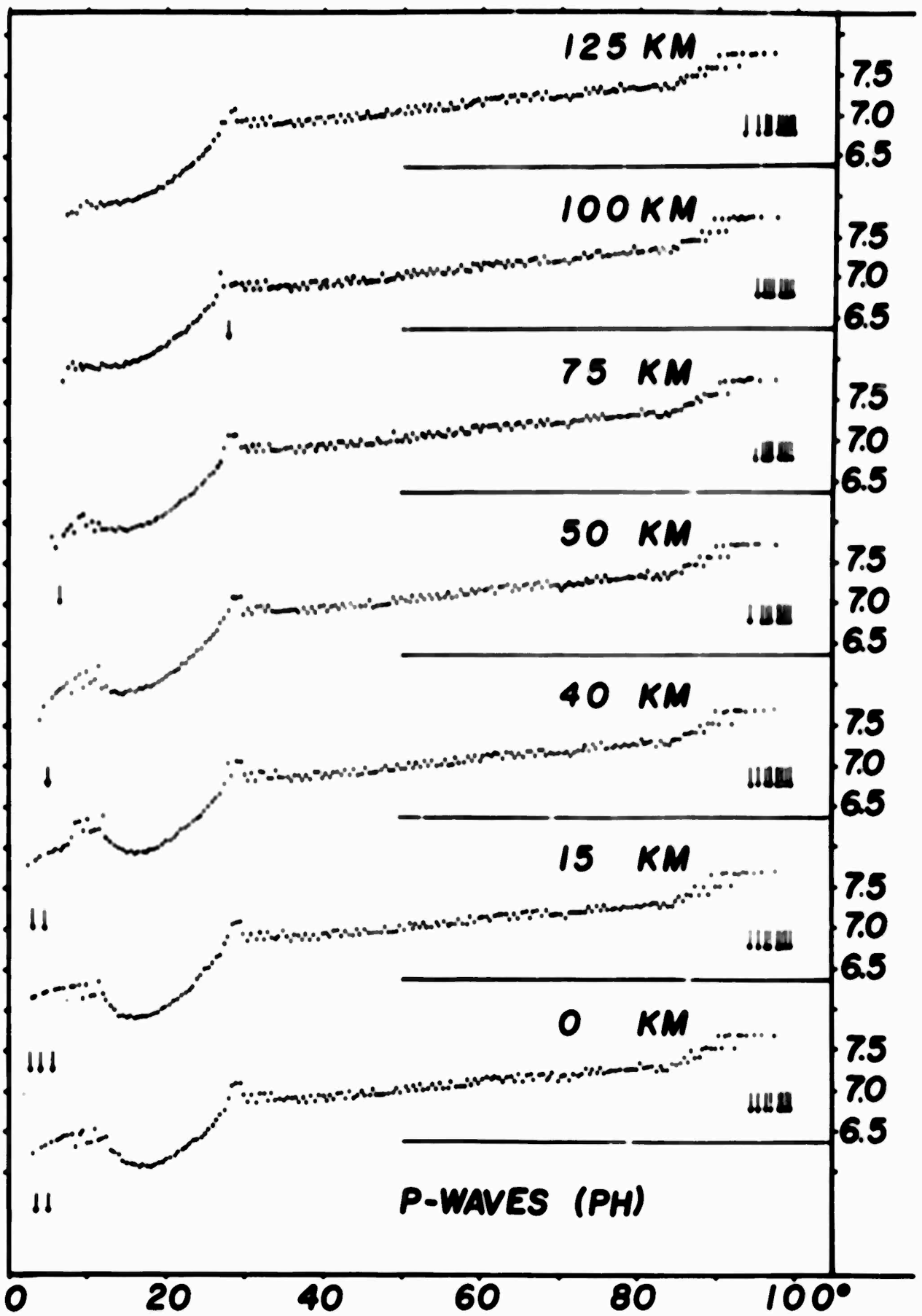
125 KM
100 KM
75 KM
50 KM
40 KM
15 KM
0 KM
7.5
7.0
6.5
P-WAVES (PH)
0
20
40
60
80
100°

FIG. 28a

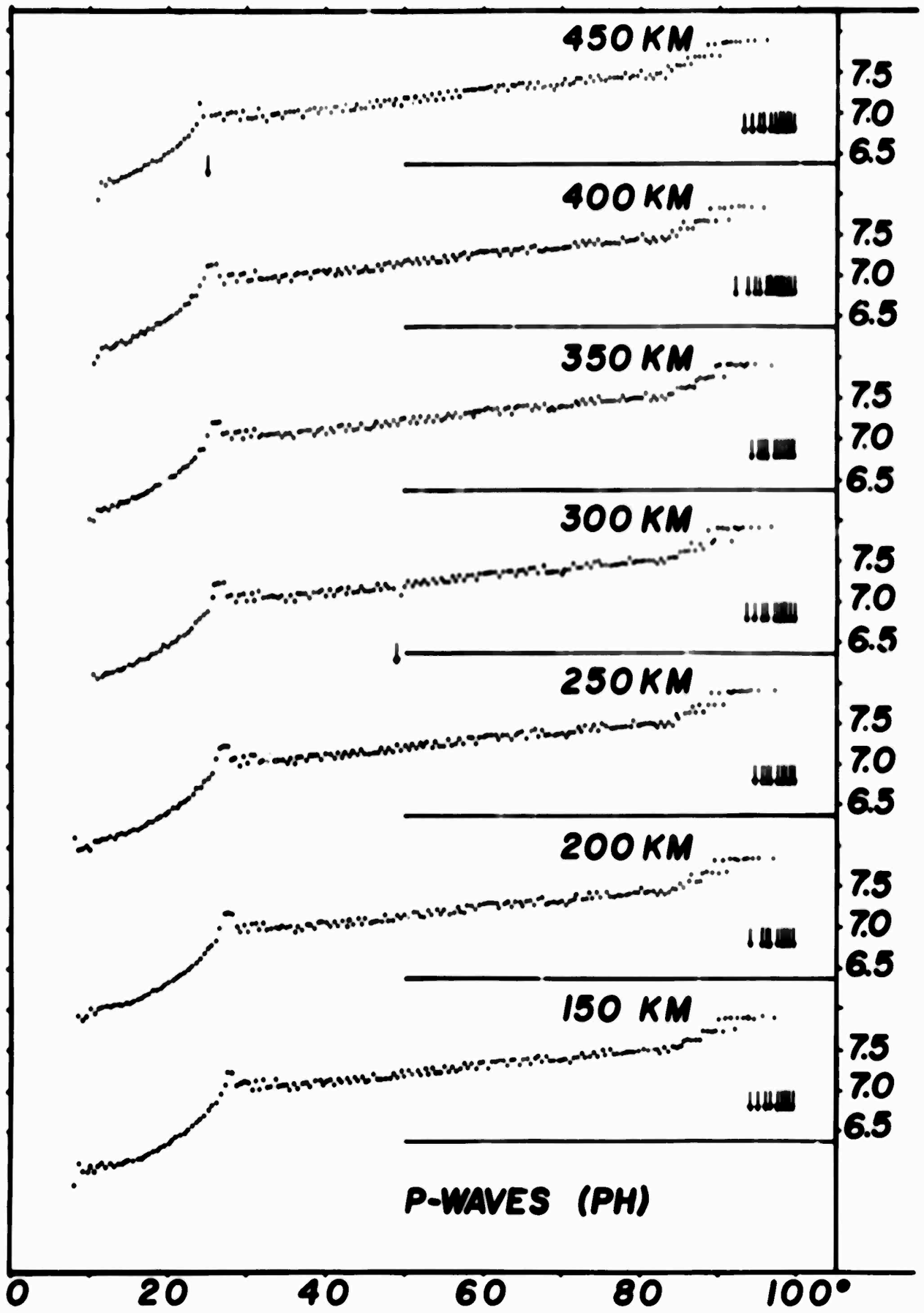
450 KM
400 KM
350 KM
300 KM
250 KM
200 KM
150 KM
7.5
7.0
6.5
P-WAVES (PH)
0
20
40
60
80
100°

FIG. 28b

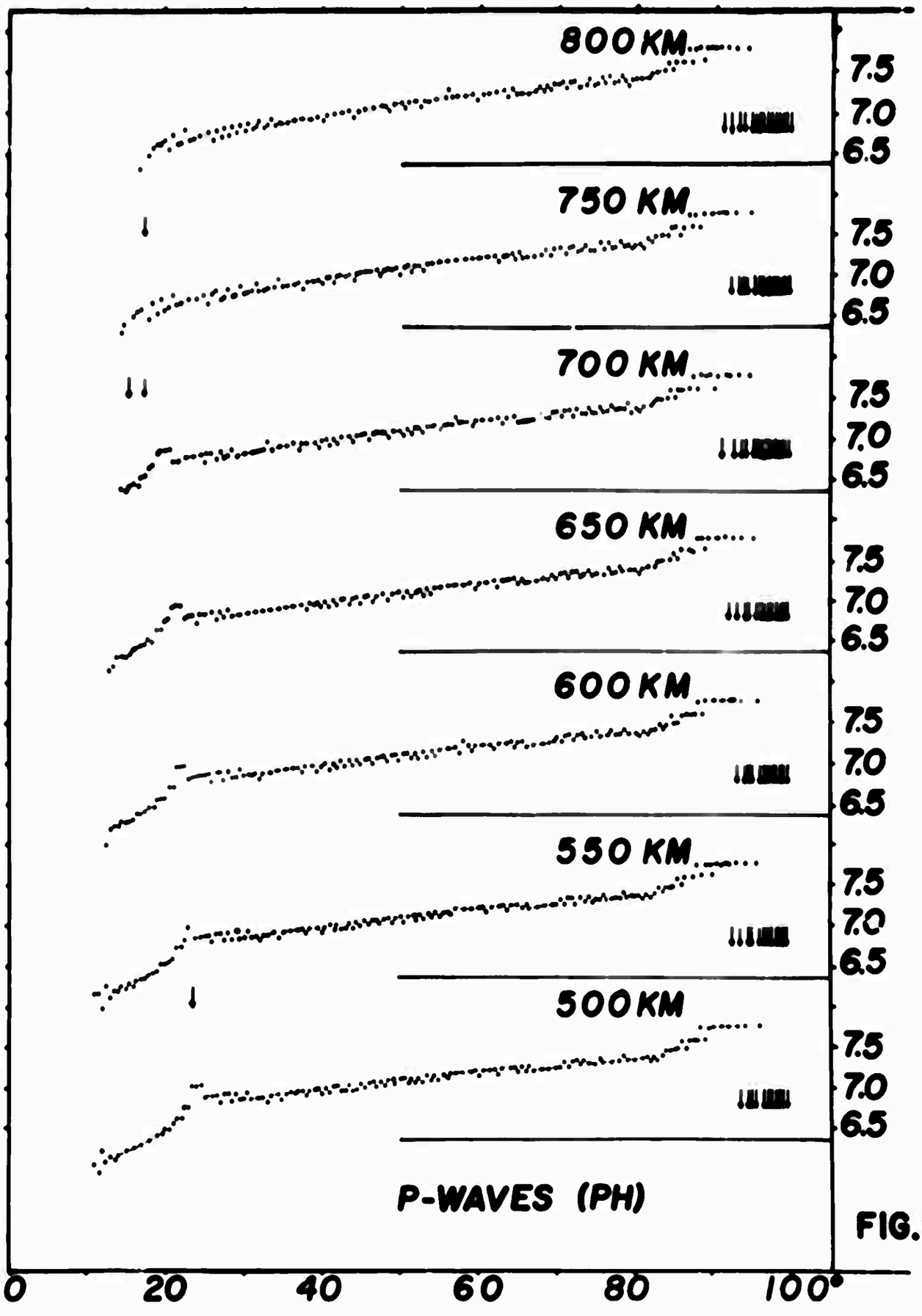
800 KM
750 KM
700 KM
650 KM
600 KM
550 KM
500 KM
7.5
7.0
6.5
P-WAVES (PH)
0
20
40
60
80
100

FIG.28c

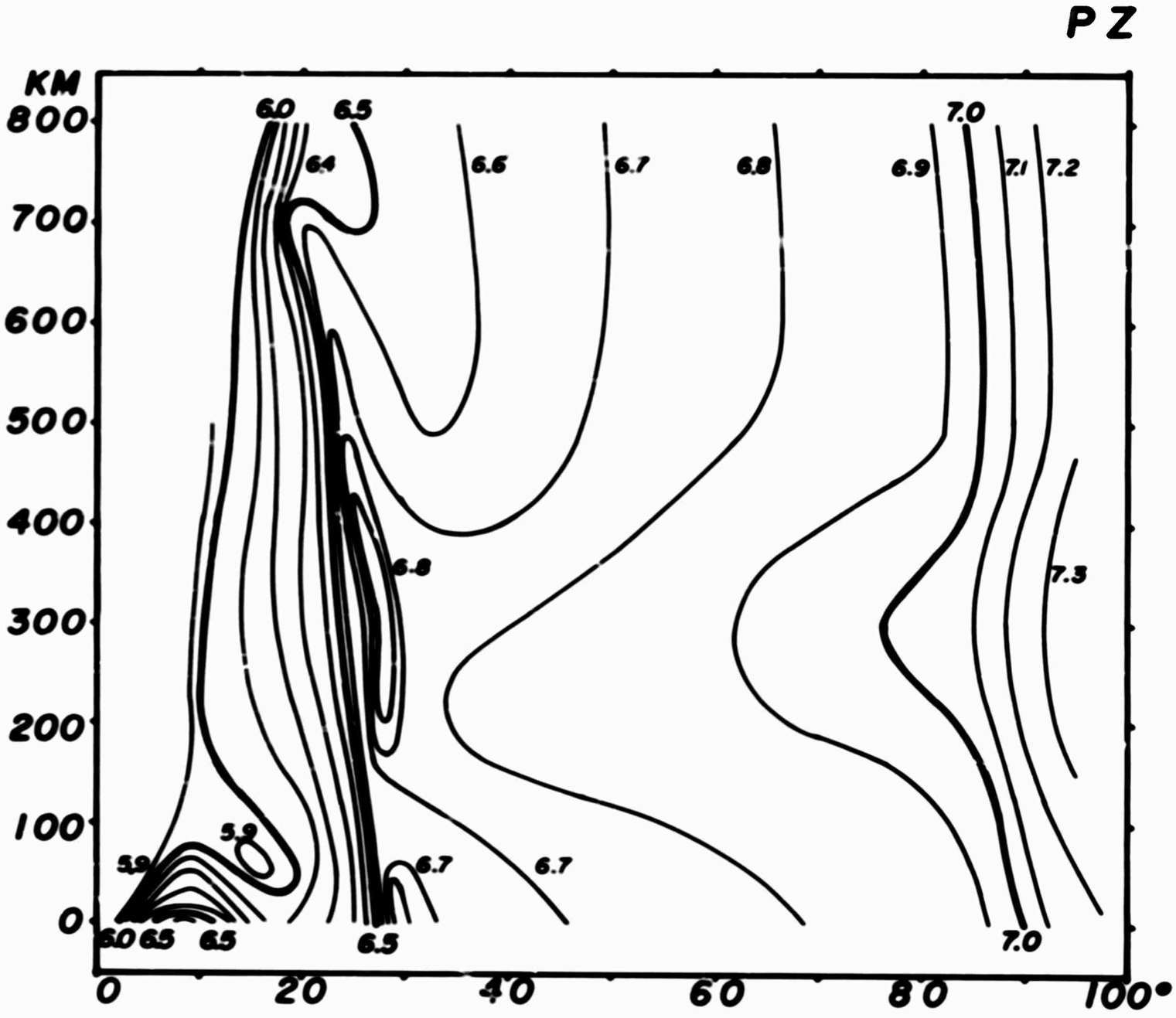
PZ
KM
800
700
600
500
400
300
200
100
0
0
20
40
60
80
100
6.0
6.5
6.4
6.6
6.7
6.8
6.9
7.0
7.1
7.2
7.3
5.9
6.7
6.5

FIG. 29

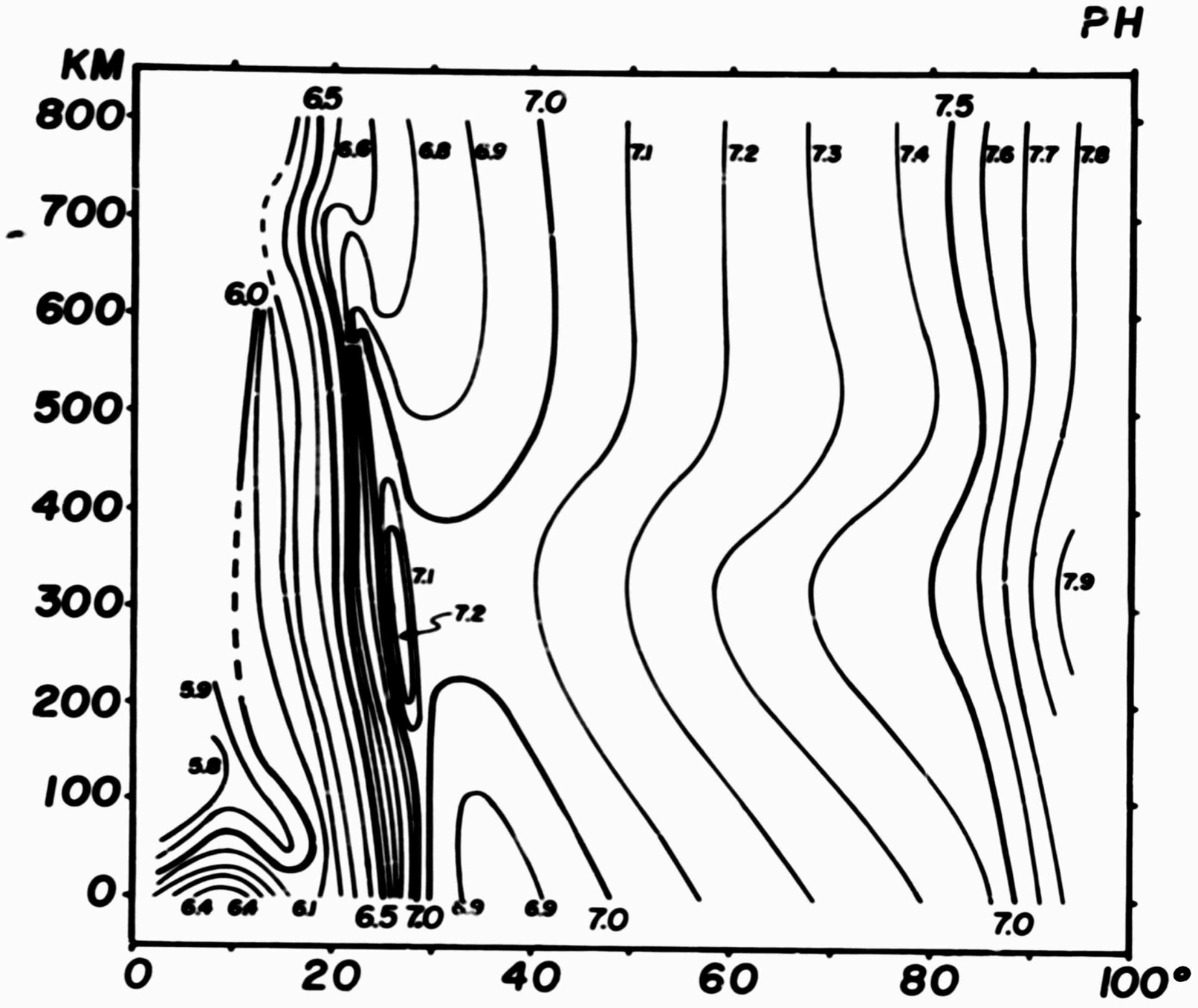
PH
KM
800
700
600
500
400
300
200
100
0
0
20
40
60
80
100°
6.5
7.0
7.5
6.6
6.8
6.9
7.1
7.2
7.3
7.4
7.6
7.7
7.8
6.0
7.1
7.2
7.9
5.9
5.8
6.4
6.4
6.1
6.5
7.0
6.9
6.9
7.0
7.0

FIG. 30

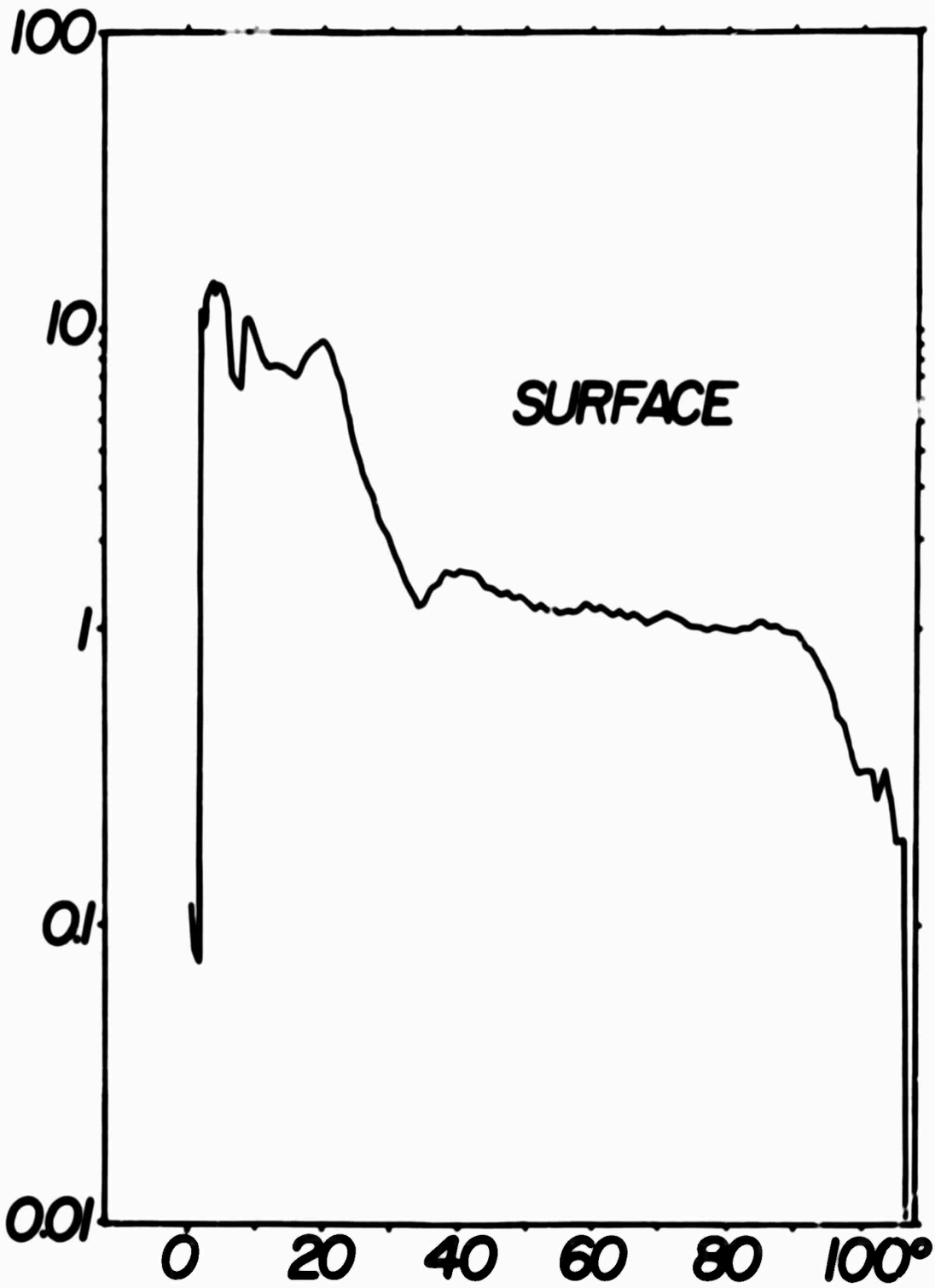

FIG. 31

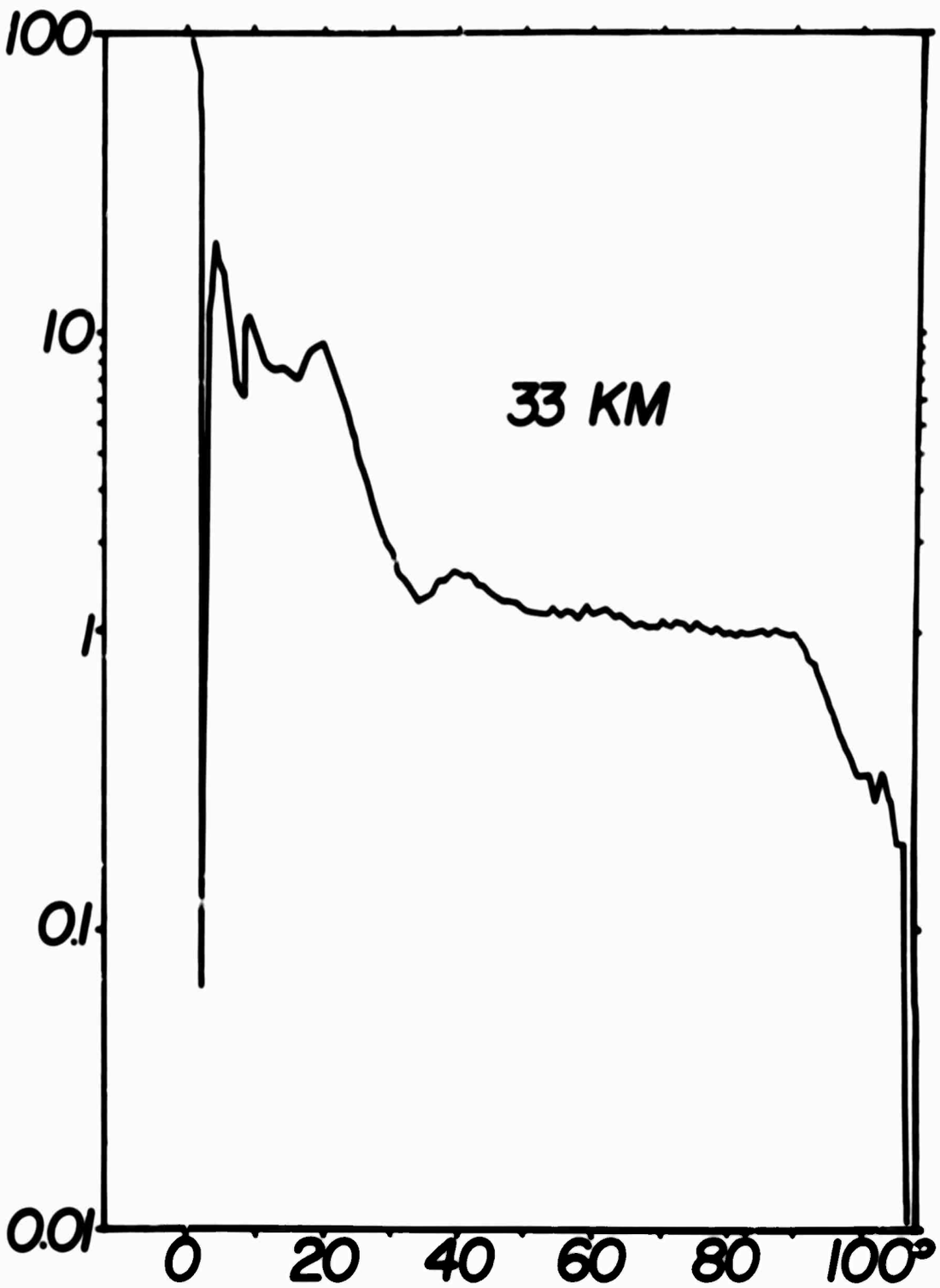

FIG. 32

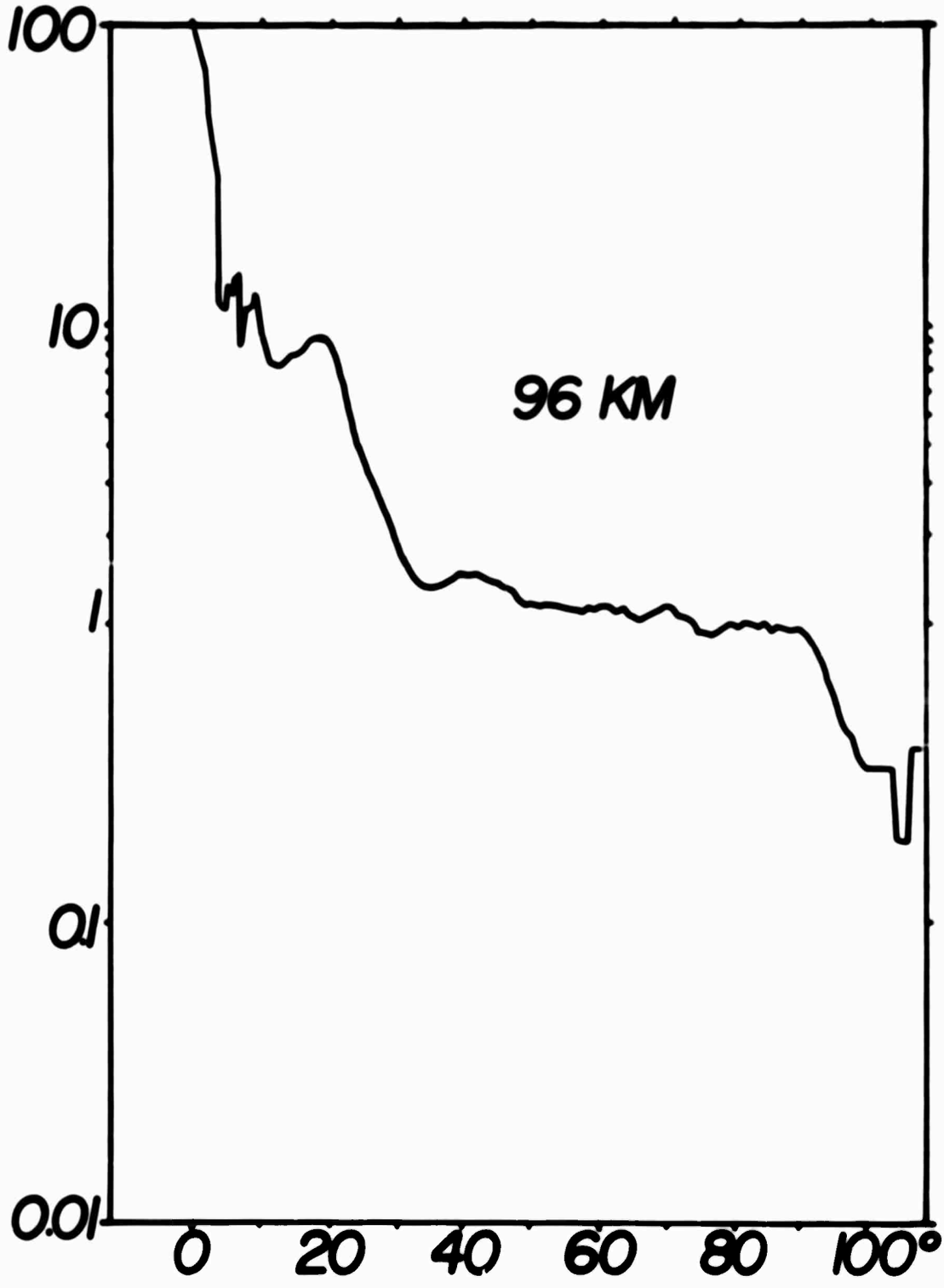

FIG. 33

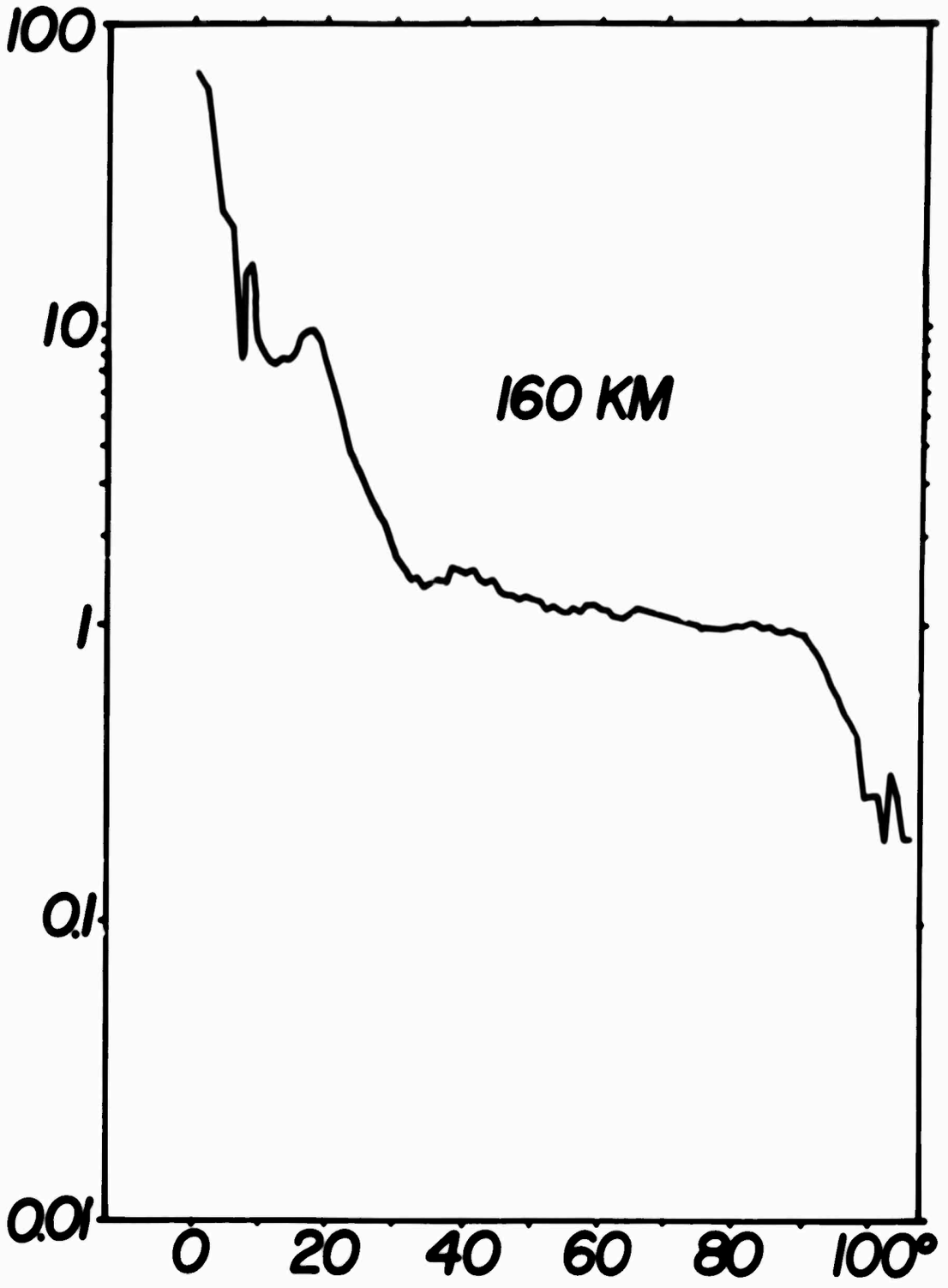

FIG. 34

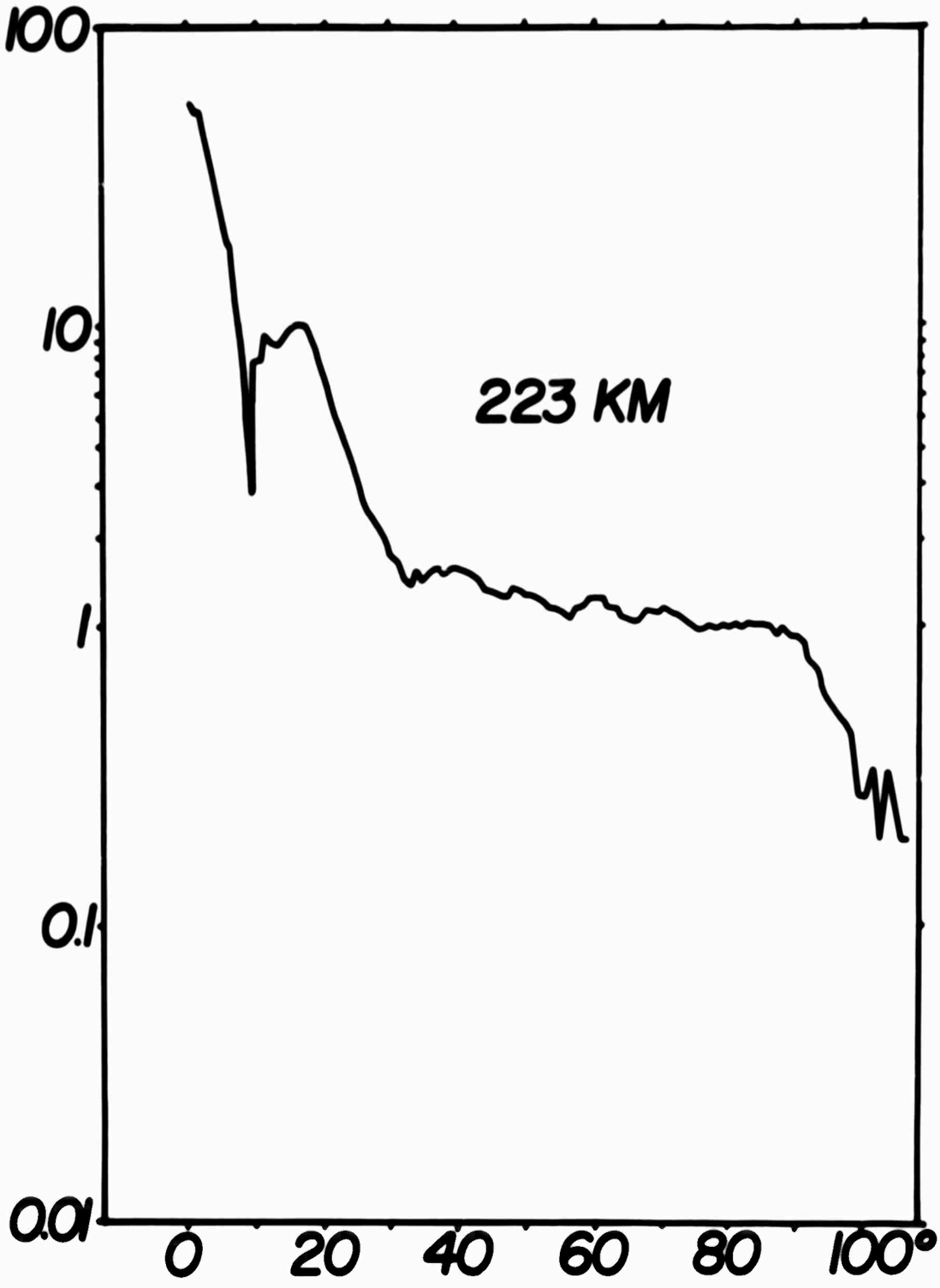

FIG. 35

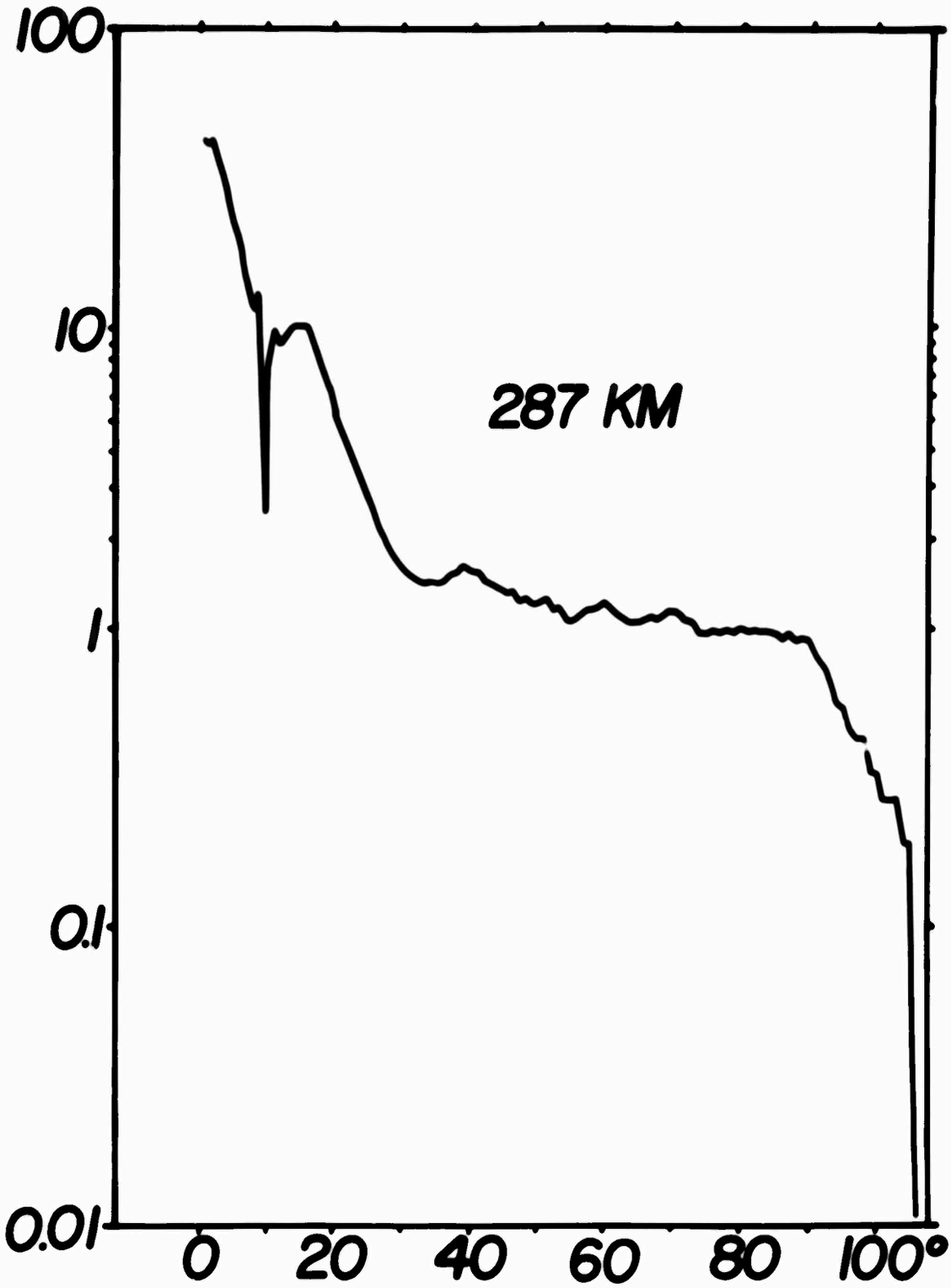

FIG. 36

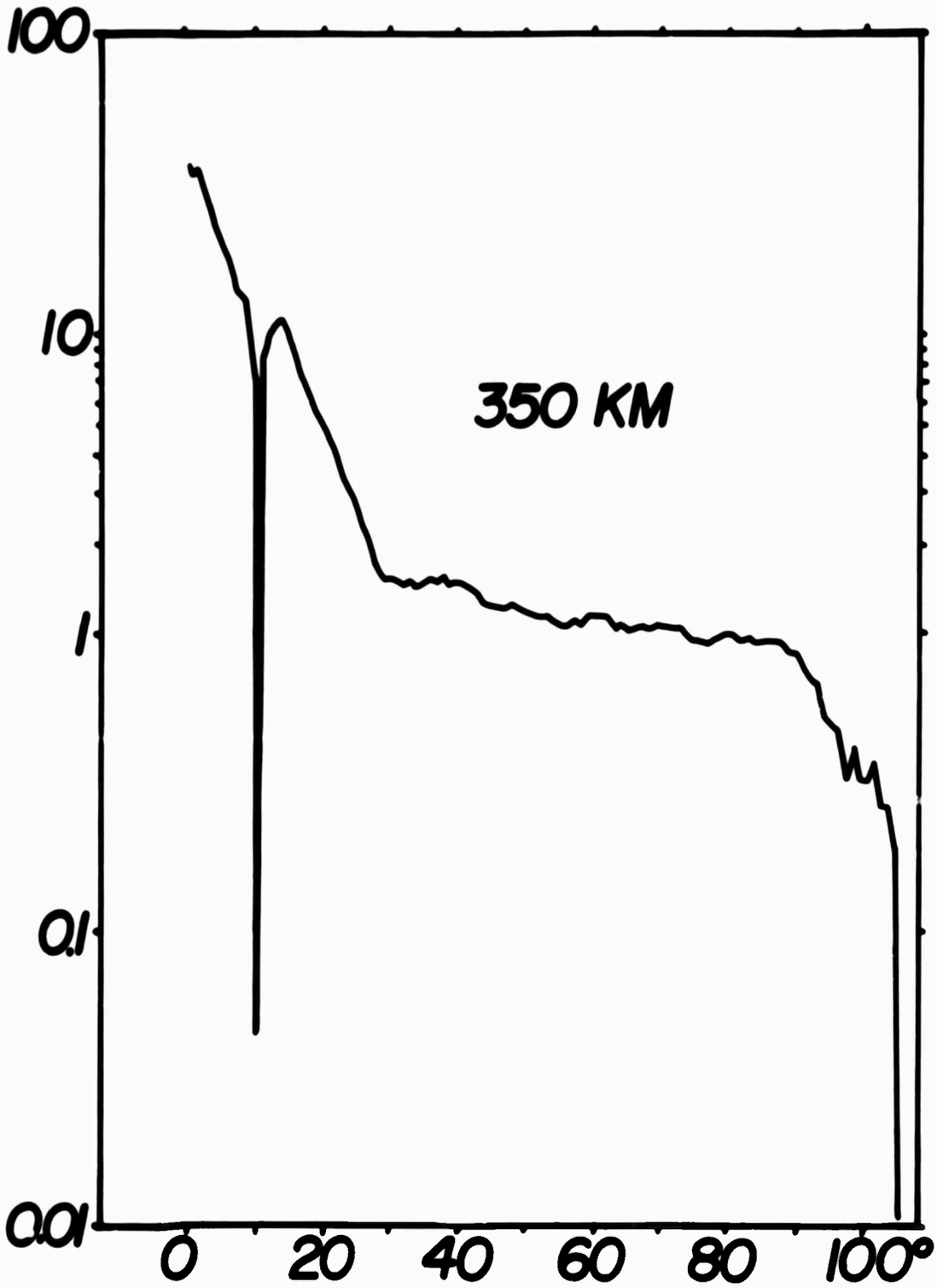

FIG. 37

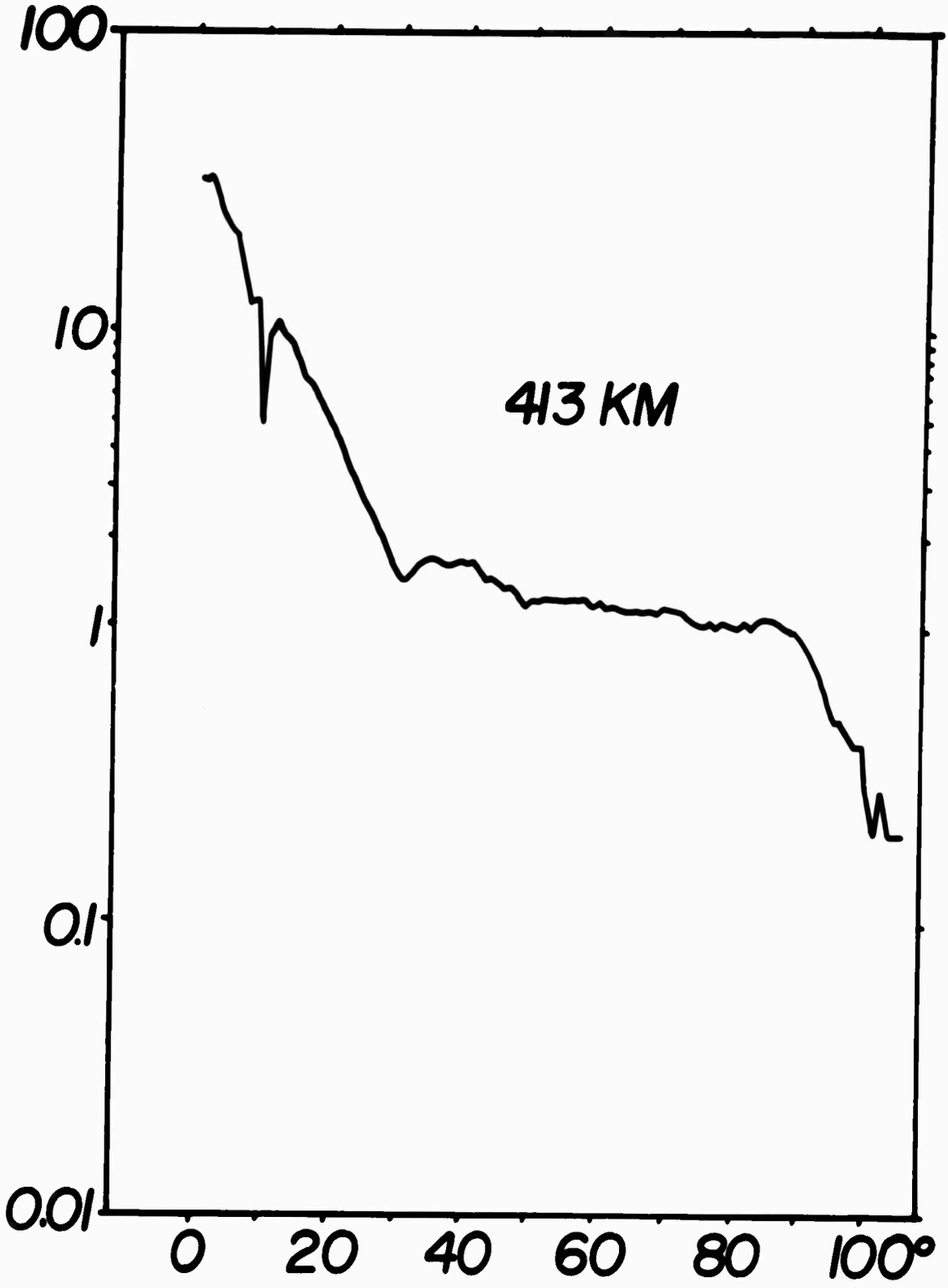

FIG. 38

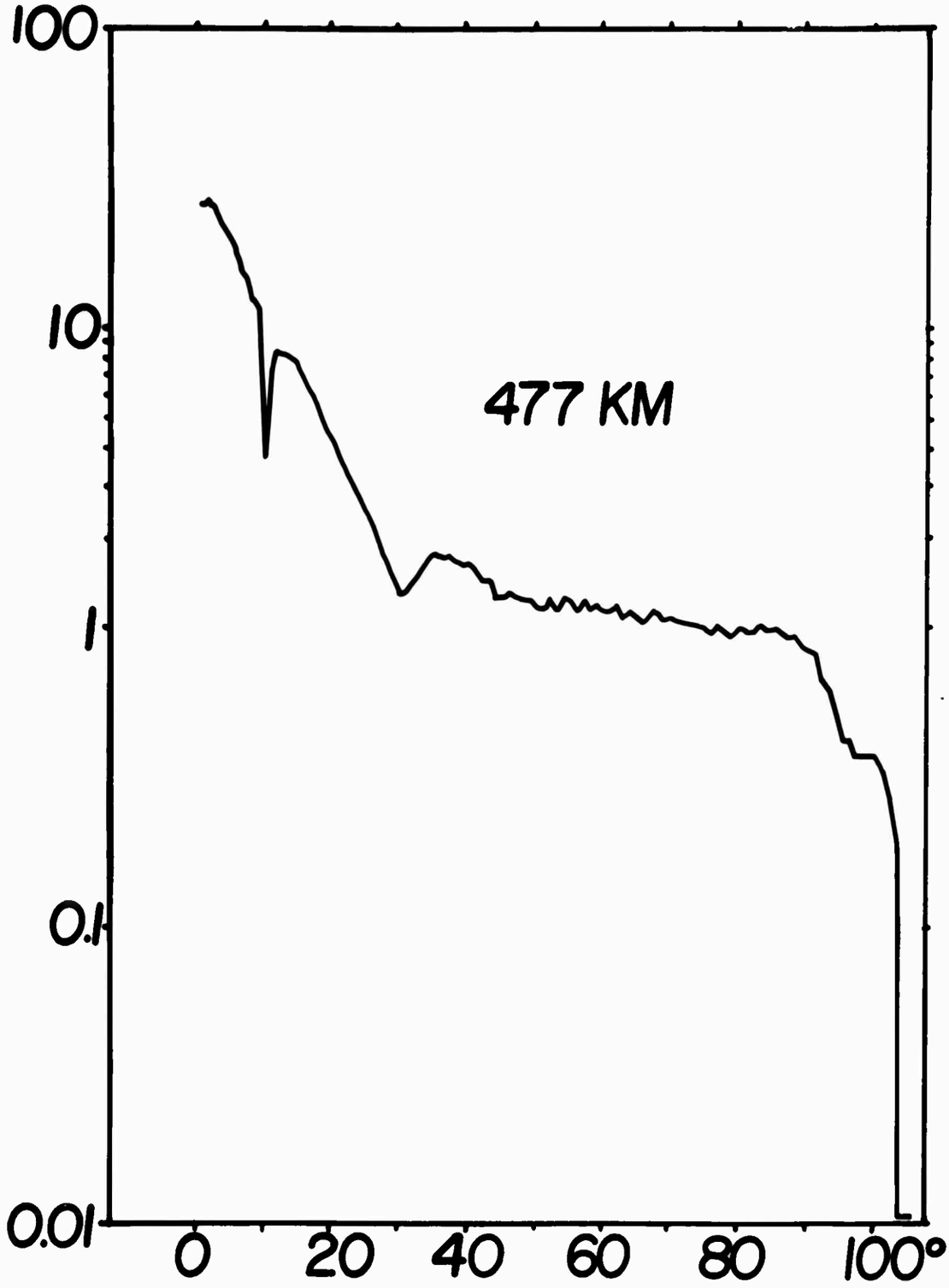

FIG. 39

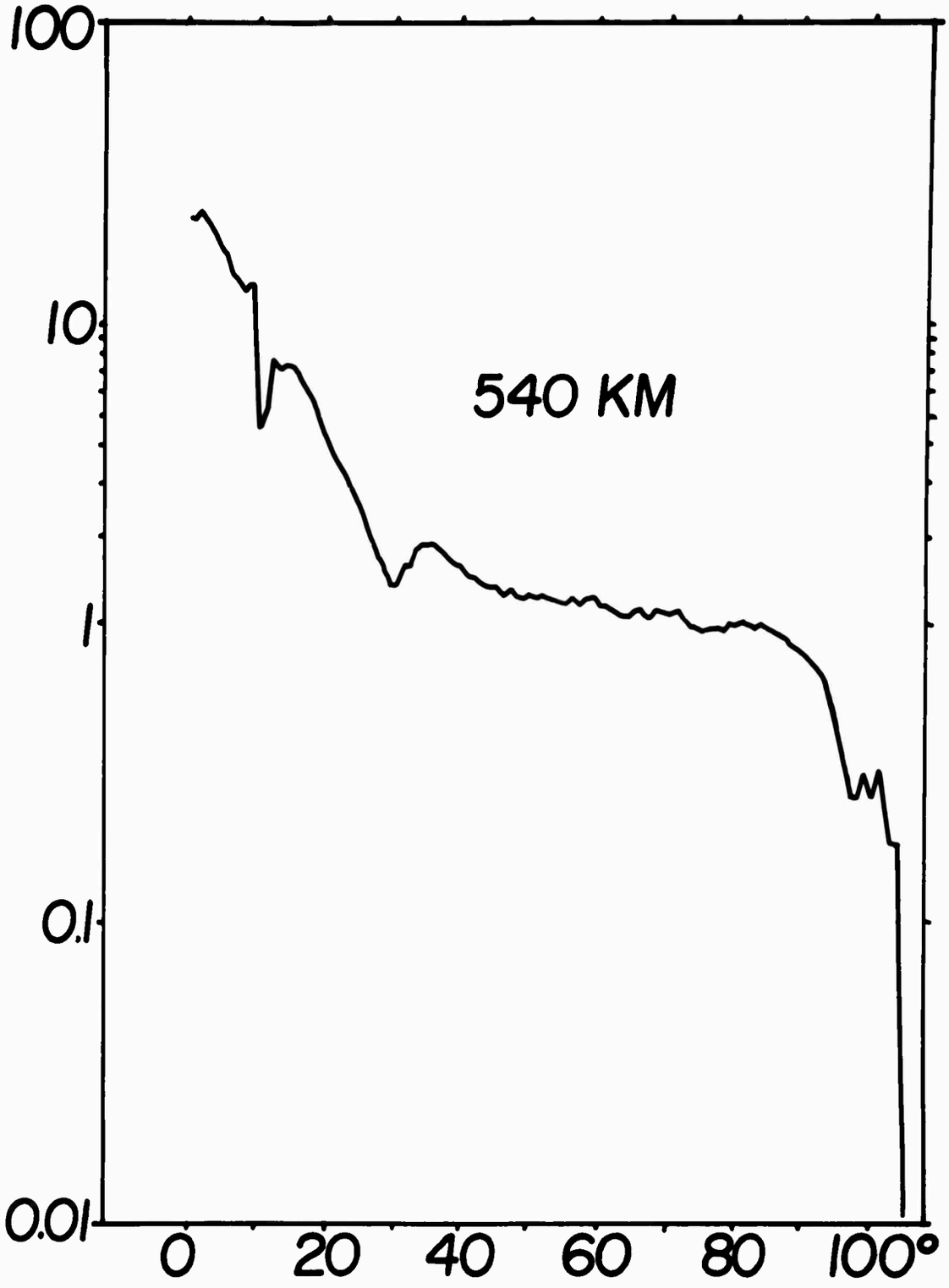

FIG. 40

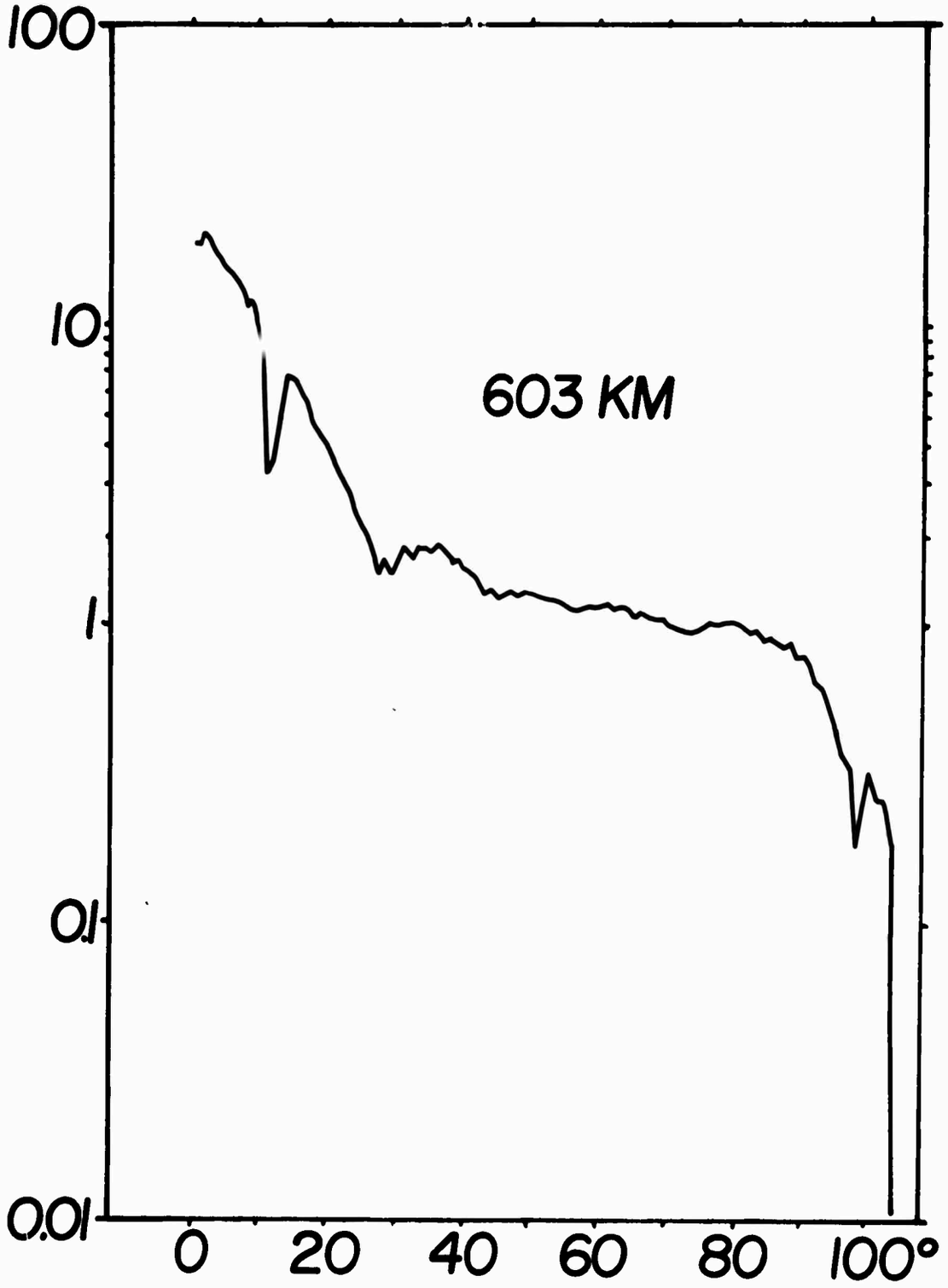

FIG. 41

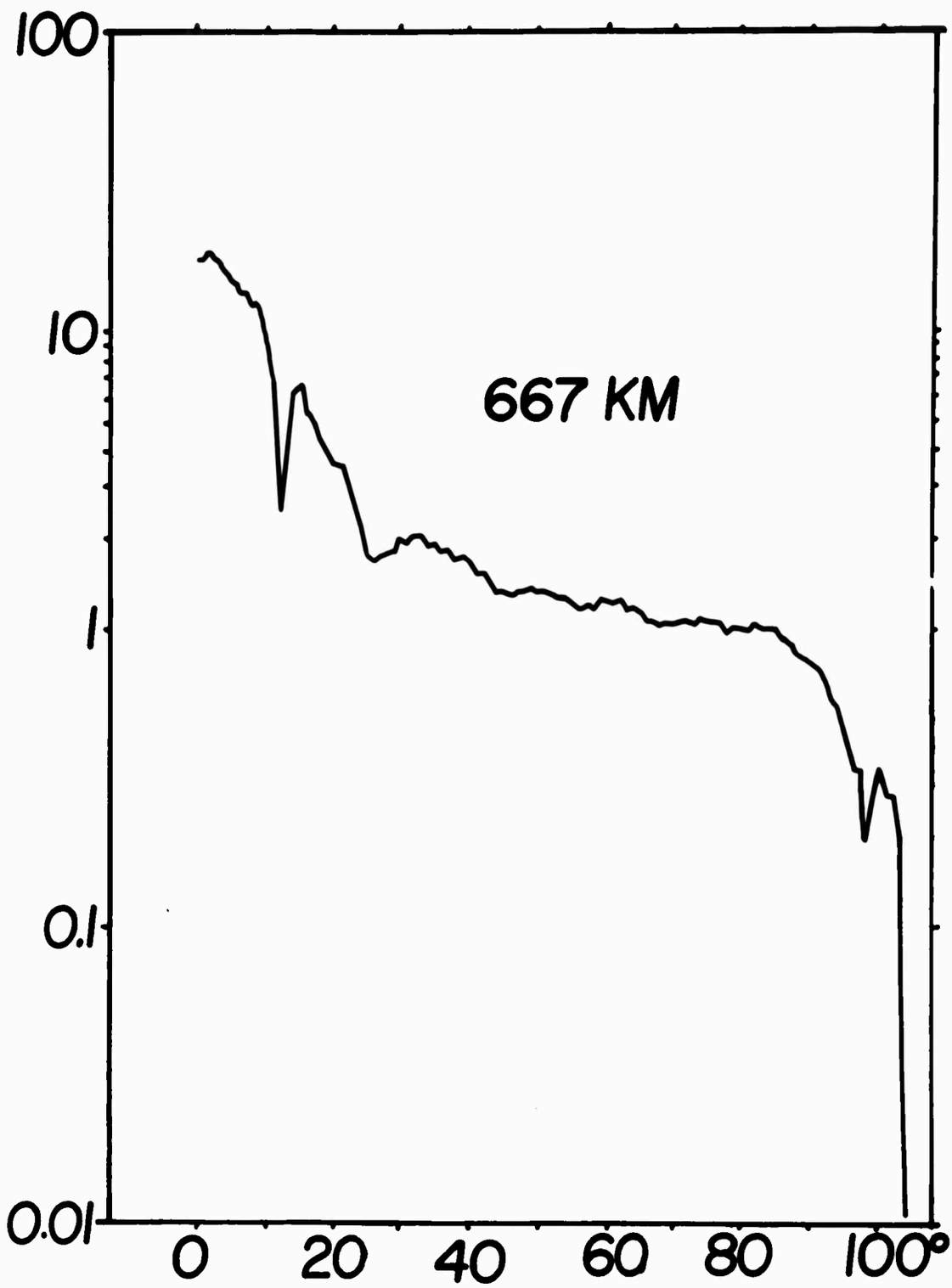

FIG. 42

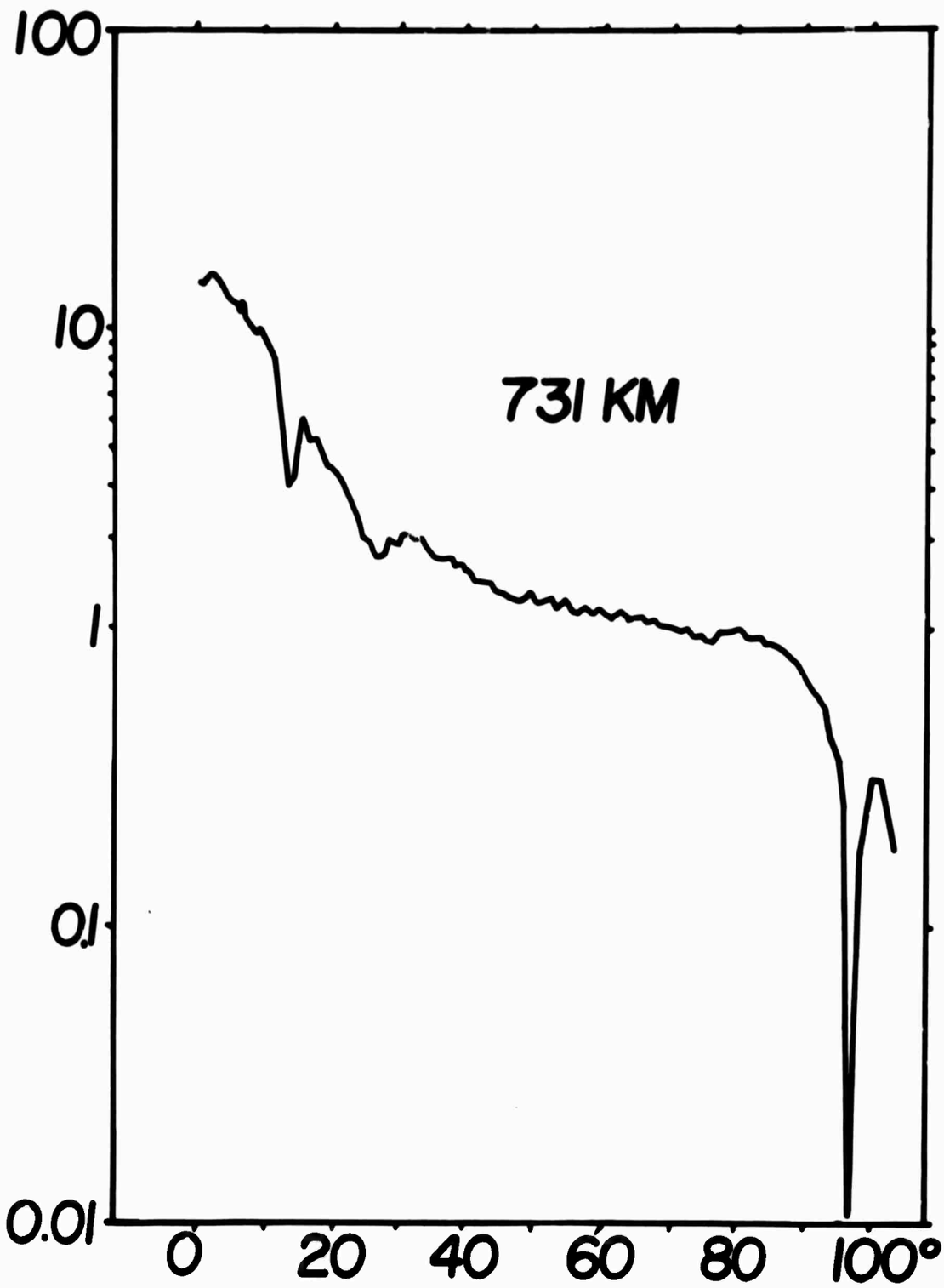

FIG. 43

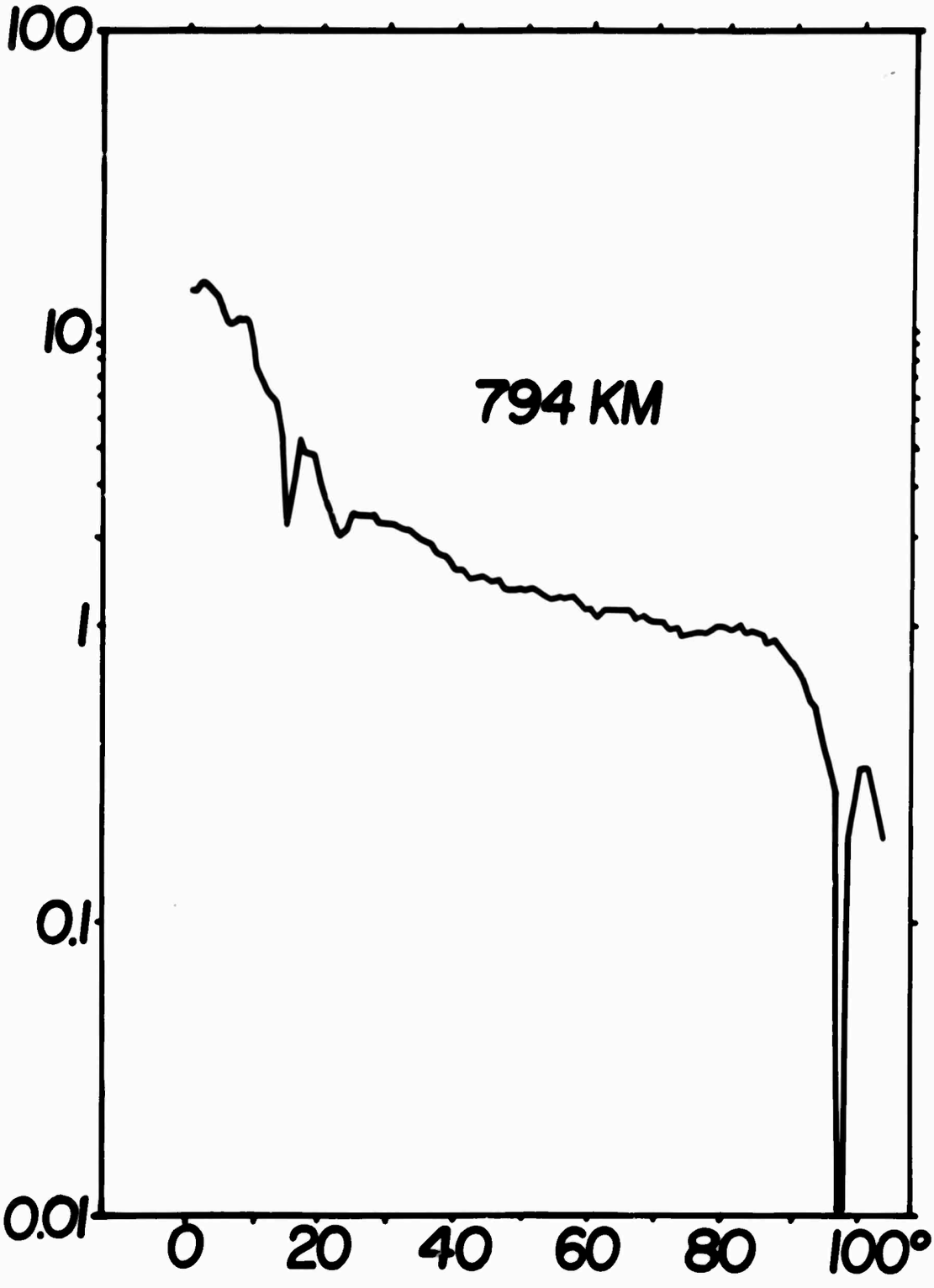

FIG. 44

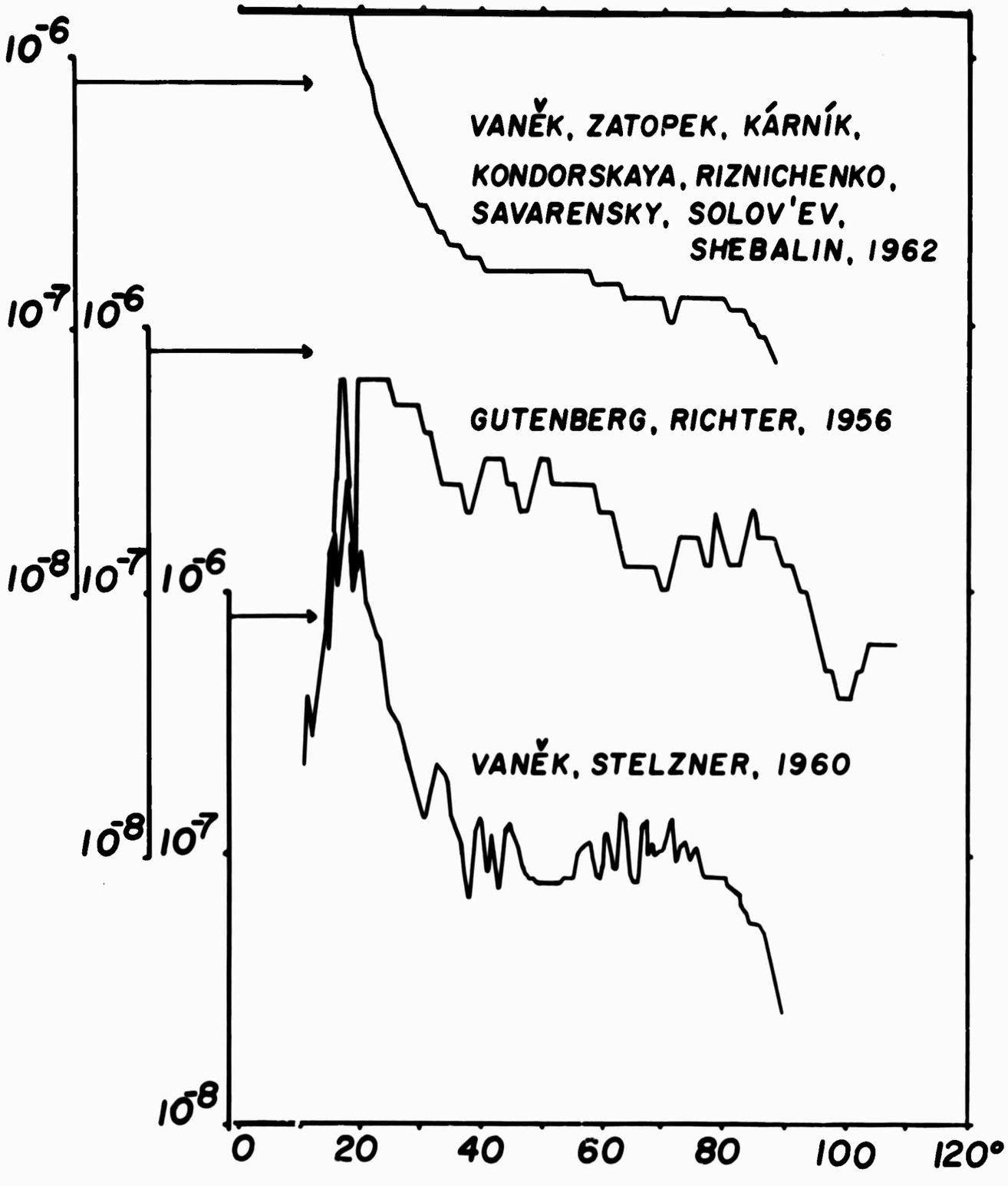
10^{-6}
VANĚK, ZATOPEK, KÁRNÍK,
KONDORSKAYA, RIZNICHENKO,
SAVARENSKY, SOLOV'EV,
SHEBALIN, 1962
10^{-7} 10^{-6}
GUTENBERG, RICHTER, 1956
10^{-8} 10^{-7} 10^{-6}
VANĚK, STELZNER, 1960
10^{-8} 10^{-7}
10^{-8}
0 20 40 60 80 100 120°

FIG. 45

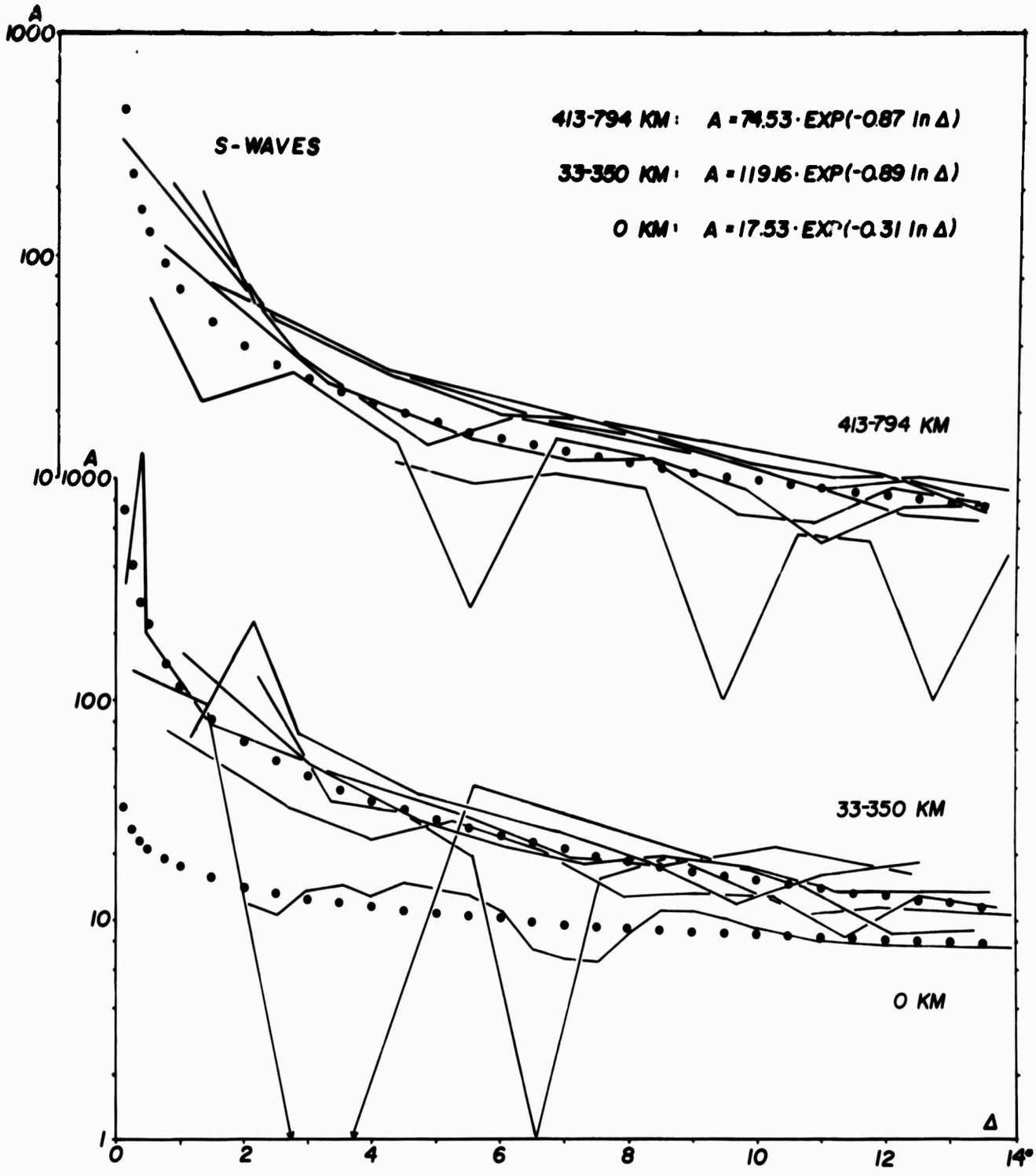
A
1000
100
10
1
S-WAVES
413-794 KM: A = 74.53 · EXP(-0.87 ln Δ)
33-350 KM: A = 119.16 · EXP(-0.89 ln Δ)
0 KM: A = 17.53 · EXP(-0.31 ln Δ)
413-794 KM
33-350 KM
0 KM
Δ
0
2
4
6
8
10
12
14°

FIG. 46

REVISED VALUES OF A FOR PZ, 1955

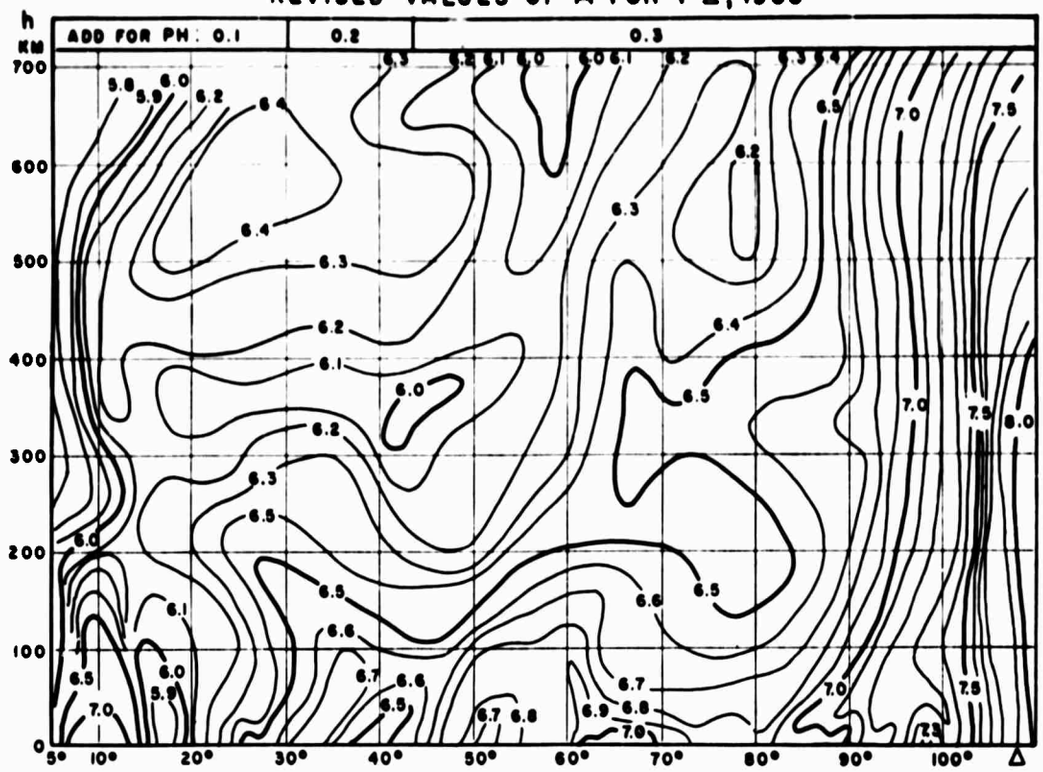

REVISED VALUES OF A FOR SH, 1955

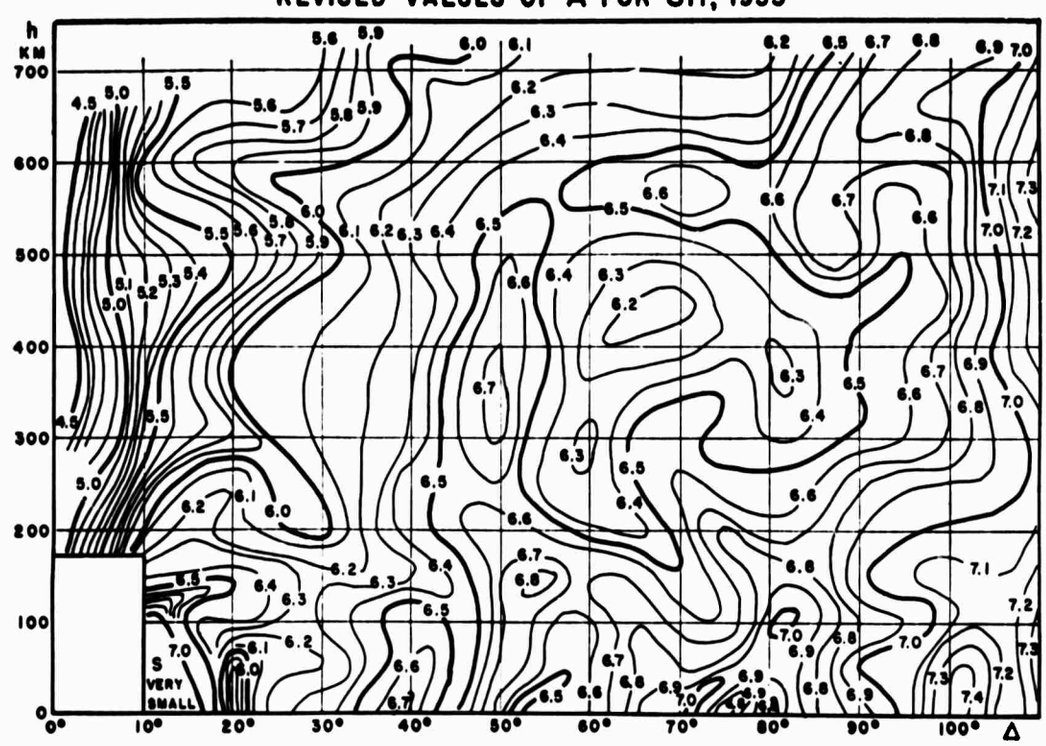

FIG.47

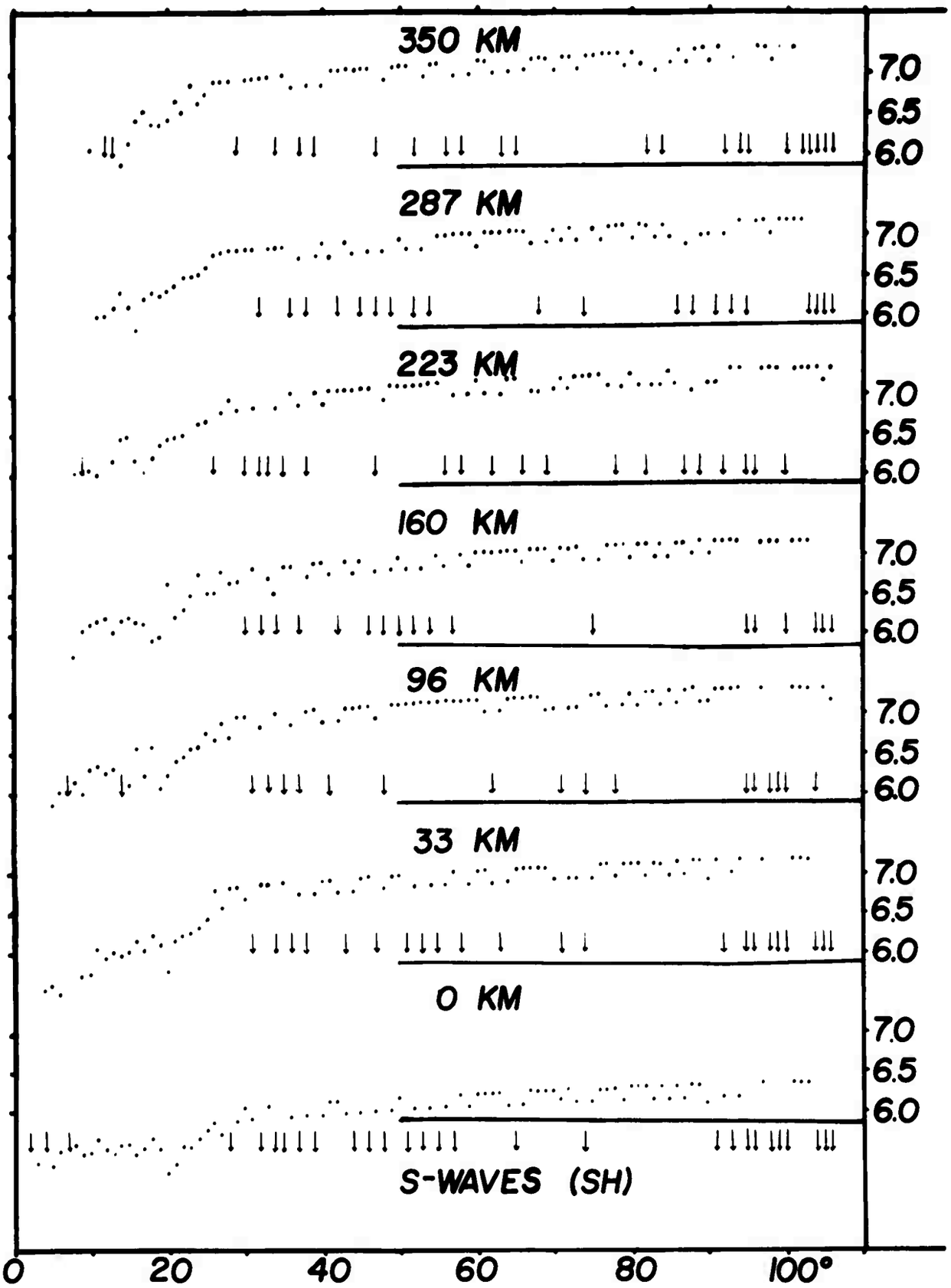
350 KM
287 KM
223 KM
160 KM
96 KM
33 KM
0 KM
7.0
6.5
6.0
S-WAVES (SH)
0
20
40
60
80
100°

FIG. 48a

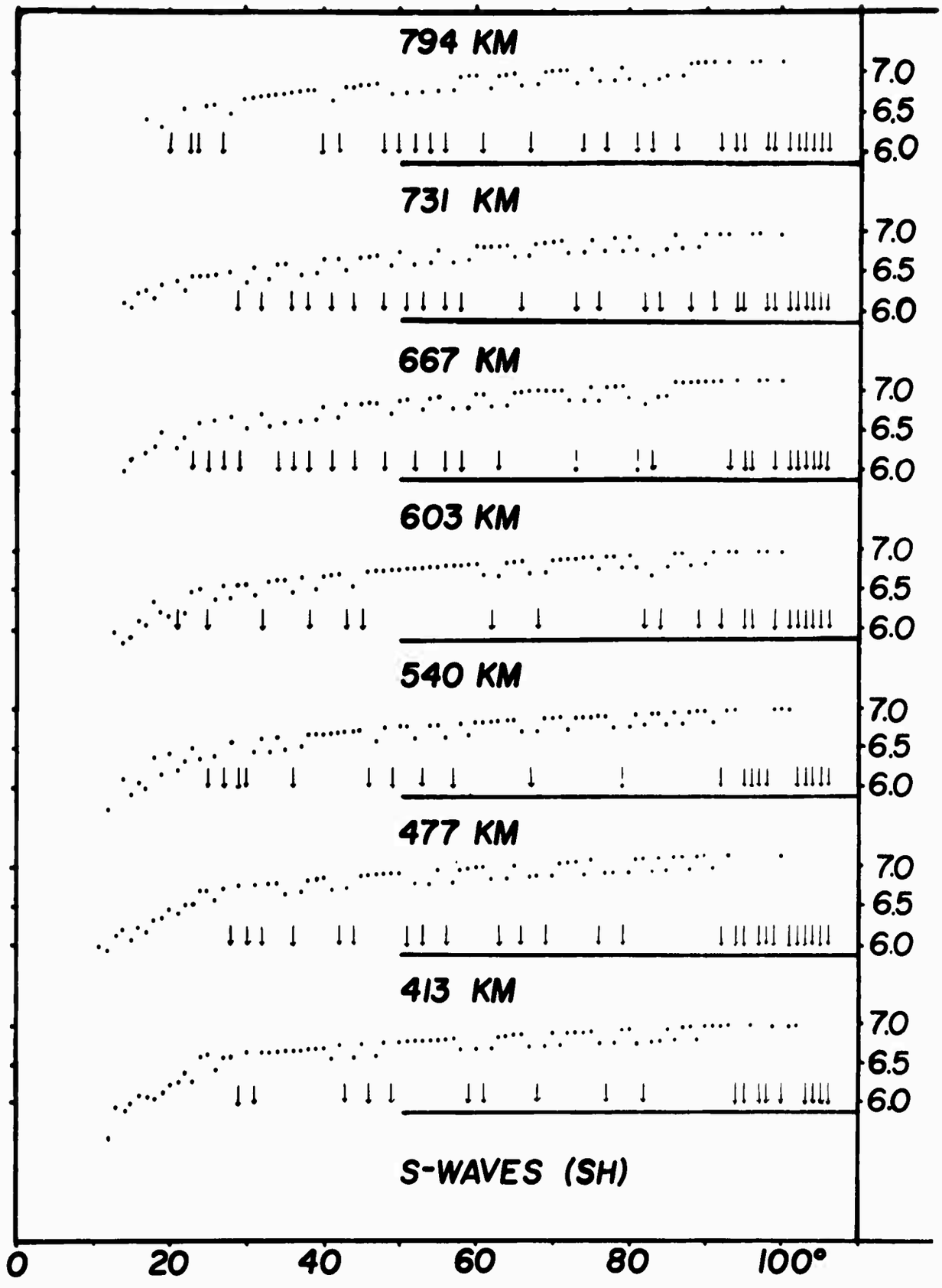
794 KM
7.0
6.5
6.0
731 KM
7.0
6.5
6.0
667 KM
7.0
6.5
6.0
603 KM
7.0
6.5
6.0
540 KM
7.0
6.5
6.0
477 KM
7.0
6.5
6.0
413 KM
7.0
6.5
6.0
S-WAVES (SH)
0
20
40
60
80
100°

FIG. 48b

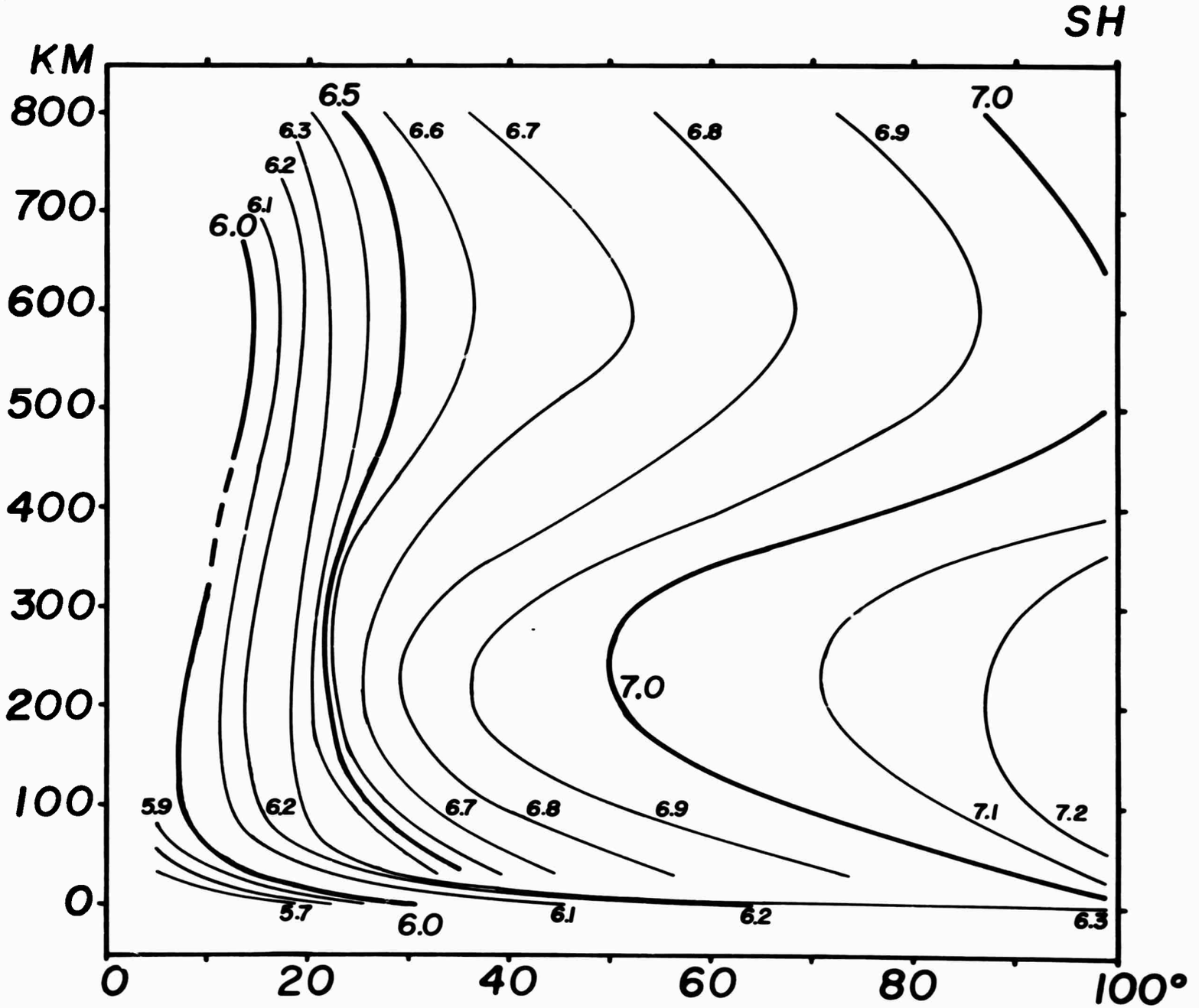
SH
KM
800
700
600
500
400
300
200
100
0
0
20
40
60
80
100°
6.5
6.3
6.2
6.1
6.0
6.6
6.7
6.8
6.9
7.0
7.0
5.9
6.2
6.7
6.8
6.9
7.1
7.2
5.7
6.0
6.1
6.2
6.3

FIG. 49

Unclassified

Security Classification

DOCUMENT CONTROL DATA · R & D

(Security classification of title, body of abstract and indexing annotation must be entered when the overall report is classified)

1 ORIGINATING ACTIVITY (Corporate author) Saint Louis University School of Engineering and Earth Science St. Louis, Missouri 63156	2a. REPORT SECURITY CLASSIFICATION Unclassified 2b. GROUP

3 REPORT TITLE

TRAVEL TIMES AND BODY WAVE MAGNITUDE.

4. DESCRIPTIVE NOTES (Type of report and inclusive dates)
Scientific Interim

5 AUTHOR(S) (First name, middle initial, last name)

Seweryn J. Duda

6. REPORT DATE	7a. TOTAL NO. OF PAGES	7b. NO. OF REFS
February 1970	87	16

8a. CONTRACT OR GRANT NO. AF 19(628)-5100, ARPA Order No. 292 b. PROJECT NO, Task, Work Unit Nos. 8652-00-01 c. DoD Element 6250601R d. DoD Subelement: n/a	9a. ORIGINATOR'S REPORT NUMBER(S) Scientific Report No. 8 9b. OTHER REPORT NO(S) (Any other numbers that may be assigned this report) AFCRL-70-0111

10. DISTRIBUTION STATEMENT

1-This document has been approved for public release and sale; its distribution is unlimited.

11. SUPPLEMENTARY NOTES	12. SPONSORING MILITARY ACTIVITY
This research was supported by the Advanced Research Projects Agency.	Air Force Cambridge Research Laboratories (CRJ) L. G. Hanscom Field Bedford, Massachusetts 01730

13. ABSTRACT The Q-charts used presently for magnitude determinations were obtained mainly from direct observations of ground motion amplitudes of several components of seismic waves (e.g. PZ, PH, SH) as functions of epicentral distance.

After the compensation of the amplitudes of body waves for the radiation pattern at the focus, the amplitude variation is caused mainly by geometrical spreading. No lateral velocity heterogeneities are permitted. Indications are given that the effect of anelasticity upon the amplitudes is secondary for magnitude scales.

Amplitude observations alone can serve for the definition of a magnitude scale applicable to events at only one particular focal depth. In order to assign the same magnitude to two earthquakes of identical "size" regardless of the focal depth, the velocity-depth and eventually anelasticity depth profile of the Earth must be known.

A set of new $\bar{Q}$-charts, obtained independently of direct amplitude observations, for PZ-, PH-, and SH-waves is presented. A refinement in the magnitude definition warrants the magnitude figures obtained with the new $\bar{Q}$-charts to be uniform with regard to focal depth. Examples show the new $\bar{Q}$-charts to decrease the scatter of magnitude determinations between stations.

Since the efficiency in generating longitudinal and transverse waves is most probably not the same for all events, separate P-wave and S-wave magnitudes are advocated.

DD FORM 1 NOV 68 1473

Unclassified

Security Classification

14. KEY WORDS	LINK A		LINK B		LINK C	
	ROLE	WT	ROLE	WT	ROLE	WT
Seismology Seismic Magnitude Seismic Wave Amplitude Seismic Wave Attenuation Seismic Travel Times						